NOTE TO USERS

Graduate School Form 9
(Revised 6/03)

PURDUE UNIVERSITY
GRADUATE SCHOOL
Thesis Acceptance

This is to certify that the thesis prepared

By David Lance Roman

Entitled

Molecular Determinants of Ligand Interaction with Serotonin Transporters

Complies with University regulations and meets the standards of the Graduate School for originality and quality

For the degree of Doctor of Philosophy

Signed by the final examining committee:

Chair

Approved by: Vincent J. Davisson 4/14/04
Head of the Graduate Program Date

☐ is
This thesis ☒ is not to be regarded as confidential.

Major Professor

Format Approved by:

Chair, Final Examining Committee or Department Thesis Format Advisor

Molecular Determinants of Ligand Interaction with Serotonin Transporters

A Thesis

Submitted to the Faculty

of

Purdue University

by

David Lance Roman

In Partial Fulfillment of the

Requirements for the Degree

of

Doctor of Philosophy

May 2004

Dedicated to my family,

for all of their support throughout this endeavor.

ACKNOWLEDGEMENTS

I thank Dr. Eric L. Barker for his guidance as my thesis advisor. I am forever indebted to him for my development as a scientist. Dr. Barker provided an environment for my Ph.D. studies that allowed success for my goals, and more importantly, was a true friend and colleague. Perhaps most important is the lesson Dr. Barker taught me was about presenting scientific information: "Science isn't a murder mystery...give your audience the 'punchline,' at the beginning of your talk." This lesson has proven valuable, and I find myself wishing that all scientists followed this adage.

I thank the members of my thesis committee for the guidance that they have provided throughout my graduate career at Purdue. Dr. Val Watts, Dr. Sandra Rossie, Dr. Gregory Hockerman, and Dr. David Nichols, have all been instrumental in completing this journey.

I also thank the great friends I have made at Purdue during my graduate career: Dr. Gustavo Rodriguez, Fariborz Rakhshan, Crystal Walline, Matthew McFarland, Dr. Deborah Kurrash-Orbaugh, Theresa Day, Dr. Maximilian A. Silvestri, Christopher Johnston, Shannon Saldana, Kellie J. White, Timothy Vortherms, Medhane Cumbay, and all of my fellow graduate students.

I thank Sally Bateman and Janine Mott, two people who were always willing to help a sometimes confused or misguided graduate student.

TABLE OF CONTENTS

Page

LIST OF TABLES

LIST OF FIGURES

Page

LIST OF ABBREVIATIONS

5-HT	Serotonin
SERT	Serotonin transporter
DAT	Dopamine transporter
NET	Norepinephrine transporter
GAT	GABA transporter
hSERT	human serotonin transporter
dSERT	*Drosophila* serotonin transporter
DA	Dopamine
VMAT	Vesicular monoamine transporter
MAO	Monoamine oxidase
HEK	Human embryonic kidney cell line
KRH	Krebs-Ringer-HEPES Buffer
PBS	Phosphate buffered saline
HeLa	Human cervical carcinoma cell line
MTS	Methanethiosulfonate
MTSET	[2-(Trimethylammonium)ethyl] Methanethiosulfonate
CoMFA	Comparative molecular field analysis
TMD	Transmembrane domain
EL	Extracellular loop
PLS	Partial least squares analysis
HDH	Chimeric human/drosophila serotonin transporter, $H^{1\text{-}281}D^{282\text{-}476}H^{477\text{-}638}$.

ABSTRACT

Roman, David L. Ph.D., Purdue University, May 2004. Molecular Determinants of Ligand Interaction with Serotonin Transporters.
Major Professor: Eric L. Barker, Ph.D.

The serotonin transporter (SERT) is a protein responsible for limiting the spatial and temporal actions of the neurotransmitter serotonin (5-HT) by regulating the concentration of 5-HT in the synapse through a reuptake mechanism. SERT is a target for a variety of drugs, including tricyclic antidepressants, selective serotonin reuptake inhibitors (SSRIs), and the abused drugs cocaine and amphetamine. The two aims of this work are the investigation of how 1) antidepressants and 2) psychostimulants are recognized by SERT. Investigation focused on the recognition of antidepressants by SERT utilized Comparative Molecular Field Analysis (CoMFA) using data generated from rat brain synaptosomes and heterologous expression systems expressing rat SERT. Using these models, I have described the molecular requirements for the interactions of antidepressants with SERTs. In addition, molecular studies were performed using chimeric SERTs and SERT point mutants. These studies focused on identifying regions or discrete amino acids of SERT that may be responsible for recognizing antidepressants. Psychostimulant studies exploited pharmacological differences between the human and *Drosophila* species variants of SERT (hSERT and dSERT, respectively), to explore the

molecular aspects of psychostimulant recognition by SERT. These studies entailed the screening of cocaine derivatives and a substituted-amphetamine library, followed by CoMFA analysis. These experiments revealed that a hSERT/dSERT chimera, $H^{1-281}D^{282-476}H^{477-638}$, exhibited pharmacology almost identical to the parental dSERT, indicating that transmembrane domains (TMDs) V-IX in SERT contained important determinants of psychostimulant recognition. Mutagenesis studies were focused on those residues that differ between hSERT and dSERT amino acid identity in TMDs V-IX. Two point mutants, F287K and Y289T, both localized to TMD V, were found to have altered recognition of some cocaine derivatives. A full cocaine derivative library screen was performed on these two point mutants, and CoMFA analysis was performed. The results of the CoMFA analysis indicate that F287K and Y289T may play a role in the recognition of cocaine derivatives. Furthermore, data from previous reports, as well as the data in this work, were used to generate models of the structural helical arrangement of SERT, as well as model of a proposed interaction site of cocaine derivatives on SERT.

Grant support: NIH MH60221.

CHAPTER I

INTRODUCTION

Cellular Transport and Homeostasis

It is estimated that there are 10^{11} neurons in the human central nervous system. On average, each of these neurons can form 1000 synaptic endings, resulting in approximately 10^{14} synapses (Ganong, 1995). Clearly, a high level of regulation must exist in order to control which cells become excited, and how the electrochemical message of neurotransmission is directed. The cycle of neurotransmission stepwise involves neurotransmitter biosynthesis, storage in vesicles, and finally exocytosis and release. Following release, neurotransmitter can be taken back into the presynaptic cell (reuptake) and then degraded as in the case of biogenic amine neurotransmitters, or it may be inactivated extracellularly, as is the case with acetylcholine.

In its simplest terms, neurotransmission is the propagation of an electrical signal, or action potential, from a neuron to its effector cell. In short, an action potential (a wave of cell membrane depolarization) travels along the axon. As the membrane becomes depolarized, voltage-gated calcium channels open, causing an increase in intracellular $[Ca^{+2}]$, which in turn, triggers the fusion of synaptic vesicles to the cell membrane at the

active zone and neurotransmitter is released into the synaptic cleft through exocytosis. Secretion of the neurotransmitter ceases when the intracellular calcium levels are lowered through either sequestration to organelles or released out of the cell by the Na^{+}/Ca^{+2} antiporter. When a presynaptic neuron releases its neurotransmitter in response to an electrochemical signal, the neurotransmitter traverses the synaptic cleft via diffusion and effects a physiological signal determined by the anatomy of the postsynaptic cell. γ-aminobutyric acid (GABA), acetylcholine (Ach) and glutamate can affect ion channels (as well as G-protein coupled receptors) and are considered to be mediators of fast synaptic neurotransmission. The monoamines, 5-hydroxytryptamine (5-HT, serotonin), dopamine (DA), and norepinephrine (NE), act on a longer time scale primarily through G-protein-coupled receptors (GPCRs), that modulate the activity of second messengers (Fon and Edwards, 2001;Loland et al., 1999).

Cellular homeostasis, and the disruption of this state, is a key concept for understanding the process of synaptic transmission. The property of cells to become excited, or deviate from a state of normal cellular functioning and tone, lies partially in the expression of cell-surface proteins that act as triggers for mechanical or chemical signaling. Receptors, ion channels, and transporters are three examples of plasma membrane-bound proteins that transduce an extracellular signal into the cell. Some receptors function as ligand-gated ion channels, others as G-protein coupled receptors (GPCRs), receptor-kinases, or mechanoreceptors. However, specific proteins physically control the flow of transmitter molecules into or out of a cell. A particular process of allowing substances into a cell falls into one of three categories: passive diffusion, facilitated diffusion, or active transport (Figure 1.1).

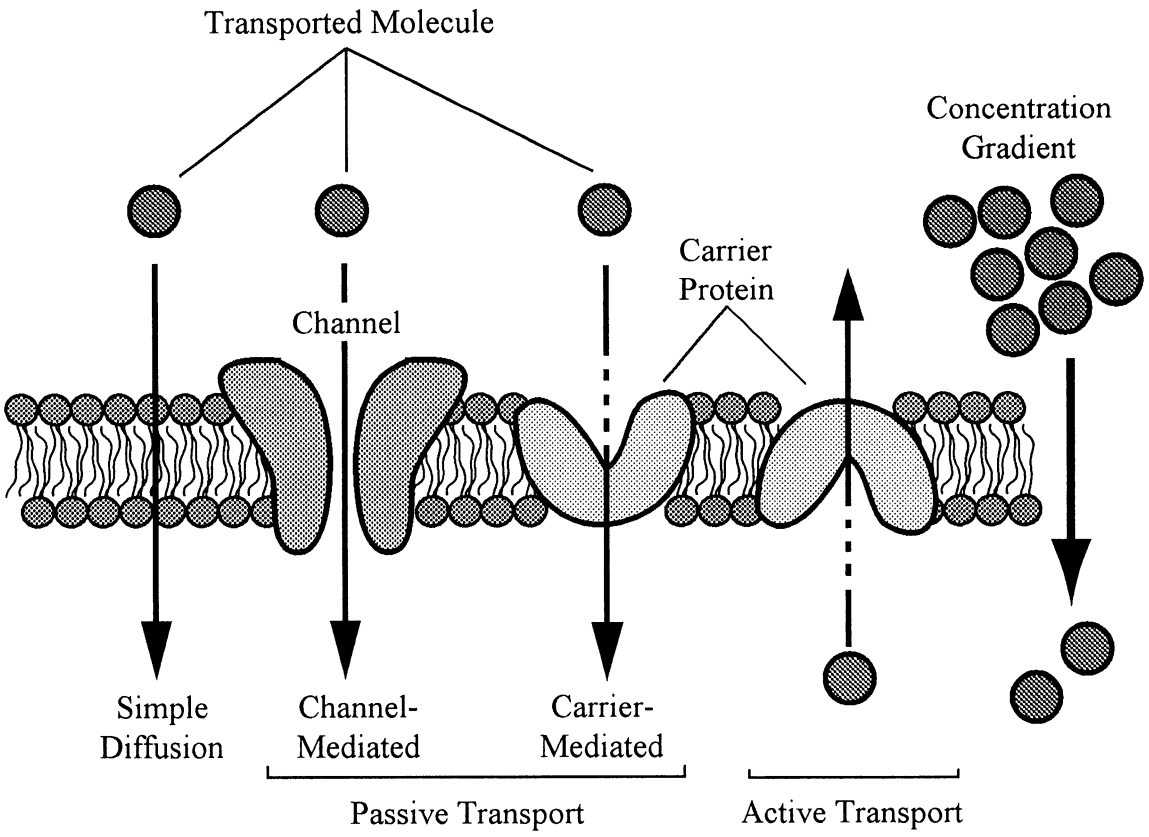

Figure 1.1. Modes of transport across cellular membranes

Passive diffusion is the simplest of the three processes of transport. Substances pass through the membrane, via no specific carrier protein or pore, following their concentration gradients, without the requirement of any cellular energy source. The ability of a substance to diffuse across the membrane is governed by the physiochemical properties of the substance (such as charge, size, lipid solubility), and environmental variables such as temperature. Some molecules that cross biological membranes through the process of passive diffusion are oxygen, nitrogen, and carbon dioxide (Berg et al., 2002).

Facilitated diffusion is a process that is also dependent on concentration gradients, but in this case, the molecules transported across the membrane are normally membrane impermeant, due to their physiochemical properties. Hydrophilic or charged molecules and ions utilize facilitated diffusion in order to cross the lipid bilayer of the membrane. Transporters and ion channels are membrane-spanning proteins which act to provide a functional "pathway" for membrane impermeant solutes to pass into or out of the cell, or subcellular compartment. As is the case for passive diffusion, the transport of substances follows the concentration gradient (Berg et al., 2002).

Transporters are membrane-bound proteins responsible for regulating the movement of molecules from one side of a membrane to another. While they are mechanistically complex, the basis of their operation is to act as carriers and move molecules across the membrane. Transporters utilize the energy from a concentration gradient to move solute through the membrane (Berg et al., 2002).

Gated ion channels are membrane-bound proteins that form a functional pore through which ions can flow down their concentration gradient. The regulation of the open state of these pores can be in response to a variety of chemical or physical stimuli, including membrane voltage, mechanical stress, or ligand binding. Ion flux is dependent on the time period that the channel is in its open state, as the rate of ion movement is somewhat limited by its diffusion rate. Ion channels are particularly important when considering the transmission of electrochemical signaling in neurotransmission because they act to regulate the membrane potential of a cell, and ultimately, the release of neurotransmitter due to changes in ion/charge concentration (Hille, 2001).

Active transport is the only mechanism of the three that requires the external input of energy, such as the hydrolysis of adenosine triphosphate (ATP), in order to move substances across a membrane. Energy is required in active transport mechanisms because in this scenario, molecules are being accumulated against their concentration gradient (movement from low to high concentration). Active transport is carried out by primary transporters, which are directly coupled to the hydrolysis of ATP for their function. One such transporter is the Na^+/K^+ ATPase, or sodium/potassium pump. This ATPase transports sodium ions to the extracellular space while countertransporting potassium ions in a 3:2 stoichiometry. This process requires energy because sodium normally exists in a higher concentration outside the cell (50 mM_i vs. 440 mM_o, whereas potassium has a higher intracellular concentration (400 mM_i vs. 20 mM_o) (values for squid giant axon, Hille, 2001). This active transport process is important for maintaining the cellular membrane potential and osmotic balance.

Another type of active transport, the secondary active transport process, does not directly couple the movement of substances to the hydrolysis of ATP, but rather relies on an established ionic gradient to drive translocation. In most cases, such as the Na^+/Cl^--dependent neurotransmitter transporters, the sodium concentration gradient established by the primary Na^+/K^+ ATPase enables the movement of solute to be coupled to the movement of ions down their concentration gradient (Rudnick, 1998). In this case, the driving force for the accumulation of a substrate against its concentration gradient is the flow of ions down their concentration gradient, thus the process does not directly involve the expenditure of cellular energy. However, because the ionic gradient that the transporter utilizes to drive its translocation process is established in an ATP-dependent manner, this transport process does ultimately have an indirect ATP dependency (Moriyama and Futai, 1990b).

Each of these transport processes provides critical roles for maintaining cellular homeostasis and signaling. In the nervous system, these transporters and their associated ions and substrates play critical roles in the propagation and termination of the electrochemical signaling that occurs between cells. In particular, these transport processes play critical roles in the processes of neurotransmitter packaging, release, and signal termination.

Neurotransmission

Vesicular Packaging: the Role of VMAT

Release of neurotransmitter critically involves two processes: packaging into synaptic vesicles and exocytosis from the presynaptic cell (Figure 1.2). Synaptic vesicles act as high-concentration storage organelles for synthesized neurotransmitter. Neurotransmitters such as 5-HT are synthesized in the cytoplasm and packaged into synaptic vesicles through transport proteins known as vesicular monoamine transporters (VMATs), specifically, VMAT1 and VMAT2. In biogenic amine-containing neurons, VMAT2 is exclusively expressed (Weihe and Eiden, 2000), and does not discriminate among serotonin, norepinephrine or dopamine, but rather the specificity is determined by the type of neuron the VMAT exists within (Uhl et al., 2000). These transporters utilize the presence of vacuolar ATPases and the impermeability of storage vacuoles to protons in order to drive the transport of these bioactive amines into the vesicles against a concentration gradient (Moriyama and Futai, 1990a;Eiden, 2000). This gradient is substantial, with an extra-vesicular concentration in the low micromolar range, and the concentration inside the vesicle approximately 10,000-fold higher. The driving force for the transport is the proton gradient or differential in chemical charge between the interior of the vesicle and the cytoplasm, with a higher concentration of protons, or lower pH, inside the vesicle. The uptake and packaging of biogenic amines into secretory vesicles closely resembles nutrient uptake by bacteria and mitochondrial ATP production in that a proton gradient drives the inward transport. However, the processes differ in that

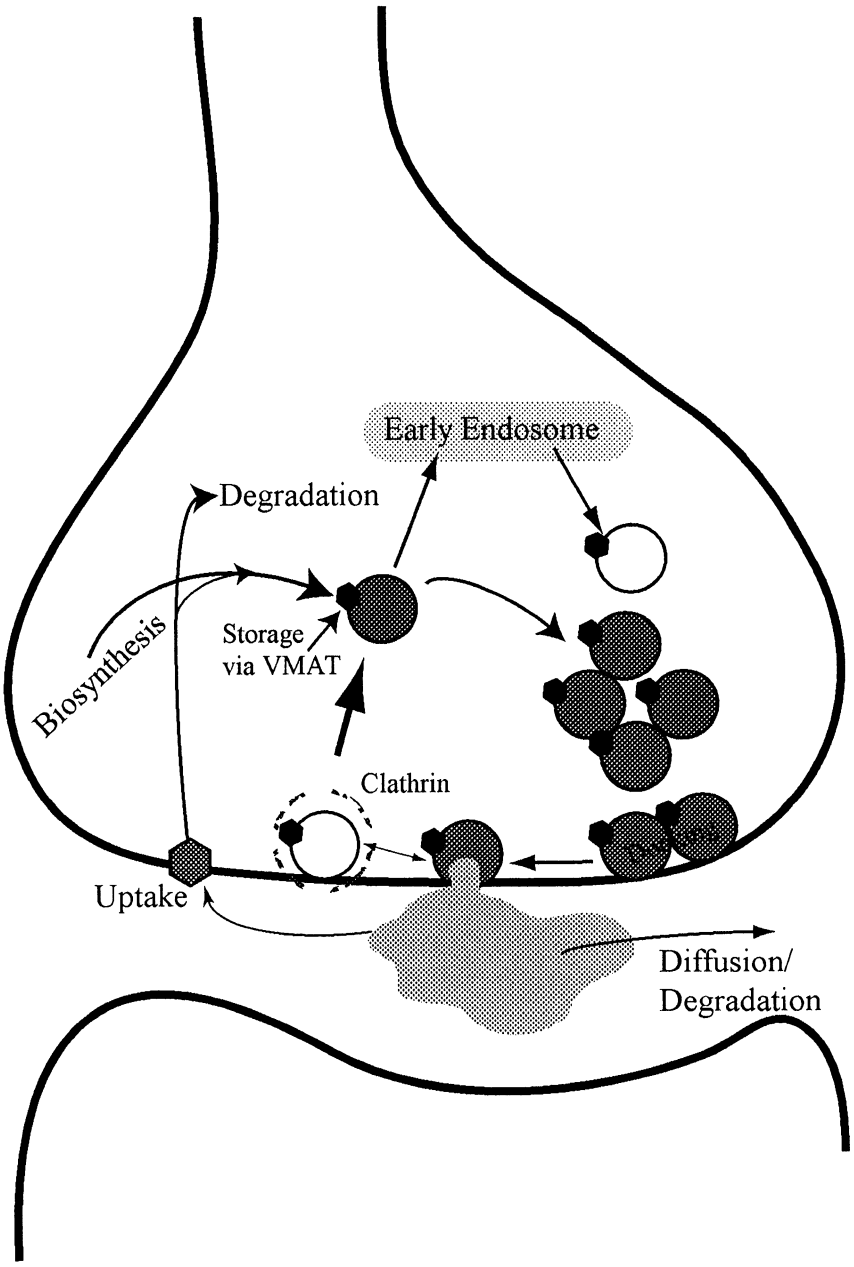

Figure 1.2. A schematic representation of the neurotransmitter synthesis, packaging, and release cycle. Free neurotransmitter, either newly synthesized or transported through a reuptake carrier can undergo degradation or repackaging through VMAT into synaptic vesicles. This packaging may occur through an early endosome intermediate step. Once the vesicles are filled, they can be recruited and docked to the active zone of the neuron awaiting their signal to release neurotransmitter. A clathrin-mediated process then can recycle the synaptic vesicles. Synaptic neurotransmitter may be transported back into the neuron, diffuse away, or be degraded.

bacterial nutrient uptake involves the cotransport of protons, whereas in mitochondria the electron transport chain initiates the gradient (Peter et al., 1997). The vesicular ATPase utilized in packaging uses the energy from ATP hydrolysis to pump H^+ ions into the vesicle. The process provides an electrical gradient necessary for loading biogenic amines against the concentration gradient between the vesicle and the cytoplasm. Concurrent to this proton pumping phenomenon, an anion (such as Cl^-) can accompany the proton, resulting in a pH gradient of increased acidity inside the vesicle, but negating the electrochemical accumulation of charge, as the net influx is neutral. In the absence of the accompanying anion, the increased hydrogen ion concentration inside the vesicle causes a net positive charge with respect to the cytoplasm (Peter et al., 1997). The high concentration of protons allows operation of the VMAT as an exchanger of two luminal protons for one cytoplasmic biogenic amine molecule during each transport cycle (Erickson and Varoqui, 2000). Interestingly, it has been calculated that the majority of driving force for *in vivo* biogenic amine uptake is the pH gradient, which provides 130-fold greater driving force than the electrical gradient established by ATPase protons without an accompanying anion (Parsons, 2000).

Vesicular Fusion

In neurotransmission, one event can be marked as the beginning of the propagation of the electrochemical signal from one cell to another: the entry of calcium into the cell. In the central and peripheral nervous system, multiple types of voltage-dependent calcium channels are expressed, including N-, P/Q-, R-, L- and T-types (Hille,

2001). Although there are a variety of expressed channels in the nervous system, immunocytochemistry experiments indicate that N-type and P/Q-type channels are predominantly involved in neurotransmission (Spafford and Zamponi, 2003). The entry of calcium through these channels allows the activation of calcium-dependent or calcium-activated proteins, such as synaptotagmin, to initiate vesicular release of neurotransmitter, thus completing the propagation step of the signaling event (Chapman, 2002).

Once calcium enters the presynaptic neuron, a series of events occurs that still is not completely understood. The concentration increase (to 10-100 micromolar) of calcium is a local event, with little diffusion occurring outside the general area of the calcium channel (Schneggenburger and Neher, 2000). This spatial limitation is due to the presence of intracellular calcium binding proteins and the general buffering capacity of the cell (Spafford and Zamponi, 2003). Due to this spatial limitation, it is not surprising that *some* presynaptic calcium channels are colocalized with proteins involved with the vesicular release machinery near the active zone of the neuron (Kasai, 1993). The presence and proximity of neuronal calcium channels, calcium binding proteins or sensors and synaptic vesicles has led to the development of the microdomain model of exocytic machinery arrangement within the presynaptic neuron (Augustine, 2001). In this model, several channels, likely of different types (such as N- and P/Q-), exist at the membrane in clusters and in close proximity to neurotransmitter filled synaptic vesicles. When the channels, due to their voltage sensitivity, allow the influx of calcium, a region of higher calcium concentration develops in the immediate area of the channels. The synaptic vesicles and associated exocytosis machinery are in close proximity, allowing

calcium-sensitive proteins to affect the release of neurotransmitter (Augustine, 2001). Note that the presence of more than one subtype of voltage gated calcium channel is evident due to the synergistic action of subtype-specific calcium channel blockers on neurotransmitter release (Takahashi and Momiyama, 1993).

Vesicular Fusion and Exocytosis of Neurotransmitter

Some of the most widely studied proteins involved in the processes of exocytosis are SNAREs (soluble N-ethylmaleimide-sensitive factor activating protein receptors). SNARE proteins can be generally classified as proteins that act as fusion factors, interacting to form extraordinarily stable complexes between membranes in close proximity. In the process of neurotransmitter release, three SNAREs are involved: VAMP-2 (synaptobrevin), SNAP-25, and syntaxin 1A (Duman and Forte, 2003). VAMP-2 is a membrane-bound protein with one transmembrane domain that is primarily localized to the synaptic vesicle membrane. SNAP-25 is a synaptosome-associated protein that is associated with the neuronal plasma membrane through a region rich in palmitolyated cysteine residues. Syntaxin 1A, like VAMP-2, is a single-transmembrane domain containing protein; however it can be found primarily associated with the plasma membrane (Lin and Scheller, 2000). The classification of SNAREs is based upon their presence in either the vesicular membrane (v-SNAREs) or plasma membrane (t-SNAREs, for target). Therefore, VAMP-2 is classified as a v-SNARE whereas Syntaxin 1A and SNAP-25 are t-SNAREs. The interactions of these proteins on the vesicular and

plasma membranes lead to membrane fusion and release of neurotransmitter into the synaptic cleft.

A large number of assorted other proteins, such as munc-18 (Dulubova et al., 1999) and Rab3 (Martelli et al., 2000) also play regulatory or structural roles in the assembly and/or interactions within the vesicular release machinery and are members of protein families involved with general membrane trafficking. Vesicle exocytosis is essentially a two-staged process. First, there is an ATP-dependent priming event involving at least two different proteins, NSF (NEM-sensitive factor) and PITPs (phosphoinositide transfer proteins). The second stage is the actual Ca^{+2} triggered membrane fusion (Lin and Scheller, 2000).

At a resting state, syntaxin exists in a "closed" conformation associated with the plasma membrane, and does not interact with the VAMP-2 on the vesicle or SNAP-25, which is also found on the plasma membrane. Another protein, synaptotagmin, is also associated with the vesicular membrane and contains calcium sensing C2 domains. Synaptotagmin is also found exclusively in neurons (Geppert et al., 1994). It has also been suggested that synaptotagmin associates directly with presynaptic calcium channels (Tucker and Chapman, 2002). In one model, upon the influx of calcium, the calcium binding loops of synaptotagmin penetrate into the plasma membrane and increases the affinity of the t-SNAREs SNAP-25 and syntaxin 1A (Tucker and Chapman, 2002). It is important to recognize that the exact role of synaptotagmin is not understood, and in fact, some data suggest that synaptotagmin may actually functionally prevent the formation of a tight SNARE complex (Chen et al., 2001). In either model, however, synaptotagmin acts as a calcium sensor and undergoes a conformational change to associate or dissociate

with other components of vesicular release machinery, allowing the formation of the SNARE complex. This action causes an increased affinity of the t-SNARES for the v-SNARE complex, and functionally causes a stronger interaction between each complex's external (non-membrane) helical domains. Once again, it is the action of calcium that causes a "zippering" effect, pulling the vesicular and plasma membranes together, resulting in the fusion of the two membranes and subsequent neurotransmitter release (Lin and Scheller, 2000).

The release of chemical from a presynaptic cell is a complicated process. The physiological process of neurotransmitter release involves a myriad of regulatory and structural proteins. Proteins such as SNAREs (Lonart and Sudhof, 2000) and vacuolar H^+ ATPases (Moriyama and Futai, 1990a) play critical roles in the overall process of cell-to-cell signaling.

Termination of Signal

Following the release of neurotransmitter, as described above, the bioactive molecules can interact with their downstream effectors, such as presynaptic or postsynaptic GPCRs, and act to enhance, transmit, or attenuate the neuronal signaling event (Figure 1.3). In the case of the biogenic amine neurotransmitters (serotonin, dopamine, and norepinephrine), the usual downstream effector is a GPCR, or in the case of 5-HT_3 receptors, a ligand-gated ion channel. Once these neurotransmitters interact with their targets, the neurotransmitters need to be deactivated, either by chemical

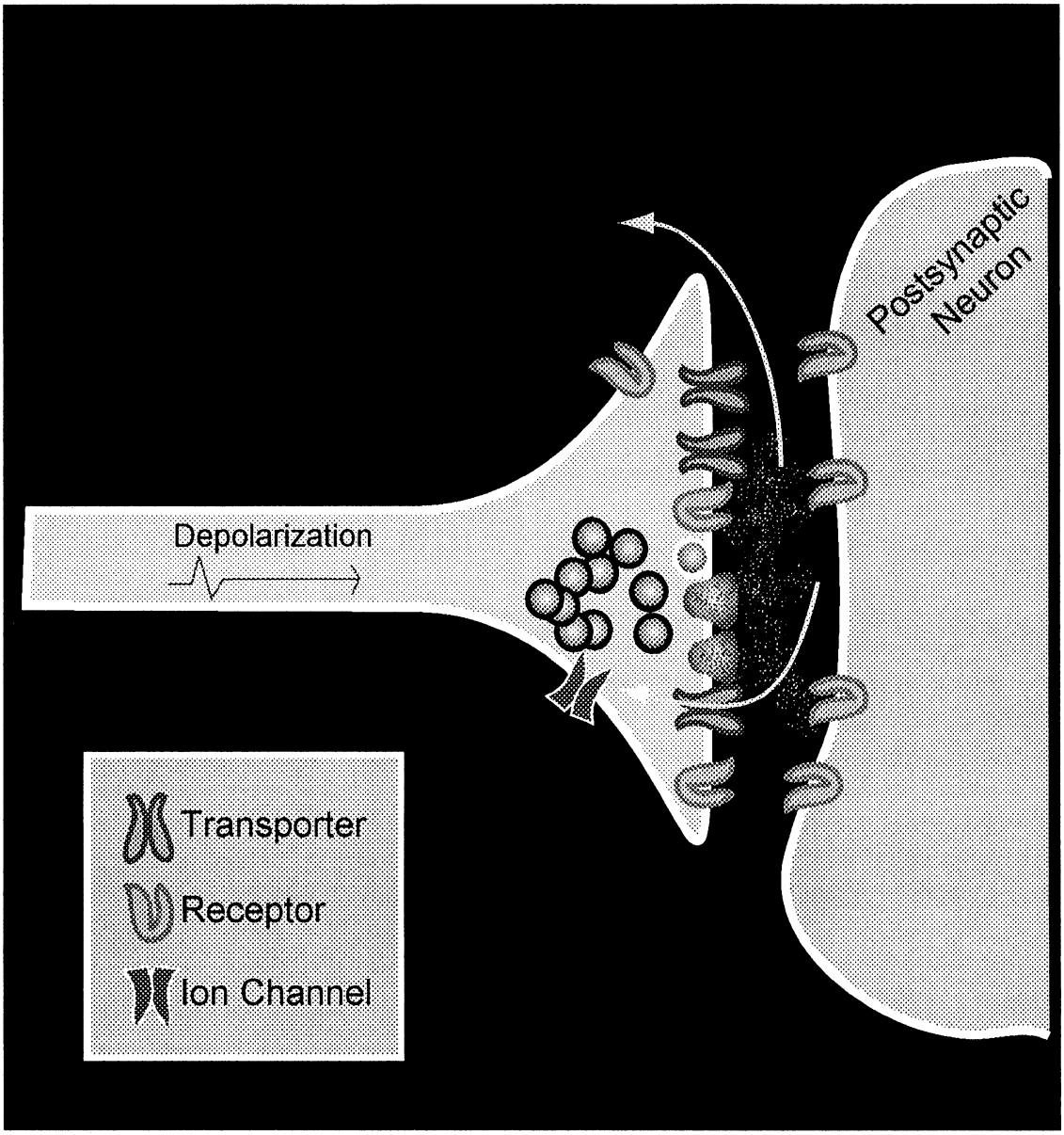

Figure 1.3. Diagram of a synaptic cleft, indicating the release of neurotransmitter and subsequent diffusion or transport into the presynaptic neuron.

modification or physical removal from the synaptic space. The signaling of biogenic amine neurotransmitters is primarily terminated through the physical removal of the neurotransmitter from the synapse, although metabolic degradation and diffusion do play a role. This physical removal is facilitated though a group of plasma-membrane bound transport proteins that are members of the Na^+/Cl^--dependent family of transporters. This gene family encompasses an extensive list of transporters, including those for 5-HT, dopamine, norepinephrine, glycine, γ-aminobutyric acid (GABA), proline, taurine, betaine and creatine (Amara and Kuhar, 1993).

Biogenic Amine Neurotransmitter Transporters

Mechanisms of 5-HT Inward Transport

My work has focused on the 5-HT transporter (SERT), the protein that functionally regulates the temporal and spatial aspects of serotonergic signaling by clearing 5-HT from the synapse following release. The molecular structure of SERT has been investigated since the transporter was cloned in the early 1990s (Blakely et al., 1991a;Hoffman et al., 1991;Ramamoorthy et al., 1993;Demchyshyn et al., 1994). The transporter is a 630 amino acid protein that is predicted to contain twelve transmembrane domains (TMDs) and intracellular amino and carboxy termini (Figure 1.4) (Barker and Blakely, 1995;Chen et al., 1998). A large extracellular loop exists between TMDs III and IV, and this loop contains several putative N-linked glycosylation sites (Blakely et al., 1996). The biogenic amine neurotransmitter transporters are believed to share this basic topology, and have approximately 48-67% overall sequence identity, with the highest degree of similarity existing within the TMDs (Shafqat et al., 1993).

Functionally, SERT couples the inward movement of substrate (5-HT) to the inward movement of Na^+ and Cl^- ions and the countertransport of K^+ (Figure 1.5). The movement of these ions and accompanying 5-HT is not directly coupled to the hydrolysis of ATP (active transport), but is indirectly facilitated through cellular ionic gradients that are established by the Na^+/K^+-ATPase. A negative membrane potential is generated that places a higher concentration of Na^+ outside the cell and a higher concentration of K^+

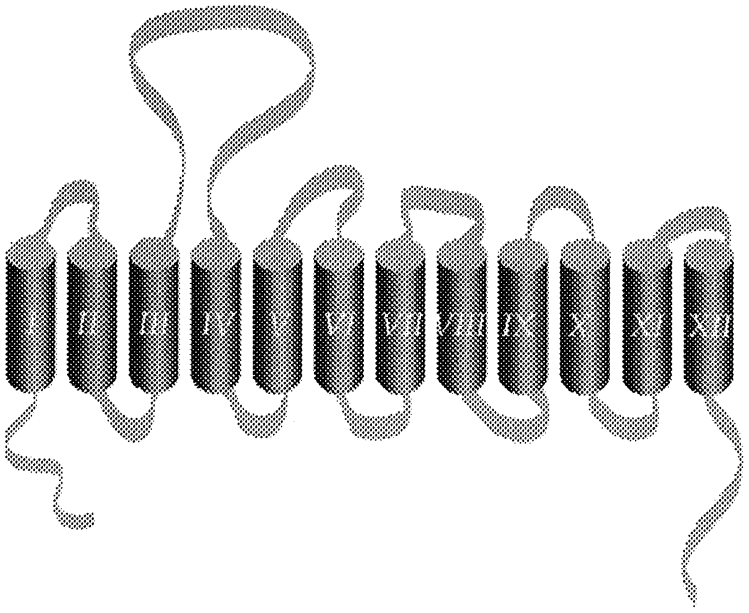

Figure 1.4. Putative topology of SERT.

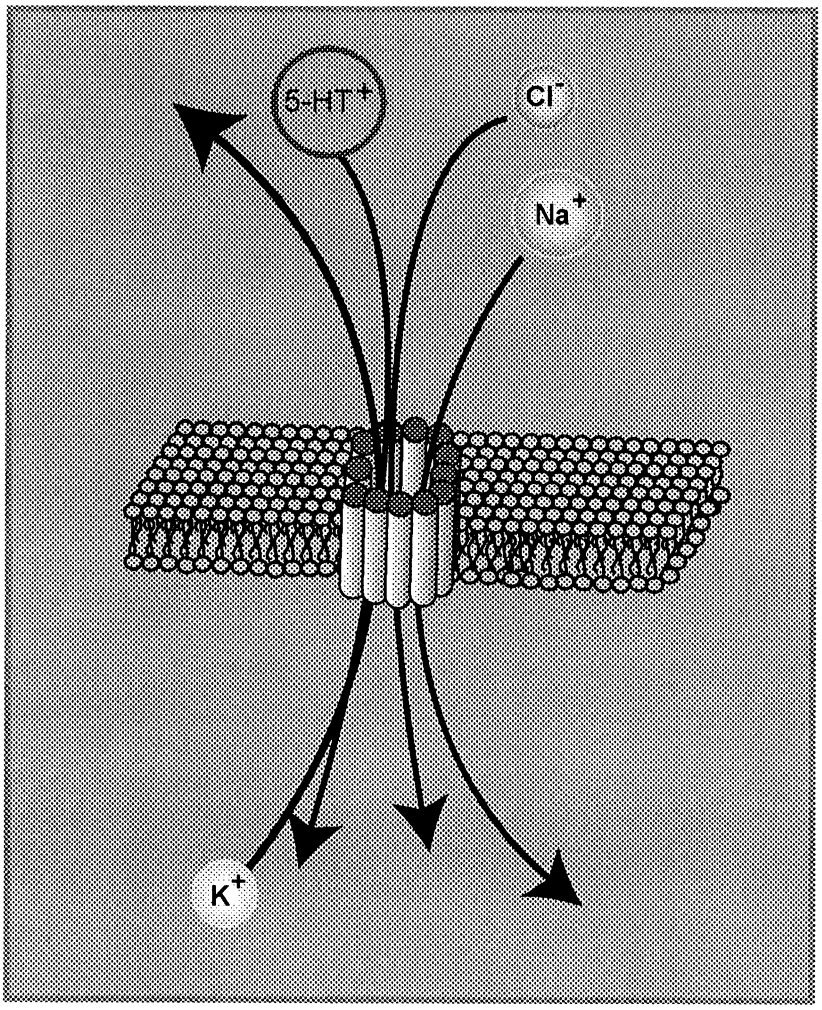

Figure 1.5. Schematic of 5-HT transport indicating ion co- and counter-transport stoichiometry.

intracellularly. In a passive manner, a Cl^- concentration gradient is also established (Rudnick, 1998).

Initial studies conducted in platelet membrane vesicle preparations, a rich source of 5-HT transporters, examined the role of ions in driving the inward transport of 5-HT. The presence of a simple Na^+ concentration gradient is sufficient to drive transport. Also, external chloride is necessary for 5-HT uptake, and destruction of the Cl^- gradient by raising the concentration of intracellular Cl^- inhibits the uptake of 5-HT (Rudnick, 1977). The role of K^+ was examined and results showed that internal K^+ could stimulate 5-HT uptake, but was not required (Nelson and Rudnick, 1979). Furthermore, Keyes and Rudnick (1982) demonstrated that internal protons could fulfill the role of antiported cation, keeping the transport cycle electrically neutral. These seminal studies provided the initial mechanistic understanding of the 5-HT transport process, by which inward Na^+/Cl^- gradients and outward K^+ or H^+ gradients provide the driving force.

Alternating Access and Channel Mode Models of Transport

The precise physical process of transporting released 5-HT back into presynaptic neurons has not yet been determined. However, the field is somewhat dominated by the "alternating access" model (Figure 1.6A). In this model, the transporter exists in either an inward or outward facing conformation in which a binding site is alternately accessible to either the intracellular or extracellular face of the membrane (Adams and DeFelice, 2003). The conversion from one face to the other would occur after ion and/or substrate binding events, thus allowing translocation. It has been proposed that 5-HT (or substrate),

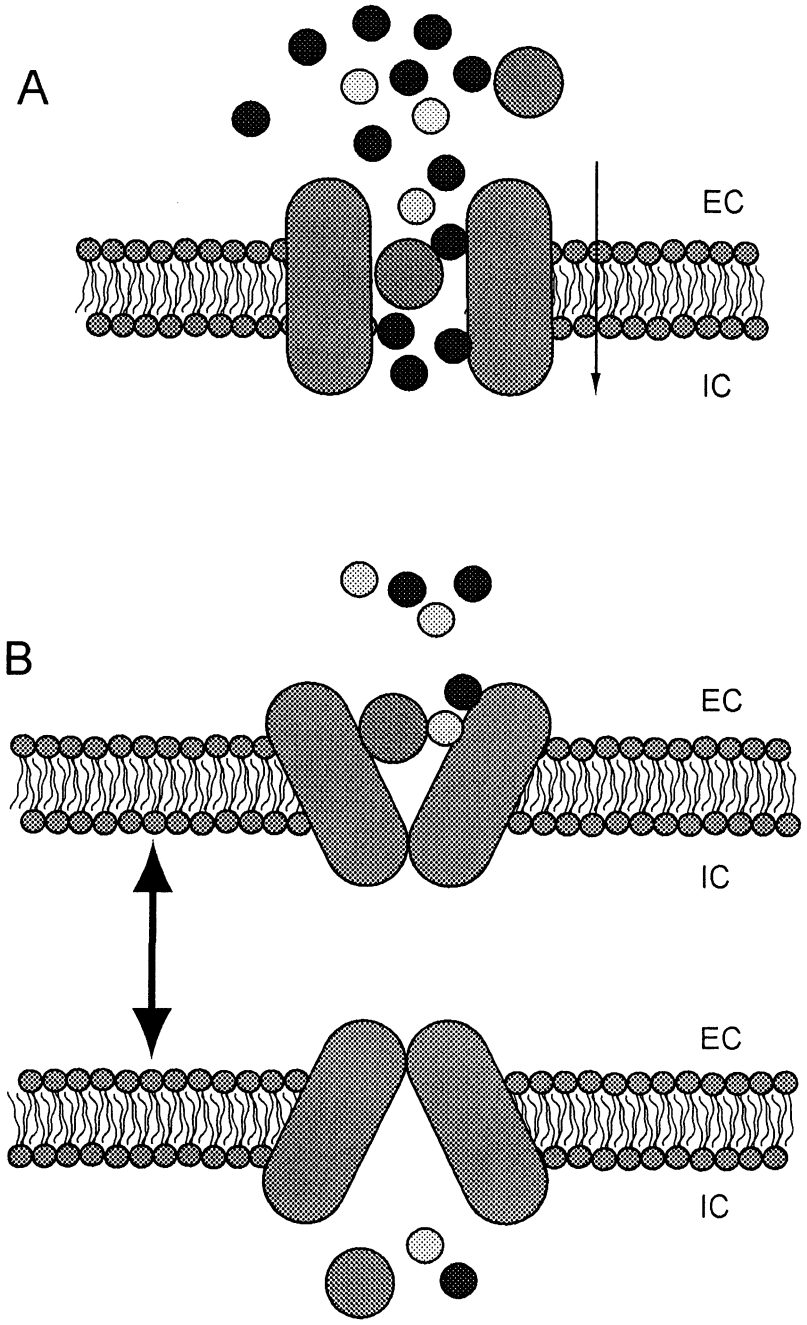

Figure 1.6. Two proposed models of SERT function. (A) Represents the channel model, or shuttling stream mode of transport. 5-HT is represented by red circles, whereas accompanying ions (sodium and chloride) are represented by yellow and blue circles. (B) Represents the Alternating Access model, whereby 5-HT and its accompanying ions bind to the external face of the transporter and then the transporter "flips" to release the neurotransmitter into the intracellular space.

Na^+, and Cl^- bind to the outward face of the transporter and induce the conformational changes necessary to "flip" the transporter to the inward facing conformation. The reorientation of the transporter would then be initiated by the dissociation of substrate and ions, and the binding of intracellular K^+ to the now inward facing, or intracellularly accessible, binding site (Torres et al., 2003b). One proposed model indicates that mechanistically, one sodium binds, one chloride binds and then substrate. Once the substrate is bound, the transporter undergoes a conformational shift to release the substrate and cotransported ions into the intracellular environment. Following this conformation change, K^+ (or a proton) binds to the now inward facing transporter and "resets" it to an outward facing conformation (Nelson and Rudnick, 1979;Rudnick and Clark, 1993;Rudnick, 1998). While this model proposes one putative mechanism, recent electrophysiological data have cast some doubt on the likelihood of its accuracy (Galli et al., 1997;Petersen and DeFelice, 1999;Adams and DeFelice, 2003).

Although the overall process of 5-HT translocation is electrically neutral, the movement of 5-HT and its accompanying ions has been observed using electrophysiological techniques, primarily two electrode voltage clamping in cRNA-injected *Xenopus laevis* oocytes. The movement of ions and 5-HT in its charged state (protonated amine nitrogen) results in a net zero charge movement across the membrane; however, currents have been measured at SERT and other members of this transporter superfamily (Corey et al., 1994;Cao et al., 1998;DeFelice and Galli, 1998;Mager et al., 1998). Initial data relating to NET and non-mammalian SERTs indicate that, according to the previously proposed stoichiometry, approximately 10^6 expressed transporters could produce a current of less than 0.2 picoAmps (pA). However, experimental data revealed a

measurable current on the order of 100 pA using HEK-293 cells transfected with hNET (Galli et al., 1996).

In light of this and other electrophysiological experiments, DeFelice and coworkers (1997;2002) have proposed a second model for the cotransport process for NET and non-mammalian (i.e. *Drosophila*) SERTs. In this second model, or alternate mechanism of transport, substrates and ions share a common pore, and coupling interactions occur between substrate and cotransported ions within this pore as they are transported (Figure 1.6B) (Adams and DeFelice, 2003). The evidence supporting this model for the monoamine transporters is that substrate-induced currents greatly exceed what can be calculated from transporter expression level and turnover rate. The calculations, when based on a 1:1:1:1 stoichiometry (5-HT:Na^+:Cl^-:K^+) and the alternating access model, do not fit the observed electrophysiological data (Blakely et al., 1994;Galli et al., 1996;Mager et al., 1998).

Additional evidence supporting a "common pore" or "channel mode" of transport is the observation of a substrate-independent or "leak" current from transporters in this family. In short, in the absence of substrate (neurotransmitter), the transporter still allows some degree of ionic flux. In this mode, the transporter exists in a conformation in which its TMDs (or, more likely, a subset of TMDs) act to surround a water-filled pore. This pore would be permeant to ions such as sodium, which will travel down their concentration gradient and be "transported" into the cell. As sodium flows into the cell, it could interact with 5-HT and Cl^- to form a "shuttling stream," moving 5-HT back into the cell. This model accounts for the presence of the "leak" current, as the transporter should

not be able to shuttle ions without being bound to 5-HT, unless the transporter existed in a conformation which allowed the flow of ions through a pore.

A final line of evidence highlighting caveats in the alternating access model, and relating to hSERT, was recently published by Adams and DeFelice (2003). In these studies, oocytes expressing hSERT cRNA were manipulated using two perfusion devices, allowing a change in the external as well as internal cellular environment. In short, these studies indicated that Na^+ can bind to the transporter from either the internal or external side of the membrane simultaneously. The presence of a binding site that is universally accessible does not fit into the alternating access model, but does fit the profile of an open, water-filled pore. However, experiments using Li^+ to substitute for Na^+ has shown that Li^+ does promote current flow through the transporter, but does not allow 5-HT to be transported (Humphreys et al., 1994). The ability to promote current flow and not 5-HT translocation does not fit with the "shuttling stream" model. The exact mechanism has not been thoroughly dissected, and differences in the way Li^+ and Na^+ interact with the transporter, for example, may affect 5-HT transport. Clearly, much research is needed in this area to understand more completely the underlying mechanisms of 5-HT transport.

While some recent data may conflict, these data as a whole suggest a reevaluation of the models proposed in the past. The data indicating that 5-HT as well as NE transporters may have a channel mode of operation is compelling and provides new avenues of research into an important pharmacological target.

Targets for the Treatment of Depression and Affective Disorders

The neuronal tone of the serotonergic system plays an important role in the determination of mood and other physiological processes such as sleep, libido, and appetite (Barker and Blakely, 1995;Zahniser and Doolen, 2001). Disruption of the finely regulated concentration of 5-HT at the cellular level appears to play a role in a host of psychiatric disorders, including depression and states of prolonged heightened anxiety such as obsessive-compulsive disorder, eating disorders, and social phobias (Barker and Blakely, 1995).

The symptoms of depression and affective disorders can be described as feelings of sadness, hopelessness, irritability, phobias and panic attacks. Anhedonia, including the inability to derive pleasure from sex, is often cited as a first warning sign of the disease. Disruptions of appetite and sleep disturbances are also common symptoms of depression.

The most recently available statistical data from the National Institute of Mental Health, based on the 1998 United States census, highlights the widespread occurrence of clinical depression. These data indicate that 9.5% of the U.S. population aged 18 or older is afflicted by a diagnosable affective disorder (2001). Perhaps even more striking is that 13.3% of the U.S. population suffers from one of the many subtypes of anxiety disorders. Clearly, in the United States and worldwide, the broadly categorized mental disorders of depression and anxiety are of major societal concern.

Many therapeutic agents for these disorders act by increasing the level of synaptic 5-HT, prolonging the downstream signaling effects of released neurotransmitter. The spatial and temporal actions of 5-HT are primarily determined by the action of SERT. Therapeutically, the blockade of this uptake process has been used to increase synaptic 5-HT and alleviate the symptoms of depression and some anxiety disorders.

Historically, some of the earliest therapeutic agents for treating depression were the tricyclic antidepressants such as imipramine and amitriptyline. This class of antidepressants has mixed activity, functioning to inhibit both SERT and NET. This mixed profile of transport inhibition yields one treatment option for those suffering from anxiety and depression. However, the adverse effects of the tricyclic antidepressants can be quite serious and, thus, their use has diminished in recent years as newer, more selective, safer agents became available. The synthesis and characterization of fluoxetine as a specific, selective serotonin reuptake inhibitor (SSRI) led to the development of a new class of compounds for the treatment of depression (Wong et al., 1974;Wong et al., 1975). The selectivity of fluoxetine for SERT vs. NET is almost 150-fold in rat brain synaptosome preparations (Robertson et al., 1988) and even more pronounced when comparing cloned hSERT to cloned hNET (0.9 nM vs.777 nM) (Owens et al., 1997). Selective 5-HT reuptake inhibitors are, to date, the most potent and selective prescription drugs available for inhibiting the action of SERT. The efficacy of SSRIs is rooted in intracellular messangers, such as cyclic adenosine monophosphate (cAMP). Administration of antidepressants up-regulates this pathway, including the expression of cAMP response element binding protein (CREB). CREB causes increased expression of brain-derived neurotrophic factor (BDNF), which has its expression lowered by stress,

causing decreased function and atrophy of hippocampal neurons. Increased expression of BDNF, through CREB is one mechanism of antidepressant activity, because it can help protect these neurons from further damage (Duman, 1998).

Transporters as Targets for Illicit Drugs

Whereas SERT has proven to be a valuable pharmacological target for the treatment of depression and certain other affective disorders, it is also the target of some illicit drugs which can be classified as psychostimulants. SERT, NET and DAT have been identified as targets for cocaine as well as amphetamine and some amphetamine derivatives. Cocaine and amphetamine remain two of the most abused drugs in present society. Widespread abuse of these substances carries grave physiological, psychological, and social consequences. Due to these problems, much research has focused on understanding how these two classes of abused drugs alter neurochemistry. Cocaine targets three major neurotransmitter systems in the brain: dopamine, serotonin, and norepinephrine (Eshleman et al., 1999;Uhl et al., 2002), in each case acting to inhibit the respective neurotransmitter transporter in a competitive manner (Ritz et al., 1987). Amphetamine and its neurotoxic derivatives are substrates for biogenic amine transporters, promoting non-vesicular release of neurotransmitter, with actions on dopaminergic, serotonergic, and noradrenergic systems (Amara and Sonders, 1998;Cozzi et al., 1999;Jones et al., 1999;Kantor et al., 1999;Reneman et al., 2002). Thus, these two structurally distinct drug classes both ultimately lead to increased neurotransmitter levels in the synapse.

Transporters as Targets for Cocaine

Cocaine, and related structural derivatives discussed in Chapter 3, are ligands for the monoamine neurotransmitter transporters. Cocaine acts as an antagonist, functioning to bind the transporter and inhibit the transport of the neurotransmitter substrate. Classically, cocaine had been thought to act primarily through the inhibition of DAT, subsequently increasing dopaminergic signaling, and leading to enhanced reward and addiction (Giros et al., 1994). This theory was revised, however, when Caron and coworkers (1998b;2002) generated a series of DAT knock-out mice. These mice still self-administered cocaine (Rocha et al., 1998a;Gainetdinov et al., 2002). Although the interaction of cocaine with SERT was well established, these behavioral data indicated that SERT might play a more critical role in the addiction process. SERT knock-out mice were also generated, and these animals showed enhanced reward properties from cocaine, indicating that SERT alone was not responsible for the self-administrative and reward schema. Only when DAT and SERT are knocked-out simultaneously do mice cease to show reward behavior after cocaine administration (Sora et al., 2001).

The interaction of cocaine with neurotransmitter transporters as its key mechanism of action has led researchers to search for a "cocaine antagonist," that is, a molecule that selectively inhibits the binding of cocaine to these transporters, but does not itself cause inhibition of neurotransmitter uptake (Howell and Wilcox, 2001;Sandhu et al., 2002). The specificity of such a drug would depend on the delineation of discrete binding or interaction sites on the transporters, specifically SERT and DAT. These sites, unfortunately, have not been completely delineated; however a great deal of functional

mutagenesis, using a comparative bioinformatics approach has been accomplished Several key residues in SERT, DAT and NET have been identified as critical for the interaction of cocaine with these transporters. The majority of the mutagenesis seeking a cocaine binding site has been focused on DAT, but due to their putative structural similarity, many of the mutations suggest residues in NET and SERT as candidates for interacting with cocaine and its derivatives.

Transporters as Targets for Amphetamines

Amphetamine (alpha-methylphenethylamine, 1-phenyl-2-aminopropane, phenylisopropylamine) and amphetamine derivatives have a unique mechanism of action involving neurotransmitter transporters. Depending on the chemical modifications on the molecule, these drugs may act as substrates for neurotransmitter transporters or more simply as antagonists. As substrates, amphetamines are transported into the intracellular space and can act as weak bases at synaptic vesicles, thus disrupting the pH gradient and causing the release of neurotransmitter into the synaptic terminal and subsequently into the synapse through "reverse transport" (Jones et al., 1998;Jones et al., 1999). The reverse transport process causes a striking increase of monoamines into the synapse. DAT and NET are thought to be the primary targets of the parental drug *d*-amphetamine, as the locomotor-activating and drug-reinforcing effects observed in animal models fit the profile for activity at these two sites (Jones et al., 1998;Jones et al., 1999;Wang et al., 1999;Gainetdinov et al., 2001;Gainetdinov et al., 2002). However, *d*-amphetamine does

have affinity for SERT, and many amphetamine derivatives have higher affinity for SERT as compared with the other two biogenic amine transporters.

The physiological changes brought about by amphetamine treatment have been the subject of recent research involving reuptake sites and specific neurotoxicity. Many researchers have shown evidence that exposure to amphetamine causes a redistribution of DAT from the cell surface to the cytoplasm in a time- and dose-dependent manner (redistribution evident after 10 minute treatment)(Kahlig et al., 2003;Loder and Melikian, 2003). The reduction in plasma-membrane bound transporters results in a decreased clearance capacity and subsequent increased synaptic DA levels.

The neurotoxic effects of amphetamine are typified by one derivative of the parental compound, methamphetamine, which has been found to have similar effects on dopaminergic neurons as *d*-amphetamine in monkeys and rats (Kogan et al., 1976;Seiden et al., 1976;Wagner et al., 1982;Ricaurte et al., 1984). These studies indicate that high doses of methamphetamine produce a consistent reduction in brain markers for dopaminergic nerve terminals. Furthermore, latter studies in rats indicated that treatment with methamphetamine also damages 5-HT containing neurons (Hotchkiss and Gibb, 1980).

Amphetamine has multiple sites of action primarily within dopaminergic neurons. Amphetamine interacts with DAT, as discussed above, to promote DA release through reverse transport. Amphetamine also has the ability to disrupt vesicular storage of DA and inhibit the activity of monoamine oxidase (MAO). Furthermore, amphetamine blocks the reuptake of released DA by antagonist actions at DAT. All of these mechanisms at these varied sites of action have the net effect of increasing intracellular as well as

synaptic dopamine levels (Kuczenski and Segal, 1994). The detection of amphetamine activity at SERT requires higher doses of the drug, and the effects appear to be transient. However, some substituted amphetamines, including 3,4-methylenedioxymeth-amphetamine (MDMA, "ecstasy") (Rudnick and Wall, 1992), fenfluramine (Berger et al., 1992) and *para*-chloroamphetamine (Huang et al., 1992) have been shown to potently affect the non-vesicular release of 5-HT. Thus, the modification of the core amphetamine structure allows for specificity for a particular transporter to be introduced.

The modification of the amphetamine core structure has been extensively studied (reviewed by Nichols, 1994). To summarize, structure-activity relationship analysis has yielded several key modifications of the core amphetamine structure that produce varying pharmacological effects. Briefly, it has been shown that *para*-substitution (halogen, methoxy) induces greater 5-HT release as compared to DA release. Also, *N*-substitution, particularly *N*-methyl substitution to yield methamphetamine ("Meth"), increases potency. Side-chain substitution of the α-methyl group decreases activity. The modification of the amphetamine molecule has produced a variety of compounds with strikingly distinct pharmacologies. Selections for serotonergic over dopaminergic neurons has been identified, as well as amphetamines that function to release 5-HT or simply block its reuptake. Also, some amphetamine derivatives are hallucinogenic (Reviewed by Nichols, 1994). The pharmacological mechanisms that these drugs affect are as distinct as the compounds themselves, with each having an underlying common thread in affecting neurotransmitter transporters.

In the published literature focused on amphetamine and its derivatives, two compounds based on amphetamine, MDA (3,4-methylenedioxamphetamine) and its N-

methyl derivative, MDMA, have been the subject of intense study since the beginning of their recreational use in the late 1960s and early 1970s. MDA has been identified as a dopaminergic toxin in rats, causing the persistent loss of markers for dopaminergic neuron function, including a loss of tyrosine hydroxylase activity and reduction in detected DA metabolites dihydroxyphenylacetic acid (DOPAC) and homovanillic acid (Kogan et al., 1976;Hotchkiss and Gibb, 1980). Sieden and coworkers also reported similar DA neurotoxicity in monkeys (Seiden et al., 1976). MDA also has toxic effects on serotonergic neurons as indicated by a loss of serotonergic markers in rats following sequential large doses of MDA (Hotchkiss and Gibb, 1980). MDMA is a very interesting compound in that it is the prototype for a new drug class called "entactogens" (Nichols, 1986). Compounds of this class, when used in a psychiatric setting, enabled patients to deal with deep and often painful emotional issues that they were previously unable to access or discuss. MDMA functions primarily as a releaser of 5-HT, however, it also functions to release DA, which is believed to be the underlying cause of serotonergic neurotoxicity according to one model (Sprague et al., 1998). In this model, MDMA-mediated release of 5-HT and DA causes depletion of intraneuronal 5-HT. The released 5-HT activates post-synaptic 5-$HT_{2A/2C}$ receptors located on GABA interneurons resulting in a decrease in GABA transmission and leading to enhanced DA release and synthesis. The additional DA released then may be transported into the depleted 5-HT terminal where it is metabolized by monoamine oxidase B (MAO-B). This metabolism causes reactive free-radical formation that subsequently damage serotonergic neurons (Sprague et al., 1998; reviewed in Green et al., 2003). This mechanism of 5-HT neurotoxicity has been examined through various methodologies, including the synthesis of related

compounds that lack the neurotoxic aspects of MDMA by maintaining great selectivity for SERT vs. DAT, including *p*-Methylthioamphetamine (Huang et al., 1992) as well as tetralin and indan analogs of MDMA (Nichols et al., 1990).

Because of the functional differences that can be derived from different substituent groups on the amphetamine core structure, it is evident that the recognition of these molecules by their targets occurs in a specific manner, leading to a specific effect. Even subtle changes in the structure of amphetamine lead to diverse mechanistic effects, and one of the facets of my studies involves the recognition of substituted-amphetamines by SERTs.

Summary

The structural diversity of molecules that interact with SERT is astounding, from its native substrate, 5-HT, to the amphetamines, cocaine and its analogs and the structurally diverse families of antidepressants. Due to SERT's ability to recognize such a large set of molecules, it is important to understand how these ligands interact with the transporter. Currently, there is a paucity of structural information available on transporters within this family. While significant mutagenesis studies have been undertaken, and some models for putative structure have been generated, the lack of a crystal structure has left a void in this area of research.

One powerful technique that is available for studying ligand-receptor (or transporter) interactions is Comparative Molecular Field Analysis, or CoMFA. This technique is useful when there is a lack of structural information for a protein, but large libraries of diverse compounds have been characterized as ligands. Such is the case for SERT. In brief, CoMFA is a technique that aligns similar molecules by their shared core structure and places this alignment into a virtual energy grid (consisting of +1 charge, sp^3 carbon molecules at the grid intersections). Binding or inhibition data are then input for each compound in the alignment. Using parameters for electrostatic and steric (hydrophobic) interactions, a graphic is generated using colored fields to designate regions of the molecule where steric bulk is favored or disfavored and where positive or negative electrostatic interactions are favorable. This technique provides a method visualize how a number of compounds interact with the transporter, and based on those

interactions, insight into what amino acid residues within the protein may be candidates for providing high-affinity interactions with characteristics of the molecule that produce favorable binding energy. This technique, coupled with rational mutagenesis can provide insight into points of transporter-ligand interaction, and perhaps direct the synthesis of more potent transporter ligands.

CoMFA methods have been used previously to study HIV-1 integrase inhibitors (Kuo et al., 2004), A3 adenosine receptor antagonists (Li et al., 1999), D1 and D2 dopamine receptor ligands (Wilcox et al., 1998), HERG channel blockers (Cavalli et al., 2002), as well as dopamine transport inhibitors (Carroll et al., 1994;Newman et al., 1999). Thus, the proof-of-concept for this methodology is well-established, and the application of this powerful computation tool to SERT ligand recognition studies should provide valuable insight about the function of this transport protein.

Scope of the Work

The overall goal of my studies is to gain insight into the recognition of ligands by the serotonin transporter at a molecular level. Briefly, my goal is to test the hypothesis that observed species differences in SERT pharmacology can be attributed to specific transmembrane domain regions and individual amino acids. Overall, my two specific aims are:

1) To investigate the differences in antidepressant interaction with SERT species variants. The specific questions that will be addressed are:
   A. Can determinants, in terms of TMD regions or specific residues, of antidepressant interaction with species variants of SERT be revealed using CoMFA modeling techniques?
   B. Following CoMFA analysis, can chimeric SERT constructs and point mutations provide information about specific points of SERT-antidepressant interaction or recognition?
2) To investigate the differences in psychostimulant interaction with SERT species variants. The specific questions that will be addressed are:

A. Do human and *Drosophila* SERT species variants exhibit different recognition patterns for substituted-amphetamines and cocaine derivatives?

B. Can differences in psychostimulant recognition be modeled using CoMFA techniques and tracked to discrete transmembrane domains and residues through the construction and use of cross-species chimeras and point mutants?

CHAPTER II

INTERACTIONS OF ANTIDEPRESSANTS WITH THE SEROTONIN TRANSPORTER: A CONTEMPORARY MOLECULAR ANALYSIS

(Results published in *The European Journal of Pharmacology*, October 2003, vol. 479, issue 1-3. p. 53-63)

Introduction

As reviewed in Chapter 1, SSRIs have marked selectivity for the inhibition of the function of SERT as opposed to the other biogenic amine neurotransmitter transporters. Interestingly, SSRIs also show selectivity for species variants of SERT. The human and other cloned species variants of SERTs exhibit markedly different sensitivities to antidepressants, as well as to other drug classes that inhibit the reuptake of serotonin (Barker et al., 1994;Demchyshyn et al., 1994;Barker et al., 1998;Adkins et al., 2001a;Rodriguez et al., 2003). These species-specific properties have been exploited in molecular studies seeking to identify domains of SERT possessing determinants for antidepressant recognition (Barker and Blakely, 1996;Barker et al., 1998).

In this section of my thesis, I will examine the structure-activity relationships of antidepressants (Figure 2.1) for inhibiting the uptake of serotonin in rat brain synaptosome preparations and cloned rat SERT (rSERT). The use of molecular modeling

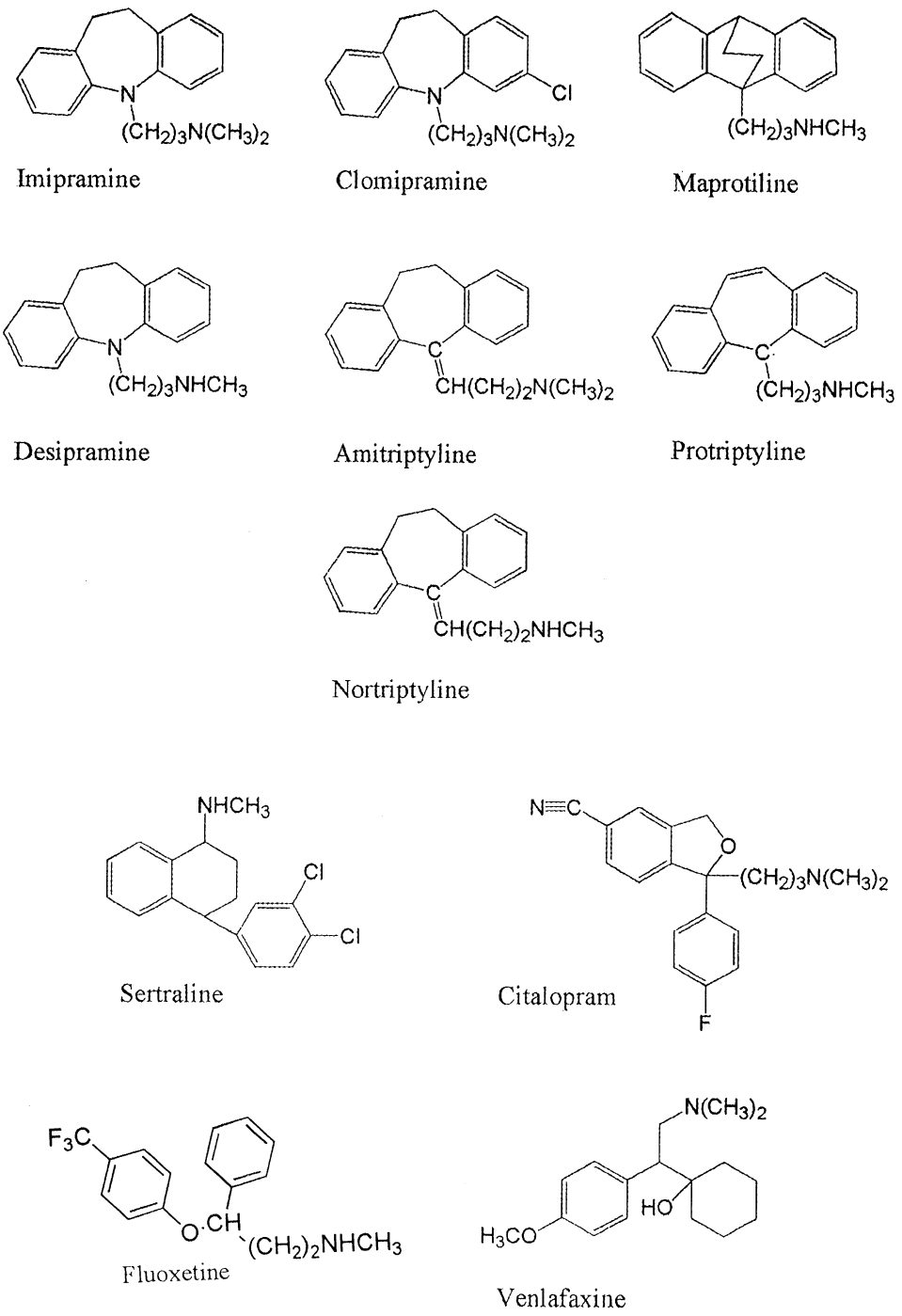

Figure 2.1. Structures of the antidepressants used in this study. Tricyclic antidepressants include imipramine, clomipramine, maprotiline, desipramine, amitriptyline, protriptyline, and nortriptyline. Selective serotonin reuptake inhibitors include sertraline, citalopram, and fluoxetine, whereas venlafaxine has activity at both SERT and NET.

and Comparative Molecular Field Analysis (CoMFA) provides insight into the structural features of these drugs that contribute to the specificity and potency for their respective targets. In particular, the role of the common amine group and free aromatic substituents will be a focus of this analysis. In addition to an exploration of antidepressant structure-activity relationships, I investigated potential mechanisms for the recognition of antidepressants by SERT at the molecular level. hSERT and *Drosophila* SERT (dSERT) were used to compare species variant sensitivity to a subset of antidepressants. These studies, coupled with experiments using a chimeric human/*Drosophila* SERT provide insight into the location of putative sites of interaction for antidepressants with the transporter.

Methods

Construction of the $H^{1-281}D^{282-476}H^{477-638}$chimera

This chimera was generated as previously described (Rodriguez et al., 2003). Briefly, it is a full-length 638 amino acid transporter constructed from amino acids 1-281 and 477-638 with identity from hSERT and residues 282-476 with identity from dSERT. The resulting chimera was cloned into pcDNA3.1(+) (Invitrogen, Carlsbad, CA) and stably transfected into HEK-293 (Human Embryonic Kidney) cells using Lipofectamine 2000 (Invitrogen, Carlsbad, CA) as per manufacturer's protocol.

Construction of S375A and P418S hSERT point mutants

The hSERT mutants S375A and P418S were generated using the Quikchange® mutagenesis kit (Stratagene, La Jolla, CA) as per manufacturer's provided protocols. The oligonucleotides used for the mutations are as follows:

S375A – Sense: 5'-GGTGAACTGCATGACAAGCTTCGTTGCGGGATTTGTC-3'

S375A – Antisense: 5'-GACAAATCCCGCAACGAAGCTTGTCATGCAGTTCACC-3'

P418S – Sense: 5'-GCGATAGCCAACATGTCAGCGTCAACTTTCTTTGCC-3'

P418S – Antisense: 5'-GGCAAAGAAAGTTGACGCTGACATGTTGGCTATCGC-3'

Bacterial colonies screened to be positive for the mutation were sequenced and subcloned into pBluescript vector before being maxiprepped (Qiagen, Valencia, CA) and used in uptake experiments.

[^{3}H]5-HT uptake assays in HEK-293 cells stably expressing SERTs

HEK-293 cells stably expressing either hSERT or dSERT were generous gifts from Dr. Randy D. Blakely, Vanderbilt University. All cells were maintained in Dulbecco's modified Eagle's medium with 10% dialyzed fetal bovine serum supplemented with 2 mM glutamine, 1% penicillin/streptomycin (10,000 U/ml), and 600 mg/l geneticin (G-418 sulfate) in a humidified 5% CO_2 incubator at 37°C.

Uptake assays were performed on cell suspensions in 96-well microtube racks. Confluent cells in 150 mm tissue culture dishes were washed with phosphate buffered saline (PBS), scraped, and resuspended in Krebs-Ringer-HEPES (KRH) buffer supplemented with D-glucose (120 mM NaCl, 4.7 mM KCl, 2.2 mM $CaCl_2$, 10 mM HEPES, 1.2 mM KH_2PO_4, 1.2 mM $MgSO_4$, 1.8 g/l D-glucose, pH 7.4). Total protein concentration was determined using the Bradford assay (Bradford, 1976). Cell suspensions were diluted in KRH to yield a concentration of 0.25 mg/ml total protein. 400 µl (100 µg) of the cell suspension was added to each tube in a 96-well microtube rack. Drugs were diluted serially in KRH buffer, and 50 µl aliquots of increasing concentrations of drug were added to triplicate microtubes. Cells were preincubated with drug at 37°C for 10 min. [^{3}H]5-HT (~110 Ci/mmol) was diluted to yield a final assay concentration of 20 nM in KRH buffer supplemented with 100 µM L-ascorbic acid and 100 µM pargyline. 50 µl of the [^{3}H]5-HT solution was added to each microtube, and uptake was allowed to proceed at 37°C for 10 min. Transport was terminated via vacuum filtration onto 96-well GF/B filter plates (presoaked with 0.3% polyethyleneimine) using

a Packard Filtermate 96-well harvester (Meriden, CT). Nonspecific uptake was determined using 10 μM cocaine. The filter plates were dried at ambient temperature overnight. The next day, scintillation cocktail (Microscint O, Packard Instrument, Meriden, CT) was added prior to counting in a Packard TopCount NXT (Meriden, CT) to determine accumulated [^{3}H]5-HT. IC_{50} values were determined using the nonlinear regression routine in GraphPad Prism v.3.0 (GraphPad Software, Inc. San Diego, CA), and K_i values were calculated using the Cheng-Prusoff equation (Cheng and Prusoff, 1973). Experiments were performed in triplicate and repeated in at least three separate assays.

[^{3}H]5-HT uptake assays in HeLa cells transiently expressing hSERT point mutants

HeLa cells were transfected using the vaccinia virus T7 (VVT7) method as previously described (Fuerst et al., 1986;Blakely et al., 1991b;Barker et al., 1994). Briefly, HeLa cells were plated at a density of 10^5 cells per well in 24-well tissue culture plates 18 hours prior to transfection. At the time of transfection, cells were washed with PBS, and then VVT7 (10 pfu/cell) diluted in 100 μl OptiMEM®/ 0.1% β-mercaptoethanol was added to each well. Infection proceeded for 30 min at 37°C. Then, 300 ng of hSERT, dSERT, S375A, or P418S pBluescript cDNA (premixed with Lipofectin transfection reagent as per manufacturer's protocol) was added to each well. Transfection with the vector pBluescript was used to define nonspecific uptake. Transfected cells were assayed 6-8 hours post-transfection.

At the time of assay, transfection media was aspirated and cells were washed with 0.5 ml KRH buffer supplemented with 1.8 g/l D-glucose (KRH/glucose). 400 µl of KRH/glucose was then added to each well. 50 µl of inhibitor (or buffer to determine total or nonspecific uptake) was then added to each well and cells were incubated for 10 min in a 37°C incubator. [^{3}H]5-HT (~110 Ci/mmol) was diluted to yield a final assay concentration of 20 nM in KRH buffer supplemented with 100 µM L-ascorbic acid and 100 µM pargyline. 50 µl of the [^{3}H]5-HT solution was added to each well, and uptake was allowed to proceed at 37°C for 10 min. Following incubation, cells were washed three times with ice-cold KRH to terminate uptake. Scintillation cocktail was added (Microscint 20, Packard Instrument, Meriden, CT), plates were shaken overnight, and accumulated tritium was determined using a Packard Topcount NXT.

Molecular modeling and CoMFA analysis of antidepressant interactions with SERT

Computational molecular modeling studies were performed using the SYBYL v.6.8 software package (Tripos Inc, St. Louis, MO) on a Silicon Graphics O2 workstation (Mountain View, CA) running IRIX v.6.5. The antidepressant analogs were modeled using library fragments in SYBYL. Atom types were automatically assigned by SYBYL and then manually checked. The compounds were subjected to a grid search (0-360 degrees, 10-degree increments) to find the lowest energy conformation for all rotatable bonds where the possibility of unfavorable torsions existed. Compounds in this conformation were then minimized using the conjugate gradient minimization method

with no initial simplex minimization, a gradient value of 0.05, and 10,000 maximum iterations. Each set of compounds was aligned, compiled into a molecular spreadsheet, and pK_i values inserted as explicit data. CoMFA data were generated using the Tripos Standard CoMFA field class with distance dielectric, no smoothing, and a steric and electrostatic cutoff of 30.0 kcal/mol. Cross-validated partial least squares (PLS) analysis was validated using the leave-one-out option. The number of optimal components was determined and a CoMFA map generated.

CoMFA analysis of imipramine analogs assayed using rat brain synaptosomes

Data for this analysis were taken from a previously published report by Horn and Trace (Horn and Trace, 1974). For this analysis, twelve compounds based on the core structure of imipramine were modeled in SYBYL using library fragments and minimized as indicated above. The molecules were aligned using their minimized structures and the common tricyclic fused ring substructure. Following alignment and subsequent PLS analysis, three components were found to be suitable, with a q^2=0.530.

CoMFA analyses of antidepressants assayed using heterologously expressed rat SERT

Data for these analyses were taken from a previously published report by Barker and coworkers (Barker et al., 1994). For the first analysis, seven compounds (imipramine, clomipramine, desipramine, amitriptyline, protriptyline, nortriptyline, and maprotiline) based on the core structure of imipramine were modeled in SYBYL using library fragments and minimized as indicated above. The molecules were aligned using their minimized structures, the two flanking aromatic rings of the fused system, and the amine of the alkylamine side chain. Following alignment and PLS analysis, two components were utilized, with a q^2=0.388. For the second analysis, eleven antidepressants (imipramine, clomipramine, desipramine, amitriptyline, protriptyline, nortriptyline, paroxetine, citalopram, maprotiline, fluoxetine, and sertraline) with much more diverse structures were modeled in SYBYL using library fragments and minimized as indicated above. The molecules were aligned using their minimized structures and the two flanking aromatic rings of the fused system. For those compounds in the set lacking the fused ring system, the equivalent positions (either aromatic or cyclohexyl) were locked in a distance constraint to match the rest of the compound set as closely as possible, while still maintaining their local energy minima. Following alignment and PLS analysis, three components were utilized, with a q^2=0.551.

CoMFA analysis of fluoxetine and related compounds assayed using rat brain synaptosome preparations

Data for this analysis were taken from a previously published report by Robertson and coworkers (Robertson et al., 1988). For this analysis, ten compounds based on the core structure of fluoxetine were modeled using SYBYL library fragments and minimized. Molecules were aligned using the amine functional group and the distal (phenoxy) aromatic ring on fluoxetine. Following alignment and PLS analysis, three components were determined to be optimal, with a q^2=0.597.

Materials

Dulbecco's modified Eagle's medium, pargyline, citalopram, and L-ascorbic acid were purchased from Sigma (St. Louis, MO). Dialyzed fetal bovine serum was purchased from Hyclone (Logan, UT). Trypsin, L-glutamine, penicillin/streptomycin, and geneticin were from Life Technologies (Grand Island, NY). Bradford Protein Assay Dye Concentrate was from Bio-Rad Laboratories (Hercules, CA). Cell culture flasks and 150 mm dishes were from Falcon/B-D Labware (Mountain View, CA). 96-well microtube racks and tubes were purchased from Marsh Bio Products (Rochester, NY). [^{3}H]5-HT trifluoroacetate (~110 Ci/mmol) was purchased from Amersham Biosciences (Piscataway, NJ). Cocaine was purchased from Research Biochemical International (Natick, MA). Venlafaxine HCl was a gift from Wyeth (Monmouth Junction, NJ), and sertraline was a gift from Pfizer, Inc. (Groton, CT). All other chemicals were purchased from Sigma Chemical Co. (St. Louis, MO) or Fisher Scientific (Pittsburg, PA) and were of the highest grade available. Integrated DNA Technologies (Coralville, IA) synthesized the mutagenic oligonucleotides, and dye-termination sequencing was performed by the University of Michigan Medical Center core facility (Ann Arbor, MI).

Results and Discussion

Three dimensional quantitative structure-activity relationships of tricyclic imipramine derivatives at rat brain synaptosomes

Studies conducted by Horn and Trace in the 1970's led to much of what is now known about the structural features of drugs that act to inhibit 5-HT uptake (Horn, 1973;Horn et al., 1973;Horn and Trace, 1974). I have performed a contemporary re-analysis of this early structure-activity relationship data. Due to observed species differences in the way SERTs recognize many of these drugs, I have focused my comparisons based on rSERT data, from early work in synaptosomes to more recent studies using cloned rSERT in a heterologous expression system. Using the data of Horn and Trace (Horn and Trace, 1974), the K_i values for twelve tricyclic antidepressants were used to generate a Comparative Molecular Field Analysis (CoMFA). The CoMFA map provides a powerful, graphical model of determinants of high-affinity interactions of drugs with SERT. In the absence of any definitive structural information for SERT, one of the few methods in which to examine quantitatively ligand-binding properties is CoMFA. CoMFA analyses are performed *in silico* using Silicon Graphics workstations (Mountain View, CA) and the SYBYL software package (Tripos Inc., St. Louis, MO). In the analysis, compounds with a similar substructure, such as the fused tricyclic rings of the imipramine derivatives, are sketched and their minimum energy conformations determined. Once the compounds in the training set are compiled into a database, the group is stacked or aligned on top of each other in a virtual energy grid. The aligned

molecules are then tabulated with their respective K_i values, and the CoMFA subroutine is executed. The CoMFA program maps regions of favorable and unfavorable electrostatic and steric interactions as colored geometric fields onto the energy grid to which the molecules have been aligned. Through thorough inspection, it is possible to analyze each atom's position in a drug molecule, and determine if that position plays a role in dictating higher or lower affinity based upon the steric and electrostatic properties of substitutions at that position. Thus, if given a large enough set of compounds with a similar core structure, one can predict how subtle changes in the molecule's structure will affect affinity.

In these original studies, rat brain synaptosomes were prepared and subsequently treated with inhibitors in the presence of radiolabeled 5-HT (Horn and Trace, 1974). These data were tabulated and published with an analysis of the structural features that provided higher or lower affinity for inhibiting the transport process. The CoMFA map (Fig. 2.2A) for tricyclic antidepressants inhibiting the uptake of 5-HT into synaptosomes (Horn and Trace, 1974) provides a graphical representation of how these compounds may be interacting with SERT. Several distinct regions on the map provide information about molecular features favored for higher affinity interactions. The green region of the figure shows an area of the molecule where steric bulk is somewhat favored for higher potency. Imipramine, the parent compound, exhibits a K_i value of approximately 285 nM, whereas 3-chloroimipramine, which places a chlorine substitution in the 3- position (as indicated in Fig. 2.2A), exhibits a K_i value of 56 nM. The blue region located near the alkylamine chain indicates that hydrogen bond donors and slight positive charge are accepted at this position, but there is a steric limitation, as shown in yellow. This yellow area correlates to

Figure 2.2. Comparative Molecular Field Analysis (CoMFA) maps of antidepressants modeled using data obtained from rat brain synaptosomes (A) and cloned rSERT (B and C). Imipramine is modeled within each field for directional orientation. Panel A depicts the CoMFA map generated with the data from twelve imipramine derivatives assayed at rat brain synaptosomes as reported by Horn and Trace (Horn and Trace, 1974). Panel B depicts the CoMFA map generated with the data from seven tricyclic antidepressants (imipramine, clomipramine, desipramine, amitriptyline, protriptyline, nortriptyline, and maprotiline) assayed at heterologously expressed rSERT as reported by Barker and coworkers (Barker, et al., 1994). Panel C depicts the CoMFA map generated with a larger group of compounds from the report by Barker and coworkers (Barker, et al., 1994), including the following eleven compounds: imipramine, clomipramine, desipramine, amitriptyline, protriptyline, nortriptyline, paroxetine, citalopram, maprotiline, fluoxetine, and sertraline. Panel C compounds include selective serotonin reuptake inhibitors (SSRIs) and as in panel B, the drugs were assayed at cloned rSERT in a heterologous expression system. Colored fields represent characteristics of the ligand that favorably or unfavorably affect high-affinity interactions. Green fields indicate molecular regions where steric bulk is favored for high-affinity binding, whereas regions indicated by yellow are areas in which steric bulk is disfavored for high-affinity interactions. Blue fields indicate regions of the molecule where more positive charge and hydrogen bond donors are favored, or negative charge and hydrogen bond acceptors are disfavored for high-affinity interactions. Red fields indicate regions where negatively charged substitutents and hydrogen bond acceptors are favored, or positive charge and hydrogen bond donors are disfavored.

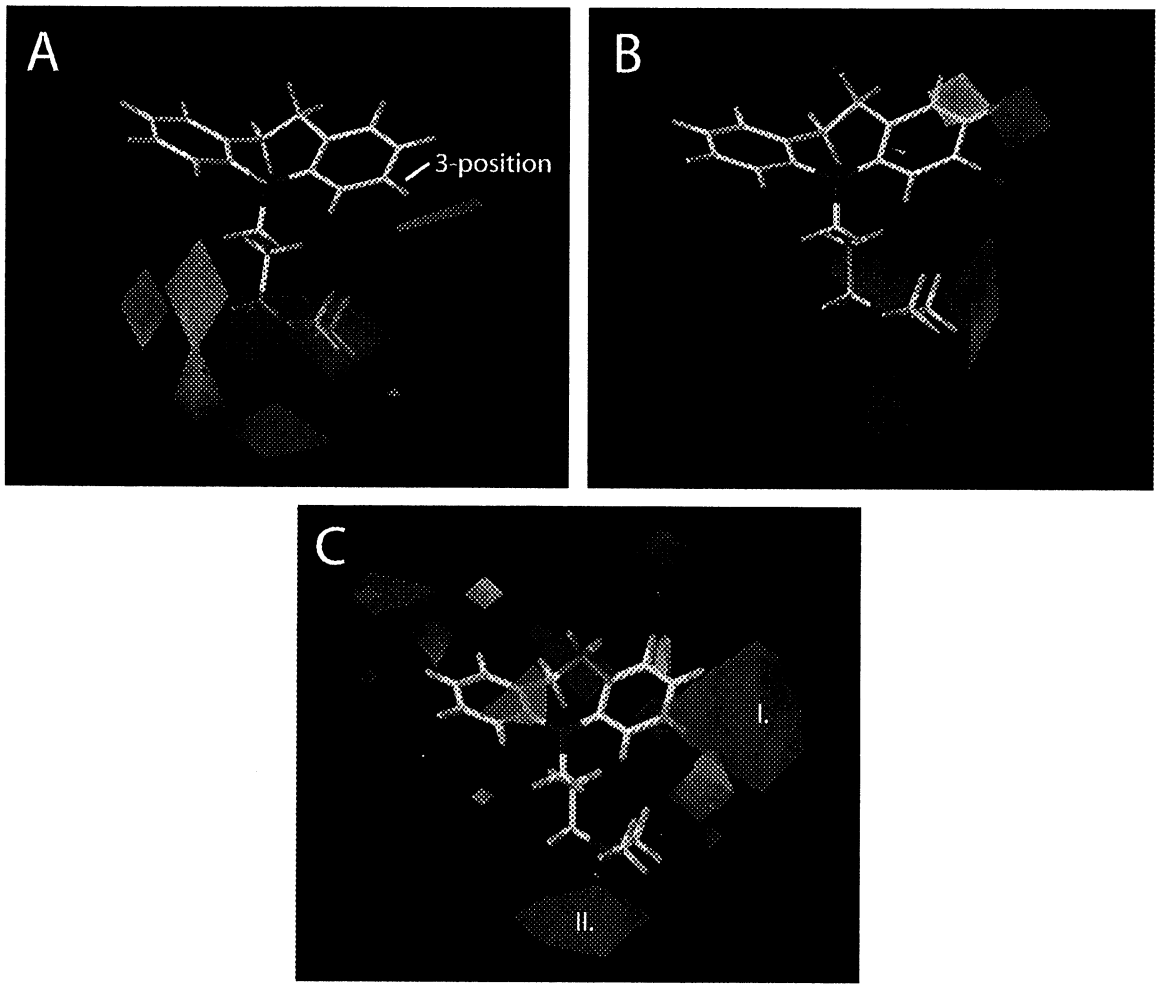

Figure 2.2

Horn and Trace's observation that α- or β- substitution on the side chain reduced potency (Horn and Trace, 1974). The red regions indicate areas where negative charge and hydrogen bond acceptors are favored, or positive charge and hydrogen bond donors are disfavored. The character of the amine, as either secondary or tertiary, affects the favorability of the drug's interaction with SERT. The secondary amine, as a hydrogen bond donor, is less favored as compared to the tertiary amine, yielding the red fields. The dual red regions indicate the location of the substitutions on the amine. Since the amine is tethered to the fused tricyclic system through the variable length carbon chain, the relative locations of the red field on the map vary as a function of the chain length, hence, two red fields are observed. As observed in the original publication, the potency of this group of compounds is greatly and adversely affected by varying the carbon chain length that, in turn, alters the position of the amine (Horn and Trace, 1974). For instance, imipramine, a three-carbon chain length species, exhibits a K_i value approximately 10-fold lower than either the two- or four-carbon chain length derivative (285 nM vs. 2450 nM and 1980 nM, respectively). Changing the length of the chain alters the distance between the fused ring system and the amine, and this distance change results in the dual red fields toward the bottom of the CoMFA map.

Three dimensional quantitative structure activity relationships of tricyclic antidepressants at the cloned rSERT

Since the cloning of several SERT species variants in the 1990's (Blakely et al., 1991a;Hoffman et al., 1991;Ramamoorthy et al., 1993;Corey et al., 1994;Demchyshyn et

al., 1994;Padbury et al., 1997) more refined studies have been undertaken in order to understand SERT function, and more specifically, how ligands interact with SERT. My next analysis was based upon data from a study by Barker and coworkers (Barker et al., 1994), focused on differences between SERT species variants in recognizing antidepressants and other ligands. An initial CoMFA map (Fig. 2.2B) was generated using a small subset of K_i values for tricyclic antidepressants at the cloned rSERT (Barker et al., 1994). Whereas the small set of seven compounds (imipramine, clomipramine, desipramine, amitriptyline, protriptyline, nortriptyline, and maprotiline) does not provide for an exhaustive CoMFA analysis, it does provide an opportunity to compare directly the data from rat synaptosomes (Fig. 2.2A) with similar compounds at the cloned rSERT. The CoMFA map generated from the data reported by Barker and coworkers (Fig. 2.2B) (Barker et al., 1994) showed remarkable similarity to the map constructed from the rat brain synaptosome data reported by Horn and Trace (1974). Specifically, the two red fields near the bottom of the map in Fig. 2.2B, indicating where negative charge and hydrogen bond acceptors are favored, match closely to the two red fields in Fig. 2.2A (note that the bottom blue field in Fig. 2.2B overlaps, to a large extent, a red field at approximately the same position). In addition, the blue region near the side chain amine correlates between the two maps, again indicating parallels between the rat synaptosome and cloned rSERT data. The minimal green field in the cloned rSERT data (Fig. 2.2B) correlates to the larger green field surrounding the 3-position of the aromatic ring from the synaptosome data (Fig. 2.2A), indicating the favorability of steric bulk at this position. One notable feature that appears in the CoMFA map for the cloned rSERT data (Fig. 2.2B), but is absent in the rat synaptosome data (Fig. 2.2A), is the presence of a

red field near the 3- and 4-position of the aromatic ring. This red field indicates that negative charge (such as from the chlorine substitution on clomipramine) is favorable for higher affinity recognition of the drug by SERT.

A CoMFA map (Fig. 2.2C) was generated using cloned rSERT K_i values for the following compounds: imipramine, clomipramine, desipramine, amitriptyline, protriptyline, nortriptyline, paroxetine, citalopram, maprotiline, fluoxetine, and sertraline. I fully recognize that these compounds are not true derivatives of one another, nor do they align in a perfect fashion when performing molecular modeling. However, for the purpose of understanding how antidepressants may be interacting with SERT globally, CoMFA methods can provide us with important structural information about how SERT may recognize these drugs. Due to the variability in structure and the imperfect alignment, the CoMFA map in Fig. 2.2C contains outlying points of color indicating smaller contributions by one, or a small subset, of the molecules assayed. These regions may provide some insight into how an individual molecule is recognized, but I will focus on the regions providing the major contributions to high-affinity interactions with rSERT, as these should provide evidence for the most crucial determinants of recognition.

The two red regions on the CoMFA map have been labeled "I" and "II" for clarity. Both of these regions are areas where negative charge and hydrogen bond acceptors are favored, or positive charge and hydrogen bond donors are disfavored. Red region I is focused around the 3- and 4-position of the aromatic ring. This area of favorable negative charge is again demonstrated by comparing the potency of imipramine with clomipramine (3-chloroimipramine) where the K_i values are 46 nM and 3.9 nM, respectively. The addition of the electronegative chlorine promotes high-affinity

interaction with SERT. Also, directly below this red region is a small green area homologous to the green field observed in Fig. 2.2A surrounding the 3-position of the aromatic ring suggesting steric bulk is favorable for high-affinity interaction. The red region II, indicates negative charge and hydrogen bond acceptors are favored. This result could indicate that the side chain amine provides higher affinity interaction when it is in a state to accept a hydrogen bond. In contrast to the CoMFA map of imipramine analogs alone (Fig. 2.2A), these latter data do not include compounds with variable length side chains or side chain substitutions (Fig. 2.2C), and this fact provides explanation for the lack of yellow sterically unfavorable areas around the alkylamine side chain.

Overall, this analysis has shown that some of the seminal data for SERT and antidepressant structure-activity relationships developed in rat brain synaptosomes correlate closely with later studies utilizing the cloned rSERT. In consideration of the species differences observed in SERT species variants, I also performed a CoMFA analysis using the same compounds used to generate Fig. 2.2C and data from the hSERT (Barker et al., 1994). Interestingly, the CoMFA maps for the hSERT and rSERT data appeared to be almost identical (data not shown). The similarity of the CoMFA maps is not surprising, because, although the absolute potencies of the compounds vary between hSERT and rSERT, the rank order of potency for the compounds does not change.

Evaluation of fluoxetine derivatives at rat brain synaptosomes

Many commercial successes in the development of drugs to treat depression came with the marketing of the selective serotonin reuptake inhibitors. Released in 1987, Prozac® (fluoxetine) became the most prescribed drug in the United States market in only two years (Stokes and Holtz, 1997). The development of fluoxetine by researchers at Eli Lilly research laboratories followed the development of another SSRI by Astra, which was removed from the market for liver toxicity exhibited in patients. Therefore, fluoxetine became the prototype for the safe, selective serotonin reuptake inhibitor class of antidepressants (Wong et al., 1974;Wong et al., 1975;Robertson et al., 1988).

My next analysis used data from a previously published report by Robertson and coworkers (Robertson et al., 1988). This report focused on the structure of fluoxetine and the *in vitro* inhibition of serotonin uptake in crude rat brain synaptosomes. I used these data and developed a contemporary re-analysis using modern computational methods. The CoMFA analyses (Fig. 2.3A and 2.3B) are presented to give an overall picture of the features of selective serotonin reuptake inhibitors that make them both very potent and very specific for SERTs. Fig. 2.3A is a CoMFA map with the molecule fluoxetine displayed for orientation. Fig. 2.3B depicts the same CoMFA fields, but instead displays nisoxetine, a norepinephrine reuptake inhibitor, which is based on the fluoxetine core structure. A prominent blue field, indicating a region where positive charge and hydrogen bond donors are favored, is common to both CoMFA maps (Fig. 2.3A and 2.3B). The blue region is localized to the amine on the selective serotonin reuptake inhibitors, indicating that this molecular feature is vital for high-affinity recognition by SERT. The

Figure 2.3. Comparative Molecular Field Analysis (CoMFA) of selective serotonin reuptake inhibitors (SSRIs) modeled using data generated at rat brain synaptosomes by Robertson and coworkers (Roberston et al., 1988). Fluoxetine is depicted in panel A and nisoxetine in panel B, for orientation of the map. For each panel, colored fields represent characteristics of the ligand that favorably or unfavorably affect high-affinity interactions. Steric contours are shown in green and yellow, whereas electrostatic contours are shown in blue and red. Green fields indicate molecular regions where steric bulk is favored for high-affinity binding, whereas regions indicated by yellow are areas in which steric bulk is disfavored for high-affinity interactions. Blue fields indicate regions of the molecule where more positive charge and hydrogen bond donors are favored, and negative charge and hydrogen bond acceptors are disfavored for high-affinity interactions. Red fields indicate regions where negatively charged substitutents and hydrogen bond acceptors are favored, or positive charge and hydrogen bond donors are disfavored.

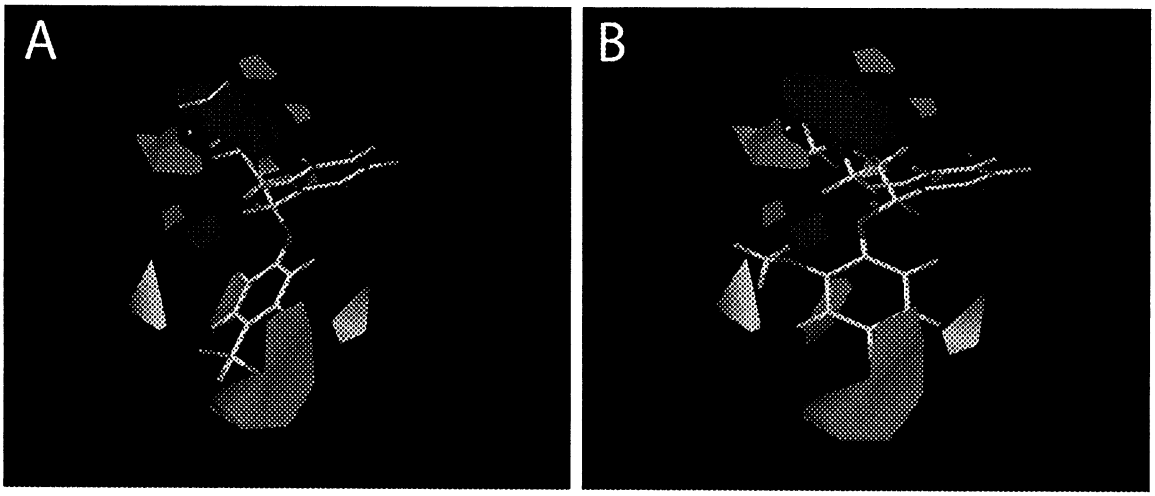

Figure 2.3

most striking components on the two maps are the green and yellow regions that flank the aromatic ring towards the bottom of the figure. The green fields indicate regions where steric bulk is favorable for high-affinity interaction with SERT, and yellow fields indicate regions where steric bulk is disfavored. When modeled with fluoxetine (Fig. 2.3A), the aromatic ring lies in the same plane as the green regions, indicating favorable interactions. However, when nisoxetine's interactions with SERT were modeled (Fig. 2.3B), the plane of the aromatic ring lies within the yellow regions, indicating the unfavorability of this geometry. The presence of the methyl ether on the aromatic ring of nisoxetine (and tomoxetine as described below) effectively causes the aromatic ring to rotate into a less favorable conformation (demonstrated by K_i values of 70 nM vs. 2000 nM, respectively). Interestingly, when examining norepinephrine transport inhibition, the potencies are virtually reversed (10 nM at NET vs. >10,000 nM at SERT), indicating a mechanism for specificity of serotonin transporters for fluoxetine and norepinephrine transporters for nisoxetine based upon the orientation of the aromatic ring. However, other minimizations of this molecule do not show a such a drastic shift in the aromatic ring orientation, indicating that the minimized structure in Figure 5.3 may represent a local, rather than global, minima (D.E. Nichols, personal communication). The orientation of the aromatic ring has also been examined in a previous three dimensional quantitative structure activity relationships study by Wellsow and coworkers (Wellsow et al., 2002), and my model correlates closely with respect to the regions of favored and disfavored steric bulk surrounding the aromatic ring.

Another compound that induces this conformational change in the highly favored fluoxetine geometry to a lower affinity geometry is tomoxetine, which places a methyl

substituent in the same position as the methyl ether on nisoxetine. Again, the geometry of the aromatic ring is shifted from the favored plane to the disfavored plane (with respect to SERT potency). The K_i values for tomoxetine at SERT and NET are 1500 nM and 4 nM, respectively. These subtle changes in the substitutions on the aromatic ring of fluoxetine induce dramatic changes in pharmacology. Both the potency of the compound, as well as the biogenic amine neurotransmitter transporter specificity, switch in an almost orthogonal manner in accordance with the orientation of the free aromatic ring. The strong dependence on the conformation of the aromatic ring for potent interactions with SERT leads to the question, what regions or discrete amino acid on SERT interact with this aromatic ring? For example, some features that might be identified include aromatic amino acids on SERT that can provide favorable pi-pi stacking interactions with the aromatic ring of the antidepressants. A more detailed discussion of potential molecular determinants of antidepressant recognition by SERT will be discussed below.

Regions of SERT containing determinants of antidepressant recognition

Previous studies by the Barker laboratory identified transmembrane domains V-IX as being important for both substrate (Rodriguez et al., 2003) and psychostimulant (Roman et al., 2004) recognition. The key to these studies was the construction of a chimeric SERT that contained amino acids 1-281 and 477-638 of hSERT identity and amino acids 282-476 of dSERT identity (Fig. 2.4A). To investigate potential domains of SERT involved with antidepressant recognition, I performed a series of [^{3}H]5-HT uptake inhibition experiments using this chimera and a set of antidepressants. As discussed

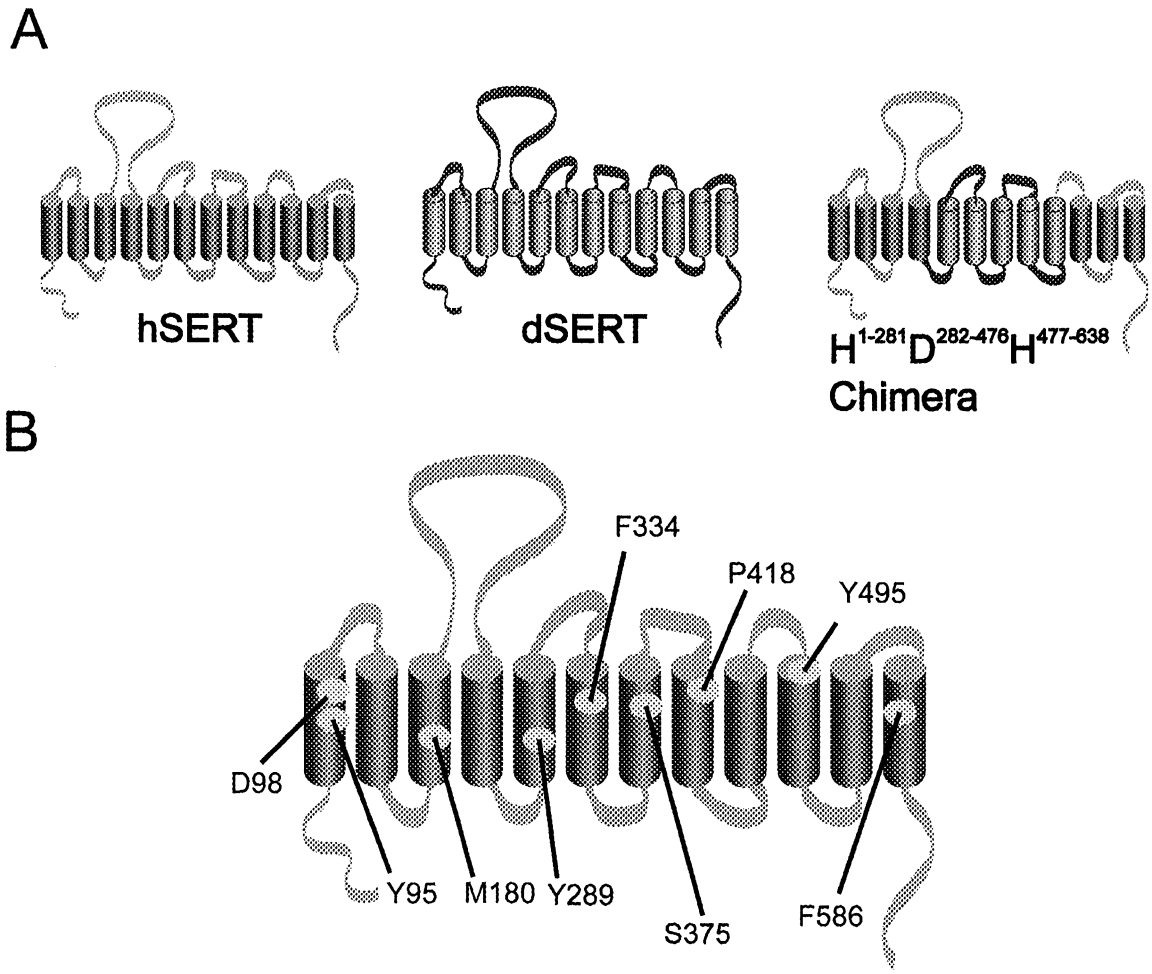

Figure 2.4. (A) Diagram of wild-type hSERT, dSERT, and the $H^{1-281}D^{282-476}H^{477-638}$ chimeric transporter. The chimeric transporter was constructed as described in Materials and Methods, with hSERT sequence indicated in blue and dSERT sequence indicated in red. (B) Representative model of SERT with amino acids implicated as sites of interaction with antidepressants (Barker and Blakely, 1996;Barker et al., 1998;Fang et al., 1998;Barker et al., 1999;Danek Burgess and Justice, Jr., 1999;Mortensen et al., 2001;Paczkowski and Bryan-Lluka, 2001;Roubert et al., 2001;Paczkowski and Bryan-Lluka, 2002).

earlier, the antidepressants have been shown to have species selectivity (Barker et al., 1994;Demchyshyn et al., 1994;Barker et al., 1998), and my experiments confirmed this phenomenon (Table 2.1). Consistent with previous results, each antidepressant was approximately 100-fold less potent at dSERT as compared to hSERT. A critical examination of the chimeric SERT data revealed a shift in potency for each antidepressant towards dSERT-like potency, but in many cases this shift was attenuated. For example, the most potent compound at hSERT, sertraline, exhibited a K_i value of 3.6 nM at hSERT, 390 nM at dSERT, and 150 nM at the $H^{1-281}D^{282-476}H^{477-638}$ chimera. Similar comparisons can be drawn for each of the other compounds except for desipramine and venlafaxine. These two compounds are relatively non-potent at dSERT and the $H^{1-281}D^{282-476}H^{477-638}$ chimera, while having modest potency at hSERT. These experiments suggest that some determinants for the interaction of antidepressants with SERTs exist within transmembrane domains V-IX. The decreased potency of each compound when transmembrane domains V-IX are switched to dSERT character in a parental hSERT construct indicate the location of some points of interaction likely to be within this region. However, the shift in potency is not a complete shift toward dSERT-like pharmacology. This finding indicates that regions or amino acids outside of the central transmembrane domain V-IX region most likely also play a significant role in recognizing antidepressants. SERT.

Previous reports have identified discrete amino acids, such as D98 (Barker et al., 1999), Y95 (Barker et al., 1998), and F586 (Barker and Blakely, 1996), as playing critical roles for the recognition of specific antidepressants by SERT. The complete shift in desipramine and venlafaxine potency at the chimera might suggest that these

Table 2.1. K_i values for inhibition of [^{3}H]5-HT uptake in stably transfected HEK-293 cells. Values are the Mean ± S.E.M. for at least three independent experiments performed in triplicate.

	K_i, nM		
	hSERT	dSERT	$H^{1\text{-}281}D^{282\text{-}476}H^{477\text{-}638}$
Sertraline	3.6 ± 0.4	390 ± 98	150 ± 37
Citalopram	6.7 ± 1.7	110 ± 30	73 ± 27
Imipramine	6.9 ± 2.7	230 ± 17	130 ± 6.0
Fluoxetine	17 ± 7.0	350 ± 40	270 ± 69
Desipramine	220 ± 90	900 ± 18	860 ± 32
Venlafaxine	310 ± 200	28000 ± 5600	32000 ± 11000

antidepressants have distinct contact sites that play a major role in their recognition and that these sites are within the transmembrane domain V-IX region. It is likely that the interaction of these critical residues, as well as other unidentified points of interaction within the transmembrane domain V-IX region, provide a site or sites through which SERT recognizes these compounds with high-affinity. These studies correlate with previous reports of transmembrane domains V-VII of the norepinephrine transporter as being important for the recognition of tricyclic antidepressants (Buck and Amara, 1995).

Amino acids implicated in providing high-affinity interactions of antidepressants with SERT

Within the transmembrane domain V-IX region, several amino acids have been implicated in antidepressant recognition (Fig. 2.4B) (Paczkowski and Bryan-Lluka, 2001;Paczkowski and Bryan-Lluka, 2002;Roubert et al., 2001). Of these amino acids, two residues (S375 and P418) represent positions where the hSERT and dSERT sequences diverge. S375 is a position that has been identified as being important for the recognition of substrates and antidepressants by NET (Fang et al., 1998;Danek Burgess and Justice, Jr., 1999). This serine in transmembrane domain VII has also been identified as a critical residue for the function of SERTs (Kamdar et al., 2000;Penado et al., 1998). As a point of sequence divergence between hSERT and dSERT, I considered the possibility that S375 might play a role in the observed species differences for antidepressant recognition. I employed species-scanning mutagenesis whereby the identity from dSERT (an alanine) was substituted into the equivalent position of hSERT (S375). Interestingly, the hSERT S375A mutant did not show any statistically significant differences in K_i values for the antidepressants as compared to the parental hSERT (data not shown, experiments performed by C.C. Walline), indicating that this residue may not play a major role in the recognition of these antidepressants. However, it is important to note that the level of [^{3}H]5-HT uptake at the hSERT S375A mutant was only

approximately 25% of wild-type. Cell surface binding experiments confirmed a lower expression of hSERT S375A as compared to wild-type hSERT (data not shown).

The other species divergent position, P418, was also converted to dSERT identity (serine). This residue, equivalent to S399 in hNET, is located in transmembrane domain VIII near the extracellular face of the helix. P418 is interesting in that it is a proline residue in the hSERT, but a serine at the equivalent position in hNET and dSERT. The presence of the "helix-breaking" proline located within a putative helix provides a unique residue to exploit using mutagenesis. Other studies (Roubert et al., 2001) have shown that this residue is critical for the recognition of tricyclic antidepressants by hNET, providing another facet of interest for this residue. However, the hSERT P418S mutant did not show significant divergence from the parental hSERT in recognizing any of the antidepressants assayed (data not shown, experiments performed by C.C. Walline). Cell surface binding and transport levels indicated that hSERT P418S expression is virtually identical to wild-type hSERT (data not shown). One explanation for this finding is that the interaction with antidepressants provided by the proline in hSERT is maintained even when the residue is mutated to a serine. More likely, however, the mutation of the proline to a serine maintains intermolecular or intrahelical interactions that provide access to high-affinity recognition sites for these antidepressants. These findings suggest that P418 (SERT) or S399 (NET) could play a role in the overall conformation of the transporter, as opposed to serving as a direct contact site for antidepressants.

Summary

The cloning of SERT provided scientists with a target for the development of antidepressants. For these analyses, I have drawn from reports published long before the molecular cloning and characterization of this protein. The initial reports of structure-activity relationships for both the tricyclic antidepressants, as well as the selective serotonin reuptake inhibitors, have been used to perform a contemporary re-analysis of several seminal findings. I have also shown the importance of the positional orientation of the selective serotonin reuptake inhibitors when interacting with SERTs. The orientation of the aromatic ring may provide both high-affinity and specificity for the selective serotonin reuptake inhibitors, which have become widely prescribed for their potency and specificity, as well as overall safety as compared to the TCAs. Finally, I have performed experiments using chimeric SERT, and experiments involving SERT point mutants have been performed in the Barker laboratory (by C.C. Walline), in order to develop a better understanding of how the protein interacts with antidepressants. Although the point mutants did not suggest critical points for recognition, the data from the cross-species chimera hint at the presence of multiple areas of SERT being involved with the recognition of antidepressants. Future studies will focus on further exploration of transmembrane domains V-IX to identify specific residues involved with high-affinity recognition of antidepressants, as well as guiding my efforts to understand how the transporter functions as a unit to recognize both tricyclic antidepressants and selective serotonin reuptake inhibitors.

CHAPTER III

DISTINCT MOLECULAR RECOGNITION OF PSYCHOSTIMULANTS BY HUMAN AND *DROSOPHILA* SEROTONIN TRANSPORTERS

(Results published in *The Journal of Pharmacology and Experimental Therapeutics*, February 2004, vol. 308, p. 679-687)

Introduction

The data presented in Chapter II, as well as previous studies have shown that human and *Drosophila* SERTs exhibit different pharmacologies even though they possess approximately 51% sequence similarity (Hoffman et al., 1991;Usdin et al., 1991;Ramamoorthy et al., 1993;Blakely et al., 1994;Corey et al., 1994;Demchyshyn et al., 1994;Barker et al., 1998). In Chapter II, my focus was to demonstrate the uniqueness of antidepressant recognition by SERT species variants. The studies presented in this chapter demonstrate differences in the way the human and *Drosophila* SERT species variants, as well as a chimeric SERT, recognize cocaine derivatives and substituted-amphetamines. In light of the structural diversity of these compounds, we hypothesize that distinct determinants of psychostimulant recognition by SERT exist and differences in these modes of recognition can be explored through molecular modeling and CoMFA. In order to test this hypothesis, we have utilized a library of 3-phenyltropane analogs and

substituted-amphetamines to examine structural components of these compounds that are critical for recognition by hSERT, dSERT, and the $H^{1-281}D^{282-476}H^{477-638}$ chimera. The structural diversity of the compound classes provides a unique collection of probes for what may be multiple binding pockets or, at minimum, unique contact sites within the same pocket, for these two prototypical psychostimulants. In our studies, both libraries of compounds were screened using a [^{3}H]5-HT uptake inhibition assay with HEK-293 cells stably expressing hSERT, dSERT, or the $H^{1-281}D^{282-476}H^{477-638}$ chimera. The K_i values for inhibition of [^{3}H]5-HT transport were calculated from IC_{50} values obtained from dose-response curves. The results of these assays were used as input for modeling using CoMFA. CoMFA has proven valuable in previous studies as a method to model protein-ligand interactions in systems that lack protein crystal structures or other definitive structural information (Carroll *et al.*, 1994;Wilcox *et al.*, 1998;Li *et al.*, 1999;Newman *et al.*, 1999). The six models presented here indicate differences in recognition on four levels. First, differences exist between the way hSERT and dSERT recognize 3-phenyltropane derivatives. Second, there are differences in the molecular recognition of the substituted-amphetamines by the two species variants. Third, and perhaps most interesting, CoMFA maps reveal differences in the way SERTs, in general, recognize these two classes of psychostimulants. Fourth, the models suggest that the $H^{1-281}D^{282-476}H^{477-638}$chimera, which is an hSERT construct with transmembrane domains (TMDs) V-IX replaced with the dSERT sequence, exhibits distinct hybrid interactions with some components similar to hSERT and dSERT for the 3-phenyltropane analogs, whereas the determinants for recognizing the substituted-amphetamines closely parallels dSERT. These maps and accompanying data indicate fundamental differences in the recognition

of psychostimulants, suggesting unique molecular interactions with SERTs that promote high-affinity interactions with these drugs of abuse.

Materials and Methods

[^{3}H]5-HT uptake assays

The $H^{1-281}D^{282-476}H^{477-638}$ chimera was generated as previously described (Rodriguez et al., 2003). Briefly, it is a full-length 638 amino acid transporter, constructed from amino acids 1-281 and 477-638 with identity from hSERT and residues 282-476 with identity from dSERT.

Human embryonic kidney cells (HEK-293) stably expressing either the human or *Drosophila* SERT were generous gifts from Dr. Randy D. Blakely, Vanderbilt University. All cells were maintained in Dulbecco's modified Eagle's medium with 10% dialyzed fetal bovine serum supplemented with 2 mM glutamine, 1% penicillin/streptomycin, and 600 mg/L geneticin (G-418 sulfate) in a humidified 5% CO_2 incubator at 37°C.

Uptake assays were performed on cell suspensions in 96-well microtube racks as described in Chapter II, with slight variation. When 3-phenyltropane analogs were assayed, the cells were pre-incubated with drug at 37°C for 10 minutes. This pre-incubation was not included when the substituted-amphetamines were assayed, as these compounds have been shown to be substrates for SERT, and the intracellular accumulation of drug could affect 5-HT transport (Wall, *et al.*, 1995; Rodriguez, *et al.*, 2003). Nonspecific uptake was determined using 10 μM fluoxetine. On average, specific 5-HT uptake was approximately 95% of total uptake. The filter plates were dried at

ambient temperature overnight. The next day scintillation cocktail was added prior to counting in a Packard TopCount NXT (Meriden, CT) to determine accumulated [^{3}H]5-HT. IC_{50} values were determined using the non-linear regression routine in GraphPad Prism v.3.0 (GraphPad Software, Inc. San Diego, CA), and K_i values were calculated using the Cheng-Prusoff equation (Cheng and Prusoff, 1973). The K_m values for 5-HT uptake at each construct were: 1.2±0.2 μM (hSERT), 0.9±0.2 μM (dSERT), and 0.8±0.1μM ($H^{1-281}D^{282-476}H^{477-638}$). Experiments were performed in triplicate and repeated in at least three separate assays.

CoMFA for 3-phenyltropane analogs

Computational molecular modeling studies were performed using the SYBYL v.6.8 software package (Tripos Inc, St. Louis, MO) on a Silicon Graphics O2 workstation (Mountain View, CA) running IRIX v.6.5. The 3-phenyltropane analogs were sketched using library fragments in SYBYL. Atom types were automatically assigned by SYBYL and then manually checked. The compounds were subjected to a grid search (0-360 degrees, 10-degree increment) to find the lowest energy conformation. This conformation was then minimized for all molecules using the conjugate gradient method with no initial simplex minimization, a gradient value of 0.05, and 10,000 maximum iterations. The compound set, as well as a consensus molecule containing the common tropane ring substructure, was inserted into the database. This consensus molecule containing the core structure of all the analogs was used as the template for SYBYL's database alignment

tool. All of the structures were aligned using the tropane ring skeleton as anchor points. The aligned molecules were then inserted into a molecular spreadsheet and pK_i values inserted as functional data. CoMFA data were generated using the parameters listed above. For the hSERT data, three components were determined to be optimal (q^2=0.63), whereas the dSERT (q^2=0.51) and $H^{1-281}D^{282-476}H^{477-638}$ chimera (q^2=0.54) models utilized two components that were determined to be optimal based on the partial-least squares analysis.

CoMFA for substituted-amphetamines

The amphetamine analogs were sketched using library fragments in SYBYL. Atom types were automatically assigned by SYBYL and then manually checked. The stereochemistry was assigned as S, based on the known S>R stereoselectivity for amphetamines at monoamine transporters. The compounds were subjected to a grid search (0-360 degrees, 10-degree increment) to find the lowest energy conformation. This conformation was then minimized for all molecules using the conjugate gradient method with no initial simplex minimization, a gradient value of 0.05, and 10,000 maximum iterations. Alignment of the database was optimized using a template molecule based on the most rigid structure of (S)-5-methoxy-6-methyl-2-aminoindan, with the aromatic ring centroid and amine nitrogen of each compound held as the anchor points. The aligned molecules were then inserted into a molecular spreadsheet with pK_i values as functional data. CoMFA data were generated using the Tripos Standard CoMFA field class, with

distance dielectric, no smoothing, and a steric and electrostatic cutoff of 30.0 kcal/mol. Partial least squares (PLS) analysis was validated using the leave-one-out option. Four components were initially selected for the PLS analysis, and then the number of optimal components was determined. For the hSERT, dSERT, and $H^{1-281}D^{282-476}H^{477-638}$chimera models three components were used with q^2 values of 0.65, 0.73, and 0.59, respectively.

Materials

Cocaine and CPT-D-tartrate were purchased from Research Biochemical International (Natick, MA). 3-phenyltropane analogs RTI-142 and RTI-121 (Neumeyer *et al.*, 1994) , RTI-55 and RTI-112 (Carroll et al., 1994), β-CFT (Neumeyer *et al.*, 1996), RTI-32 (Holmquist *et al.*, 1996), RTI-31 (Carroll *et al.*,1995), RTI-83 (Blough *et al.*, 1996), and RTI-311 (Scheffel *et al.*, 1997), were synthesized as previously described. Substituted-amphetamines were synthesized using conventional methodologies and their structures confirmed with NMR, MS, and elemental analysis, all of which matched expected criteria. All cell culture supplies, common chemicals, and supplies were purchased from sources described in Chapter II.

Results

Comparison of 3-phenyltropane analogs and substituted-amphetamines at hSERT, dSERT, and $H^{1-281}D^{282-476}H^{477-638}$ chimera

Initial studies determined the sensitivities of hSERT, dSERT, and $H^{1-281}D^{282-476}H^{477-638}$ to cocaine and amphetamine derivatives. The potency of the 3-phenyltropane analogs and substituted-amphetamines for inhibition of [^{3}H]5-HT uptake was determined (Figure 3.1). The K_i value for inhibition of 5-HT uptake at HEK-293 cells expressing hSERT (hSERT-HEK) was 10- to 100-fold lower, depending on the compound, as compared to dSERT and $H^{1-281}D^{282-476}H^{477-638}$ expressing cells (dSERT-HEK and $H^{1-281}D^{282-476}H^{477-638}$-HEK, respectively) (Tables 3.1 and 3.2). Interestingly, potencies at $H^{1-281}D^{282-476}H^{477-638}$ generally paralleled dSERT for all compounds assayed. For the 3-phenyltropane analogs, the rank order of K_i values at hSERT was: RTI-55 < [RTI-] 112 < -311 < -31 < -142 < -83 < -32 < -121 < cocaine < β-CFT and < CPT-D-tartrate. At dSERT, the rank order of K_i values was: RTI-55 < RTI-142 < -121 < -311 < -32 < -112 < Cocaine, <-31, <-83 < β-CFT and < CPT-D-tartrate. At the $H^{1-281}D^{282-476}H^{477-638}$ chimera, the rank order of K_i values was: RTI-55 = RTI-142 < cocaine < -121 < -112 < -311 < -83 < -31 < β-CFT < -32 and < CPT-D-tartrate.

For the substituted-amphetamines, the order of increasing K_i values at hSERT was: DCA < 4-MTA < 2-Me-MDA < MMAI < MDA < 3-MTA < AMMI < DFA < 6-Me-MDA < 4-TFMA < AMMT. The order of increasing K_i values for the substituted-

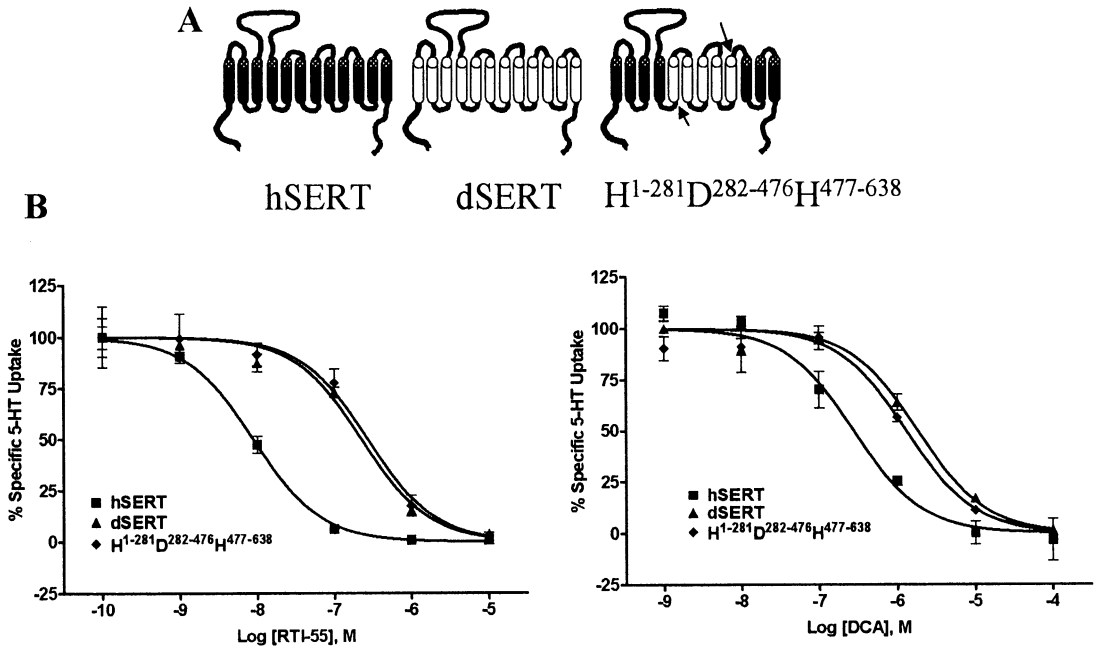

Figure 3.1. (A) Diagram of wild-type hSERT, dSERT, and the $H^{1-281}D^{282-476}H^{477-638}$ chimera. The transporters were constructed as described in Materials and Methods, with hSERT sequence indicated in black and dSERT sequence indicated in white. Arrows indicate chimeric switch point. (B) Inhibition of [^{3}H]5-HT uptake at (■) hSERT, (▲) dSERT, and (◆) $H^{1-281}D^{282-476}H^{477-638}$ using RTI-55 and 3,4-dichloroamphetamine (DCA). [^{3}H]5-HT uptake assays were performed as described in Materials and Methods. Nonspecific uptake was determined with 10 μM fluoxetine. Data were plotted as a percentage of specific [^{3}H]5-HT uptake. Dose-response curves depicted are representative of at least three experiments performed in triplicate.

Table 3.1. 3-phenyltropane derivative K_i values for [^{3}H]5-HT uptake inhibition at hSERT, dSERT, and $H^{1-281}D^{282-476}H^{477-638}$ chimera.

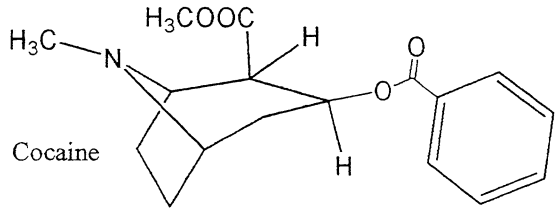

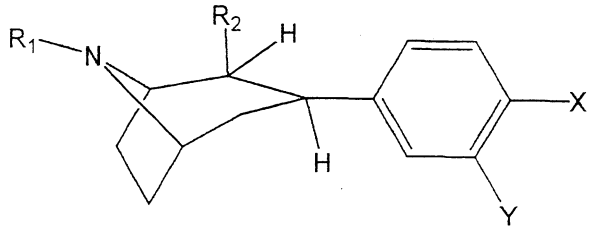

Name	R_1	R_2	X	Y	K_i, nM ± SEM		
					hSERT	dSERT	$H^{1-281}D^{282-476}H^{477-638}$
Cocaine	-	-	-	-	250 ± 90	750 ± 140	220 ± 60
CPT-D-tartrate	CH_3	$COOCH_3$	H	H	1500 ± 100	38000 ± 10000	14000 ± 10000
RTI-142	H	$COOCH_3$	F	H	45 ± 10	320 ± 90	200 ± 40
β-CFT	CH_3	$COOCH_3$	F	H	990 ± 110	4300 ± 1300	2600 ± 450
RTI-31	CH_3	$COOCH_3$	Cl	H	40 ± 7	800 ± 140	890 ± 270
RTI-112	CH_3	$COOCH_3$	Cl	CH_3	12 ± 2	580 ± 90	550 ± 210
RTI-32	CH_3	$COOCH_3$	CH_3	H	110 ± 30	580 ± 240	5800 ± 1600
RTI-83	CH_3	$COOCH_3$	CH_2CH_3	H	60 ± 10	2600 ± 1300	660 ± 320
RTI-55	CH_3	$COOCH_3$	I	H	7 ± 2	190 ± 10	200 ± 30
RTI-121	CH_3	$CO_2CH(CH_3)_2$	I	H	180 ± 40	340 ± 150	360 ± 170
RTI-311	$CH_2CH{=}CH_2$	$COOCH_3$	I	H	30 ± 4	470 ± 160	600 ± 160

Table 3.2. Substituted-amphetamine K_i values for [^{3}H]5-HT uptake inhibition at hSERT, dSERT, and $H^{1-281}D^{282-476}H^{477-638}$ chimera.

Name	Abbrev.	Structure	K_i, μM ± SEM		
			hSERT	dSERT	HDH[1]
3,4-Dichloro-amphetamine	DCA	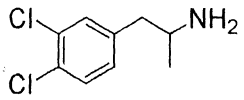	0.20 ± 0.1	1.5 ± 0.5	1.5 ± 0.2
3,4-Difluoro-amphetamine	DFA	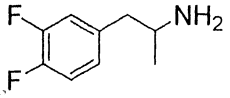	4.3 ± 2.2	56 ± 30	12 ± 6
4-Methylthio-amphetamine	4-MTA	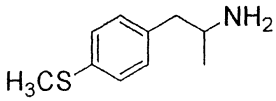	0.45 ± 0.1	4.6 ± 0.2	3.8 ± 0.6
3-Methylthio-amphetamine	3-MTA	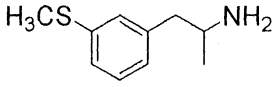	1.8 ± 0.9	7.3 ± 2.1	14 ± 0.9
1-Aminomethyl-5-methoxyindan	AMMI	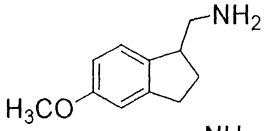	2.1 ± 0.3	13 ± 3.1	16 ± 4.7
1-Aminomethyl-6-methoxytetralin	AMMT	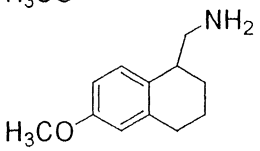	7.0 ± 1.3	11 ± 1.9	15 ± 2.8
5-Methoxy-6-methyl-2-aminoindan	MMAI	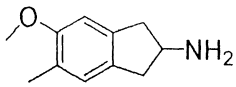	0.83 ± 0.1	19 ± 1.0	20 ± 3.2
3,4-Methylenedioxy-amphetamine	MDA	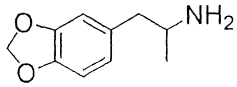	1.1 ± 0.3	19 ± 2.4	13 ± 2.0
2-Methyl-3,4-methylene-dioxy amphetamine	2-Me-MDA	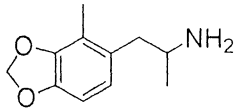	0.70 ± 0.1	27 ± 2.0	19 ± 3.0
6-Methyl-3,4-methylene-dioxy amphetamine	6-Me-MDA	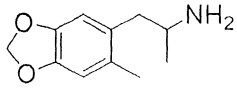	4.4 ± 0.2	26 ± 1.9	12 ± 2.0
4-Trifluoromethyl-amphetamine	4-TFMA	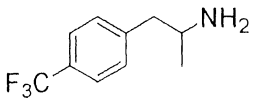	5.2 ± 1.0	86 ± 19	55 ± 22

[1] $H^{1-281}D^{282-476}H^{477-638}$

amphetamines at dSERT was: DCA < 4-MTA < 3-MTA < AMMT < MMAI < MDA < 6-Me-MDA < 2-Me-MDA< DFA < 4-TFMA. The order of increasing K_i values for $H^{1-281}D^{282-476}H^{477-638}$ chimera was: DCA < 4-MTA < 3-MTA = MDA = 6-Me-MDA < AMMT = AMMI < MMAI = 2-Me-MDA < 4-TFMA.

CoMFA of 3-phenyltropane analogs at hSERT, dSERT, and $H^{1-281}D^{282-476}H^{477-638}$ chimera

A Silicon Graphics O2 workstation and the SYBYL software package were used to generate CoMFA maps for distinct models of 3-phenyltropane analog interaction with human (Fig. 3.2A), *Drosophila* (Fig. 3.2B), and the $H^{1-281}D^{282-476}H^{477-638}$ chimeric (Fig. 3.2C) SERTs, using RTI-55 as a model compound for reference. Overall, upon inspection, a high degree of similarity exists between the dSERT (Fig. 3.2B) and $H^{1-281}D^{282-476}H^{477-638}$ (Fig. 3.2C) models. Also, the compounds assayed share very similar potencies for dSERT and the $H^{1-281}D^{282-476}H^{477-638}$ chimera. Four prominent features stand out in all three models. First, the region of disfavored steric bulk, near the bridgehead amine, depicted in yellow is reduced in size in the dSERT and $H^{1-281}D^{282-476}H^{477-638}$ models (Fig. 3.2B and 3.2C), as compared to hSERT (Fig. 3.2A). The pharmacological data indicate that addition of bulky groups to the amine nitrogen or to the C2 carboxylic acid carbon results in a loss of potency. For example, RTI-121 and RTI-311 are congeners of RTI-55 with bulky substitutions at position C2 or the amine nitrogen, respectively. Both of these compounds showed profound loss of activity at all three

constructs as compared to RTI-55 (Table 3.1). A second prominent feature is the blue field, denoting positive charge and hydrogen bond donors being favored. In hSERT (Fig. 3.2A), the blue field surrounds the aromatic ring, whereas in dSERT and $H^{1-281}D^{282-476}H^{477-638}$ (Fig. 3.2B and 3.2C) the blue region is reduced in size and does not envelop the aromatic ring as completely as in the hSERT model. The third region of interest is the area denoting favored steric bulk, in green, near the 4'-substituted position of the aromatic ring. All three models share this green field. The effect of this region of steric bulk is evident when comparing β-CFT, RTI-31, and RTI-55. The potency of the compound increases in going from F-, to Cl-, to I- , following increasing hydrophobicity of the substituent. The favorability of steric bulk is evident in that the 4'-ethyl substitution (RTI-83) was more potent than the 4'-methyl congener (RTI-32) of the 3-phenyltropane series (60 nM vs. 110 nM at hSERT). The $H^{1-281}D^{282-476}H^{477-638}$ model shows this region of favored steric bulk that is larger than either parental hSERT or dSERT. In both hSERT and $H^{1-281}D^{282-476}H^{477-638}$ lengthening the 4'-substituent from methyl to ethyl affords a modest increase in potency. By contrast, at dSERT, this changes leads to decreased affinity. The small yellow regions in this location in dSERT may indicate a reduced tolerance to steric bulk at this site, relative to hSERT and $H^{1-281}D^{282-476}H^{477-638}$.

Figure 3.2. Comparative molecular field analysis (CoMFA) maps of cocaine analog interactions with (A) hSERT, (B) dSERT, and (C) $H^{1-281}D^{282-476}H^{477-638}$ chimera, arranged for cross-eyed viewing. RTI-55 is modeled within the field for directional orientation. Colored fields represent characteristics of the ligand that favorably or unfavorably affect high-affinity interactions. Steric contours are shown in green and yellow, whereas electrostatic contours are shown in blue and red. Green fields indicate molecular regions where steric bulk is favored for high-affinity interactions, whereas regions indicated by yellow are areas in which steric bulk is disfavored for high-affinity interactions. Blue fields indicate regions of the molecule where more positive charge and hydrogen bond donors are favored, and negative charge and hydrogen bond acceptors are disfavored for high-affinity interactions. Red fields indicate regions where negatively charged substitutents and hydrogen bond acceptors are favored, and positive charge and hydrogen bond donors are disfavored.

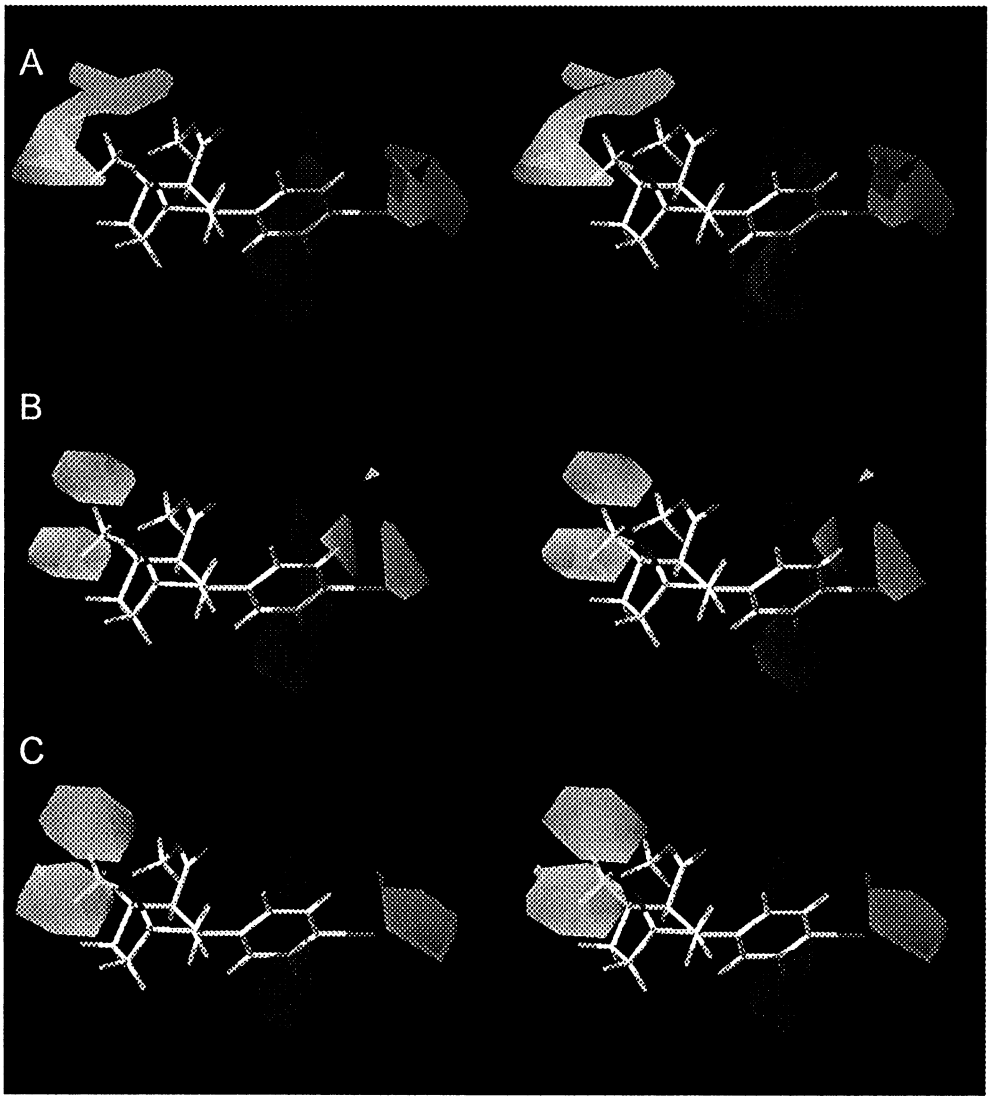

Figure 3.2

The fourth region of interest is the red field region of favored negative charge on the $H^{1-281}D^{282-476}H^{477-638}$ model (Fig. 3.2C) also located near the 4'- position that is shared by the hSERT model (Fig. 3.2A) but not the dSERT model (Fig. 3.2B). The somewhat higher potency of RTI-31 (4'-Cl) over RTI-32 (4'-CH_3) at the hSERT and $H^{1-281}D^{282-476}H^{477-638}$ chimera may reflect this favorability for negative substituents (such as chlorine or iodine) at the 4'-position.

CoMFA of substituted-amphetamines at hSERT, dSERT, and $H^{1-281}D^{282-476}H^{477-638}$ chimera

A Silicon Graphics O2 workstation and the SYBYL software package were used to generate CoMFA maps for distinct models of amphetamine derivative interaction with the 5-HT transporters. Figure 3.3 is the pharmacological data as a CoMFA model, using 3,4-dichloroamphetamine for orientation, for interactions with the human (Fig. 3.3A), *Drosophila* (Fig. 3.3B), and the $H^{1-281}D^{282-476}H^{477-638}$ chimeric (Fig. 3.3C) SERTs. The compounds in this training set all possess the aromatic core and ethylamine of the parent compound *d*-amphetamine, but vary by either single substitutions on the aromatic ring or the creation of a fused, sterically constrained bicyclic system with the aromatic ring and another saturated five- or six-membered ring. As with the 3-phenyltropane derivatives, inspection of Table 3.2 shows that the majority of compounds have similar potencies at dSERT and $H^{1-281}D^{282-476}H^{477-638}$ that are, in general, lower than their potencies at

Figure 3.3. Comparative molecular field analysis (CoMFA) maps of substituted-amphetamine interactions with (A) hSERT, (B) dSERT, and (C) $H^{1\text{-}281}D^{282\text{-}476}H^{477\text{-}638}$ chimera, arranged for cross-eyed viewing. 3,4-dichloroamphetamine is modeled within the field for directional orientation. Colored fields represent characteristics of the ligand that favorably or unfavorably affect high-affinity interactions. Steric contours are shown in green and yellow, whereas electrostatic contours are shown in blue and red. Green fields indicate molecular regions where steric bulk is favored for high-affinity interactions, whereas regions indicated by yellow are areas in which steric bulk is disfavored for high-affinity interactions. Blue fields indicate regions of the molecule where more positive charge and hydrogen bond donors are favored, and negative charge and hydrogen bond acceptors are disfavored for high-affinity interactions. Red fields indicate regions where negatively charged substituents and hydrogen bond acceptors are favored, and positive charge and hydrogen bond donors are disfavored.

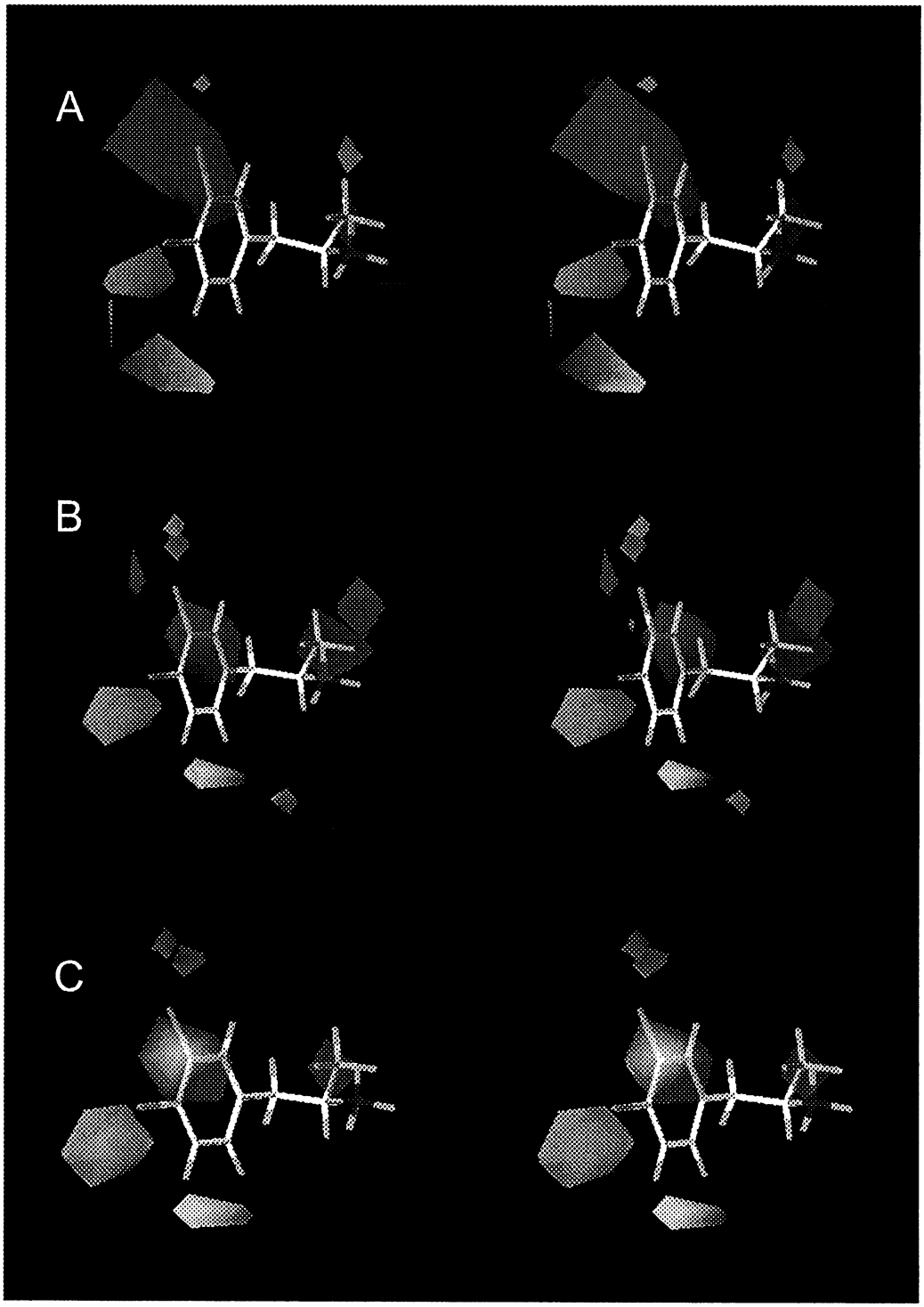

Figure 3.3

hSERT. Inspection of the CoMFA fields shows a general similarity between those of dSERT and $H^{1-281}D^{282-476}H^{477-638}$ consistent with the experimental data. The CoMFA fields for all three substituted-amphetamine models show a region of favored steric bulk (green) in the vicinity of the 4-position of the aryl ring. This field changes size very slightly among the three models. In addition, a red region exists near the 3-position of the aryl ring, indicating a region where electronegative substituents would increase potency. This red region is considerably larger on the hSERT model (Fig. 3.3A) as compared to the models in Figures 3.3B and 3.3C. There is also a sterically disfavored yellow region in the vicinity of the 5,6-positions of the aryl ring on all three models. The hSERT CoMFA (Fig. 3.3A) differs principally in that it has a much larger negative field at the 3-aryl position. In addition, the disfavored yellow region is displaced from its hSERT location in both the dSERT and $H^{1-281}D^{282-476}H^{477-638}$ models (Fig. 3.3B and 3.3C). Each of the amphetamines tested in this training set contain the ethylamine moiety. The region around the amine differs in each of the three models. For hSERT (Fig. 3.3A), the region around the amine shows a small red field (negative electrostatics favored) as well as a slightly distal small blue (positive electrostatics favored) field. The dSERT and $H^{1-281}D^{282-476}H^{477-638}$ models show much larger red fields in this region. These results suggest a contact site with the amphetamine amine moiety exists on hSERT, but is different in dSERT and the $H^{1-281}D^{282-476}H^{477-638}$ chimera.

Discussion

The studies described in this chapter seek to examine the structural features of two different psychostimulants in the context of their common ability to interact with SERTs. Due to the striking differences in their molecular structure, yet common target, one might predict some overlapping features responsible for molecular recognition if shared contact sites exist.

Structure-activity relationships of 3-phenyltropane analogs at hSERT, dSERT, and $H^{1-281}D^{282-476}H^{477-638}$ chimera

The most potent 3-phenyltropane analog tested in this study at both hSERT and dSERT was RTI-55 (Carroll et al., 1994), whereas RTI-55, RTI-142, and cocaine are equipotent at the $H^{1-281}D^{282-476}H^{477-638}$ chimera. The 3-phenyltropane analog RTI-55 differs from cocaine in two ways. First, it lacks the ester linkage between the tropane substructure and the aromatic ring. Second, RTI-55 contains an iodine atom at the 4'-(para) position on the aromatic ring. These two changes to cocaine's structure combine to promote an increase in potency approximately 40-fold at hSERT (250 nM vs. 7 nM) and greater than 3-fold at dSERT (190 nM vs. 750 nM), but little difference at $H^{1-281}D^{282-476}H^{477-638}$, possibly indicating a unique mode of recognition by the chimera. Using RTI-55 and my CoMFA models, several possible conclusions were drawn about the high-potency interaction between 3-phenyltropane analogs and SERTs. Substitutions at the 4'-

position on the aromatic ring appear to be important for potent interactions with SERT (as reflected by the red fields in Figs 3.2A and 3.2C). The 4'-fluoro is the most electron withdrawing substituent, followed by the 4'-chloro and 4'-iodo. In rank order of potency, the iodine-containing compound RTI-55 is most potent, followed by the chlorine-containing (RTI-31) and then the fluorine-containing analog (β-CFT). These results are similar to those reported in previous studies focused on the cocaine binding site in purified rat brain striatum, a rich source of dopaminergic neurons (Carroll et al., 1994). This study, while performed on tissue containing DAT, supports the hypothesis that the importance of the substitution at the 4'- position may be general for high-affinity 3-phenyltropane analog interactions with biogenic amine neurotransmitter transporters. (Carroll et al., 1994).

Our CoMFA models revealed similarities among hSERT, dSERT, and the $H^{1-281}D^{282-476}H^{477-638}$ chimera interaction with the aromatic ring of the 3-phenyltropane analogs. In the models, the electron withdrawing substituents seem to exert their effect through a delocalization of electrons in the aromatic ring. Interestingly, the dSERT and $H^{1-281}D^{282-476}H^{477-638}$ chimera models (Fig. 3.2B and 3.2C) show a much smaller area of favorable interactions around the aromatic ring faces. It has been proposed that pi-pi stacking interactions with aromatic residues in DAT may contribute to high-potency interactions with cocaine analogs (Blough *et al.*, 2002). Aromatic amino acids present in hSERT, possibly in TMDs I-IV or X-XII, but absent in dSERT, could be important points of interaction or provide unique conformations. The $H^{1-281}D^{282-476}H^{477-638}$ chimera may have contact points for cocaine in both its central dSERT (TMDs V-IX) and its hSERT (TMDs I-IV and X-XII) regions. The effect of alkyl substitutions on the aromatic ring

have been shown previously to effect binding to both SERT and NET (Blough et al., 1996). The green region of favorable steric bulk in the vicinity of the 4-position is common to all three models (Fig. 3.2A-C). The effect of this steric region is evident when comparing β-CFT, RTI-32, and RTI-55. The potency of the compounds increases when going from F-, to Cl-, to I-, with increasing hydrophobicity of substituents. Steric bulk effects have also been observed for DAT binding sites in rat striatum, where a 4'-bromo substitution had similar potency as a 4'-methyl substitution (1.8 nM vs. 1.7 nM) (Carroll *et al.*, 1991). Similar Van der Waals radii of the bromine and methyl substituent could explain the similarity in potency. This steric constraint has been observed with other cocaine derivatives at biogenic amine transporters (Neumeyer et al., 1996). Interestingly, my CoMFA models do not suggest a significant role for the charge associated with the amine nitrogen in contributing to potency. This observation is supported by the recent synthesis of non-nitrogen containing phenyltropanes by Goulet and coworkers that effectively and potently inhibit 5-HT transport (Goulet *et al.*, 2001).

Structure-activity relationships of substituted-amphetamines at hSERT, dSERT, and $H^{1-281}D^{282-476}H^{477-638}$ chimera

Amphetamine and its neurotoxic derivatives are known to interact with the biogenic amine transporters to cause an increase in synaptic neurotransmitters. Structure-activity relationships for substituted-amphetamines have been studied at SERT, DAT, and NET. For instance, amphetamines with dual substitutions in the 3- and 4-positions

become more selective for serotonergic effects (Nichols, 1994). Also, primary amines are the most potent for the biogenic amine neurotransmitter transporter family, but N-ethyl substitutions can differentially improve interactions with SERTs (Nichols, 1994). My studies have focused on these two molecular areas to contribute to the understanding of substituted-amphetamine structure-activity relationships.

In this study, I have generated CoMFA maps from pharmacological data for hSERT, dSERT, and the $H^{1-281}D^{282-476}H^{477-638}$ chimera using a set of substituted-amphetamines. Similarities and differences in their characteristics can be identified from these analyses. At all three SERT constructs the most potent substituted-amphetamine assayed was 3,4,-dicholoroamphetamine, although the compound was 10-fold more potent at hSERT than dSERT and the $H^{1-281}D^{282-476}H^{477-638}$ chimera (0.20 μM for hSERT vs. 1.5 μM for dSERT and $H^{1-281}D^{282-476}H^{477-638}$). Structurally, the closest derivative in this study to 3,4-dicholoroamphetamine was 3,4-difluoroamphetamine, which differs only by the identity of the halide substitution. This fluorine-substituted compound, however, had markedly decreased potency at species variants as compared to the chlorine-substituted variant (4.3 μM at hSERT, 56 μM at dSERT, and 12 μM at $H^{1-281}D^{282-476}H^{477-638}$). The CoMFA models indicate a region of favored negative charge (in red, Fig. 3.3) in the area around the 3-position of the aromatic ring on each of the three models. However, this field is slightly displaced from the 3-position, indicating that this electrostatic effect may not be solely determined by the substitution at the 3-position. The green field near the 4-position indicates that the bulk of the substitution plays a major role in potency. The role of this position was examined in a previous study that revealed that bulk at the 4-position is critical in determining potency (Marona-Lewicka, *et al.*,

1995). The second most potent compound at hSERT, dSERT, and the $H^{1-281}D^{282-476}H^{477-638}$ chimera was 4-methylthioamphetamine (0.45 μM, 4.6 μM, and 3.8 μM, respectively). The position of the methylthiol group affects potency, with the 4-methylthioamphetamine exhibiting higher potency as compared to 3-methylthioamphetamine, due to favorable steric interactions as indicated by the green region in Figure 3.3.

In addition to distinctions surrounding the aromatic ring, differences in molecular fields are present near the amine. These species-specific interactions revealed similarities between dSERT and the $H^{1-281}D^{282-476}H^{477-638}$ chimera. The *Drosophila* SERT sequence in the $H^{1-281}D^{282-476}H^{477-638}$ chimera is localized to the TMD V-IX region, implicating these domains as possessing residues involved with interacting with the amine functionality. Previously published reports have identified TMD I as an important region of SERT involved with recognition of the amine of both 5-HT (Barker et al., 1999) and tryptamine derivatives (Adkins et al., 2001b). Together, my data and these previous studies indicate that substrates likely interact with multiple TMDs, including TMD I and the TMD V-IX region, and, consequently, any model of SERT structure should consider multiple points of contact within the transporter to form a substrate translocation pathway. The models show two additional sites of similarity among the three SERTs. The green field (steric bulk favorability) could suggest that these bulky, hydrophobic substituents interact with a corresponding hydrophobic region on SERT. In addition, a sterically-disfavored yellow region in the vicinity of the 5,6-positions of the aryl ring is common to all three models, however its location is displaced in the dSERT and $H^{1-281}D^{282-476}H^{477-638}$ model as compared to hSERT.

In conclusion, comparing and contrasting the two models of psychostimulant recognition by SERT provides a unique opportunity to reveal evidence of unique interaction sites for cocaine and substituted-amphetamines at SERT. For the 3-phenyltropane analog models, differences exist in the way SERT species variants recognize these compounds on several levels: recognition of the phenyl ring, different substituents in the 4'-position of the aromatic ring, and the electrostatics of the phenyl ring. Similarity among these three models exists in the steric bulk components around the bridgehead amine and the 4'-position substitutions. For the substituted-amphetamines, favored negative charge around the 3- and 4-position is shared by all three SERTs. Also, differences exist in the way the three SERTs recognize the amine functionality. Because all known substrates for SERTs contain amine groups, the site involved with coordinating the amine may be critical for substrate recognition and translocation. The overall dissimilarity of the CoMFA fields for 3-phenyltropane and substituted-amphetamine interactions is suggestive that the sites for interaction on SERT are very different. It is possible that the regions that bind to the 4'-aryl of the 3-phenyltropane analogs and the 4-aryl position of the substituted-amphetamines could be the same, but there are no other structural features to suggest other similarities. I would argue, therefore, that the sites of interactions for these two families of psychostimulants are distinct, but have major determinants within the TMD V-IX region. Also, the uniqueness of the molecular interactions can likely be explained by differences in mechanism of action for these psychostimulants; the substituted-amphetamines can act as substrates for the transporter, whereas the 3-phenyltropanes act as transport blockers (Wall, *et al.*, 1995). Future

molecular studies should identify specific amino acids involved with recognition of psychostimulants and provide important new information about SERT function.

CHAPTER IV

INTERACTIONS OF PSYCHOSTIMULANTS WITH SERT POINT MUTANTS

Introduction

In the previous chapter, I focused on regions of SERT that dictated the species-specific interactions of the psychostimulants amphetamine and cocaine with SERT. As discussed in chapter III, the distinct recognition of these two groups of psychostimulants at hSERT, dSERT, and the cross species chimera $H^{1-281}D^{282-476}H^{477-638}$ provided information that allowed me to narrow my focus to TMDs V-IX when considering possible amino acids that could be involved with the recognition of cocaine derivatives and substituted amphetamines.

The shared sequence identity between hSERT and dSERT, overall, is approximately 51%. Recognition sites for psychostimulants should lie within the transmembrane helices, as the connecting intracellular and extracellular loops have not been implicated in recognition of ligands by SERT or the other monoamine transporters. Thus, I focused on TMDs V-IX, and searched for candidate residues that may be important for the recognition of these drugs. In consideration of the available literature, TMDs VI and IX were not focused on, primarily because these TMDs have neither been

implicated in being part of the permeation pathway, nor have they been implicated in the recognition of substrates or antagonists. Given the sequence divergence, I focused on the TMDs, within the V-IX subset, that had been implicated in recognition of substrates or antagonists. Thus, I chose mutations within TMDs V, VII, and VIII. Once the TMDs were identified, a search for candidate amino acids was based on a logical, bioinformatics approach, in which those residues having shared identity with dSERT and hDAT, but divergent at hSERT, were selected. This criterion was based on the observed pharmacology of dSERT, which is more similar to cloned DATs than mammalian SERTs. An alignment of these TMD sequences, and the selected residues are depicted in Figure 4.1. Subsequent mutagenesis of candidate residues in hSERT to the corresponding dSERT identity was accomplished, and a first-round set of nine point mutants was evaluated. These mutants are highlighted in blue in the sequence alignment represented in Figure 4.1. The mutants were characterized using 5-HT uptake inhibition assays, with the goal of identifying residues important for the recognition of amphetamines and/or cocaine. In summary, none of these single point mutants showed a statistically significant deviation from the parental hSERT construct in regard to the potency of cocaine analogs or amphetamine derivatives.

A second round of mutagenesis was undertaken, in which I narrowed my focus to two aromatic residues in TMD V. These aromatic residues were chosen based on their position and the report that an aromatic interaction existed between cocaine derivatives and other monoamine transporters (Blough et al., 2002). Moreover, the CoMFA analyses performed in chapter III indicated a common interaction with the phenyl ring of the cocaine derivatives and each construct tested. One of these amino acids, Y289, had been

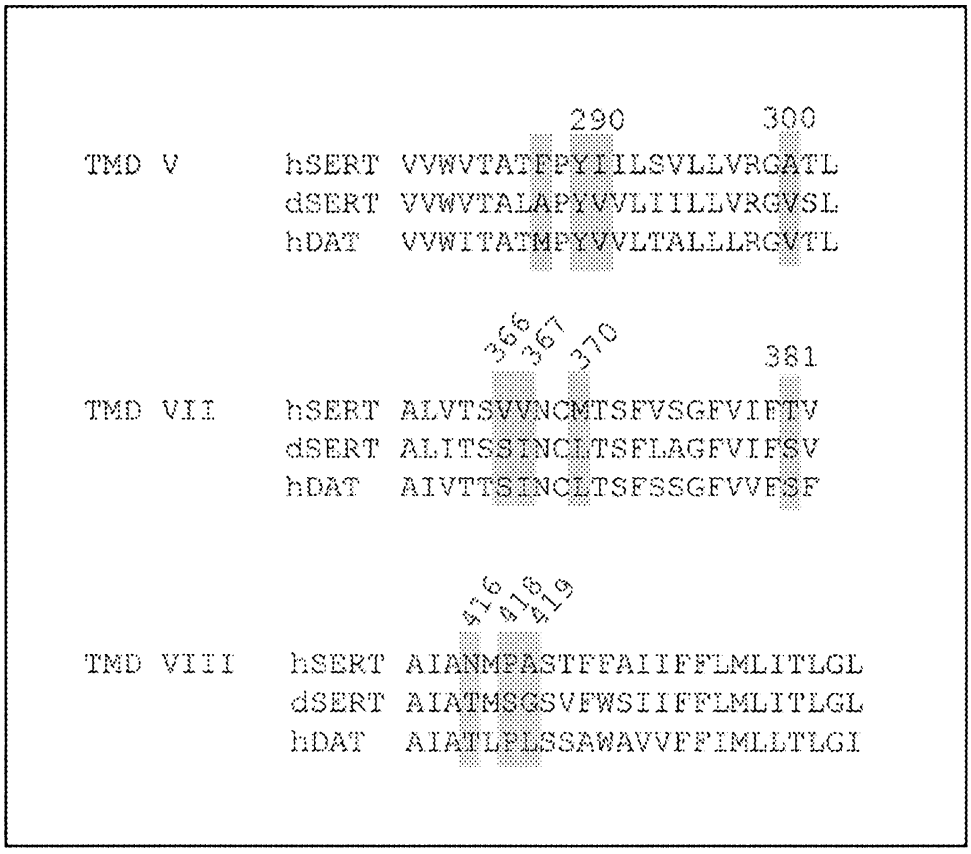

Figure 4.1. Aligment of TMDs V, VII, and VIII. hSERT mutant positions for the first round of mutagenesis are indicated in blue. Two positions, indicated in orange, represent hSERT F287 and Y289, which were mutated in a second round of mutagenesis.

identified in DAT (Y273) as being important for cocaine recognition (Kitayama et al., 1996). Y289, an aromatic amino acid had been previously implicated as a determinant of cocaine recognition, but had not been well-characterized. Another hSERT residue, F287 also located in TMD V was focused on, as aromatic residues seem to be important in the recognition of cocaine by SERTs (see chapter III). Multiple mutants of these two residues were created in order to dissect the role of interactions between these residues and cocaine derivatives.

Following mutagenesis and a screen of four initial cocaine analogs, RTI-31, RTI-32, RTI-55, and RTI-142 (see Table 3.1), two mutants, F287K and Y289T, were found to have K_i values that were divergent from the parental hSERT. These two mutants were then fully characterized with the library of cocaine analogs used in the studies discussed in chapter III, and CoMFA maps were generated in an attempt to visualize how the mutated transporters recognized the cocaine derivatives.

Materials and Methods

Generation of hSERT point mutants

hSERT point mutants were generated using the site-directed mutagenesis method described in chapter II. The sense and antisense oligonucleotides used for mutagenesis for the first round of mutants are described in Table 4.1, and for the second round of mutants in Table 4.2. Restriction endonuclease sites were either introduced or deleted with the construction of each mutant, to be used as an initial screen, before dye-termination sequencing was performed by the University of Michigan Medical Center Core Facility (Ann Arbor).

[^{3}H]5-HT uptake assays

Uptake assays were performed on transiently transfected HeLa cells as described in the Methods section of Chapter II. Experiments were performed in triplicate and repeated in at least three separate assays. Statistical analysis was performed with the ANOVA program in Graphpad Prism 3.0 (Graphpad Software, San Diego). Dunnet's tests for mutants determined to be significantly different than hSERT were performed, with hSERT values used as control.

Materials were purchased as described in chapters II and III.

Table 4.1. Oligonucleotides used for the generation of hSERT mutants. REN indicates the restriction endonuclease site introduced or deleted.

Mutant			Sequence		REN
I290V	S	5'	CCTTCCCTTATGTCATCCTTTCAGTACTGCTGGTGAG	3'	ScaI
	AS	5'	CTCACCAGCAGTACTGAAAGGATGACATAAGGGAAGG	3'	
A300V	S	5'	GGTGAGGGGTGTCACCCTCCCGGGAGCCTGGAG	3'	SmaI
	AS	5'	CTCCAGGCTCCCGGGAGGGTGACACCCCTCACC	3'	
V366S	S	5'	CCCTGGTGACCAGCTCGGTCAACTGCATGACGAG	3'	HincII
	AS	5'	CTCGTCATGCAGTTGACCGAGCTGGTCACCAGGG	3'	
V367I	S	5'	GACCAGCGTGATCAACTGCATGACAAGCTTCGTTTC	3'	HindIII
	AS	5'	GAAACGAAGCTTGTCATGCAGTTGATCACGCTGGTC	3'	
M370L	S	5'	GGTGAACTGCTTGACAAGCTTCGTTTCG	3'	HindIII
	AS	5'	CGAAACGAAGCTTGTCAAGCAGTTCACC	3'	
T318S	S	5'	GTCATCTTCTCAGTGCTCGGGTACATGGCTGAG	3'	AvaI
	AS	5'	CTCAGCCATGTACCCGAGCACTGAGAAGATGAC	3'	
N416T	S	5'	GAAGCGATAGCCACCATGCCAGCGTCC	3'	(-)NspI
	AS	5'	GGACGCTGGCATGGTGGCTATCGCTTC	3'	
P418S	S	5'	GCGATAGCCAACATGTCAGCGTCAACTTTCTTTGCC	3'	HincII
	AS	5'	GGCAAAGAAAGTTGACGCTGACATGTTGGCTATCGC	3'	
A419G	S	5'	GCCAACATGCCAGGGTCAACTTTCTTTGCC	3'	HincII
	AS	5'	GGCAAAGAAAGTTGACCCTGGCATGTTGGC	3'	

"(-)" Indicates restriction site native in hSERT and deleted from the mutant SERT

Table 4.2. Oligonucleotides used to generate second-round hSERT mutants. REN indicates the restriction endonuclease site introduced or deleted.

Mutant			Sequence		REN
F287A	S	5'	TGGGTGACAGCCACTGCACCTTATATCATCCTTTCTGTC	3'	BstEII
	AS	5'	GACAGAAAGGATGATATAAGGTGCAGTGGCTGTCACCCA	3'	
F287D	S	5'	AGGTGGTGTGGGTGACCGCCACCGACCCTTATATCATCC	3'	BstEII
	AS	5'	GGATGATATAAGGGTCGGTGGCGGTCACCCACACCACCT	3'	
F287K	S	5'	GGTGGTGTGGGTGACCGCCACCAAGCCTTATATCATCCT	3'	BstEII
	AS	5'	AGGATGATATAAGGCTTGGTGGCGGTCACCCACACCACC	3'	
Y289F	S	5'	CCACCTTCCCTTTTATCATCCTTTCTGTGCTGCTGGTGA	3'	BbvI
	AS	5'	TCACCAGCAGCACAGAAAGGATGATAAAAGGGAAGGTGG	3'	
Y289T	S	5'	CCACCTTCCCTACTATCATCCTTTCTGTGCTGCTGGTGA	3'	BbvI
	AS	5'	TCACCAGCAGCACAGAAAGGATGATAGTAGGGAAGGTGG	3'	

CoMFA for cocaine analogs

Computational molecular modeling studies were performed using the SYBYL v.6.8 software package (Tripos Inc, St. Louis, MO) on a Silicon Graphics O2 workstation (Mountain View, CA) running IRIX v.6.5, as described in chapter III. Briefly, the 3-phenyltropane analogs were sketched using library fragments in SYBYL. A consensus molecule containing the core structure of all the analogs was used as the template for SYBYL's database alignment tool. All of the structures were aligned using the tropane ring skeleton carbon atoms as anchor points. For each of the modeled mutants, three components were determined to be optimal, and q^2 values were as follows: hSERT 0.59, F287K 0.48, and Y289T 0.52.

Results

Initial studies outlined in chapter III determined the differential sensitivity of species-variants of SERT to cocaine and amphetamine derivatives. The potencies of psychostimulants for inhibition of [^{3}H]5-HT uptake were determined at each mutant and are presented in Tables 4.3 and 4.4. The N416T mutant was nonfunctional for 5-HT uptake and will not be further discussed. The K_i values (uptake inhibition) for the initial set of eight active mutants, I290V, A300V, V366S, V371, M370L, T381S, P418S, and A419G, were found to not be statistically different than the values for the parental hSERT. However, mutants V366S, M370L and T381S showed a decrease in transport activity for 5-HT, likely due to decreased V_{max} and K_m values, as well as markedly decreased levels of surface expression (Rodriguez, 2004).

Attempts to make multiple point mutations at positions 287 and 289 provided some interesting results. F287K and Y289T were found to have statistically different K_i values for a subset of the cocaine analogs, as indicated in Table 4.5, whereas two other mutants, F287D and Y289F, did not exhibit a significant level of 5-HT transport, and were thus not able to be characterized. Furthermore, an F287A mutant showed no difference in pharmacology as compared to the parental hSERT. Thus, my efforts focused on a full characterization of the F287K and Y289T mutants with our library of eleven cocaine analogs.

CoMFA of cocaine analogs at hSERT, F287K, and Y289T Mutants

Overall, the CoMFA models depicted in Figure 4.2 are strikingly similar to one another. As was discussed in chapter III, prominent features stand out in each of the three models, and are common to all of them. These features are common to those of the hSERT CoMFA, generated with HEK-293 cell data as discussed in chapter III. Fine differences in the fields depicted in Figure 4.2, as compared to those in chapter III, are likely due to the higher potency of these compounds in transiently-transfected HeLa cells as compared to stably transfected HEK-293 cells. This phenomenon has been observed in the Barker lab as well as other laboratories (Owens et al., 1997). Briefly, the pharmacological data indicate that addition of bulky groups to the amine nitrogen or to the C2 carboxylic acid carbon results in a loss of potency. Furthermore, the blue field, denoting positive charge and hydrogen bond donors being favored, surrounds the aromatic ring. Another region of interest is the area denoting favored steric bulk, in green, near the 4'-substituted position of the aromatic ring. The favorability of steric bulk is evident in that the 4'-ethyl substitution (RTI-83) was more potent than the 4'-methyl congener (RTI-32) of the 3-phenyltropane series (20 nM vs. 42 nM at hSERT).

In summary, the CoMFA maps presented in this chapter show agreement with those in chapter III. No striking differences are evident when comparing the parental hSERT CoMFA with the CoMFA maps generated from data at the F287K and Y289Y mutants (Figure 4.2A-C), but some fine differences exist. Primarily, the yellow field indicating the unfavorability of steric bulk is larger in the CoMFAs for the F287K and Y289T mutants as compared to the same field in the hSERT CoMFA (Figure 4.2A-C).

Also, the green field, indicating favorable steric bulk interactions is larger in the F287K CoMFA as compared to the same field in the hSERT and Y289T models. The red and blue fields, indicating electrostatic interactions with the molecules are identical among hSERT, F287K, and Y289T models.

Table 4.3. K_i values for uptake inhibition of [^{3}H]5-HT in transiently transfected HeLa cells by cocaine derivatives. Values are the Mean ± SEM, and were calculated from at least three independent experiments performed in triplicate.

Construct	Compound, K_i (nM)				
	RTI-55	RTI-311	RTI-121	RTI-120	RTI-32
hSERT	6.8±2	30±10	175±40	28800±1000	60±10
I290V	1.2±0.4	50±10	192±30	>30μM	300±100
A300V	1.2±0.2	50±20	56±20	>30μM	120±40
V366S	3.1±1.9	70±30	190±50	19800±2900	310±80
V367I	16±6	60±10	200±30	>30μM	111±30
M370L	16±2	23±10	235±20	20100±1000	45±10
T381S	7.2±1	50±20	64±11	>30μM	320±220
N416T	Nonfunc.				
P418S	9.2±6	90±20	30±7	>30μM	390±140
A419G	12±2	40±6	78±2	>30μM	50±20

Table 4.4. K_i values for uptake inhibition of [^{3}H]5-HT in transiently transfected HeLa cells by amphetamine derivatives. Values are the Mean ± SEM, and were calclulated from at least three independent experiments performed in triplicate.

Construct	**Compound**						
	K_i, µM						
	MMAI	**DCA**	**DFA**	**3-MTA**	**4-MTA**	**6-Me-MDA**	**2-Me-MDA**
hSERT	0.8±0.3	0.2±0.1	4.0±1.2	1.8±0.4	0.46±0.2	4.4±0.2	0.67±.04
dSERT	12±1.0	1.6±0.4	56±34	7.3±3	4.6±0.2	26±2	27±2
I290V	1.2±0.2	0.32±0.1	4.0±2.9	1.8±0.2	0.03±0.01	7.7±6	0.82±0.1
A300V	0.9±0.3	0.2±0.03	2.0±0.7	0.70±0.5	0.22±0.1	3.6±0.3	1.0±0.05
V366S	1.9±0.7	0.5±0.2	7±1	1.6±1	0.78±0.2	5.2±1	0.49±0.1
V367I	2.9±1	0.3±0.1	4.0±1.2	2.1±0.8	0.7±0.1	3.7±1	0.9±0.4
M370L	0.9±0.1	0.07±.02	2.8±1	0.07±0.3	1.7±1.3	0.19±0.8	1.7±0.4
T381S	2.9±0.9	0.4±0.2	1.2±1.0	0.89±0.3	0.78±0.4	2.0±0.8	1.3±0.8
N416T				NF			
P418S	1.5±0.4	0.2±0.02	4.0±1	1.4±0.7	0.75±0.5	4.0±0.5	1.4±0.1
A419G	1.1±0.2	0.3±0.1	4.0±0.5	0.98±0.3	0.52±0.2	1.9±0.5	1.2±0.5

Table 4.5. K_i values for uptake inhibition of [^{3}H]5-HT in transiently-transfected HeLa cells. Values given are Mean ± SEM, and were calculated from at least three experiments performed in triplicate.

Compound	hSERT	F287K	Y289T
		K_i (nM)	
RTI-55	4 ± 0.1	9.5 ± 0.9**	8.5 ± 0.2**
RTI-112	6.3 ± 1	14± 1**	13 ± 0.6*
RTI-311	14 ± 3	22 ± 4	31 ± 1*
RTI-142	19 ± 2	61 ± 13	46 ± 13
RTI-83	20 ± 0.2	23 ± 4	44 ± 6**
RTI-31	24 ± 2	76 ± 20**	28 ± 4
RTI-32	43 ± 13	9 ± 20	71.7 ± 20
RTI-121	62 ± 13	118± 13*	290 ± 5**
Cocaine	76 ± 17	114 ± 20	104 ± 13
β-CFT	483 ± 36	581 ± 128	780 ± 120
CPT-D-Tartrate	1400 ± 510	1000 ± 148	1400 ± 546

* $P<0.05$, ** $P< 0.001$ as compared to hSERT

Discussion

The studies described in this chapter highlight an important goal of my thesis research: the determination of amino acid residues on SERT that may provide contact sites for cocaine interaction. The species-scanning mutagenesis, producing my first nine mutants, unfortunately did not provide any positive data about the recognition of cocaine or amphetamines by SERT, but did provide a rough roadmap for future studies, namely those involving mutations at positions F287 and Y289.

The data presented in Table 4.5 do show a few key differences in the way the cocaine derivatives are recognized by the mutant transporters F287K and Y289T as compared to hSERT. It is important to recognize that the shifts exhibited for a small subset of these compounds at F287K and Y289T are quite subtle. The loss of potency of some of the derivatives, such as RTI-55, RTI-112, RTI-83, RTI-31 and RTI-121 are subtle, with the most remarkable decrease of potency being approximately four-fold, in the case of β-CFT at Y289T.

While the potency shifts of these compounds is subtle, slight changes in the CoMFA maps depicted in Figure 4.2 can be seen. Both of these subtle changes are steric in nature, and are reflected in the green and yellow fields of the CoMFA maps. First, the green field in the F287K CoMFA map is slightly larger as compared to the same field in the hSERT and Y289T maps. The green field protrudes toward the 3'-position of the aromatic ring of the cocaine analog depicted, RTI-55, indicating a higher degree of favorable steric interactions at this position of the molecule. Considering the data, this interaction is predicted when comparing the compound RTI-112 and RTI-31, which

differ only by the addition of a methyl group at the 3'-position on RTI-112. At hSERT, RTI-112 is somehwhat more potent than RTI-31 (6.3 vs. 23.5 nM), indicating a favorable steric interaction with the addition of the 3'-methyl group. Replacement of phenylalanine with a lysine (F287K) is a dramatic shift in amino acid character, from a non-polar, hydrophobic residue to a basic residue of approximately the same length. At this mutant, the potency shift with the addition of the 3'-methyl group is favorable, with a shift from 76 nM to 14 nM. The addition of the steric bulk is quite favorable for recognition by the F287K mutant, perhaps indicating a higher degree of freedom when a smaller amino acid side chain is occupying this region of interaction. Interestingly, the change in amino acid character from an aromatic phenylalanine to a basic, positive lysine does not appear to reflect any changes in electrostatic effects in the CoMFA maps. This model could explain some distal interaction with an area of SERT near position 287, but it is very difficult, due to the subtle nature of the shifts to be more definitive about the interactions.

Another region of the CoMFA maps that exhibits slight differences between the constructs modeled is in the yellow field of unfavorable steric interactions, located near the amine and the core tropane ring. The Y289T mutant shows a greater level of steric bulk intolerance at this position as compared to hSERT and the F287K mutant. The data indicate that substitution near the amine with bulkier groups, typified by RTI-311 and RTI-121, is less tolerated by the Y289T mutant. The potency shift between hSERT and Y289T for RTI-311 is approximately 2-fold, and the potency shift for RTI-121 is approximately 4-fold. Again, these are subtle pharmacological changes, and the nature of the mutation does not provide a direct explanation for the slight differences in interaction between Y289T, hSERT, and these two compounds. The replacement of the aromatic,

polar tyrosine residue with a polar threonine residue is more of a change in the "reach" of the hydroxyl group on the amino acid, with the tyrosine residue providing a bulkier and longer side-chain. The apparent greater intolerance of steric bulk at this region of the molecule by the Y289T mutant is difficult to explain, and a direct residue-drug contact point does not seem likely. A more reasonable explanation seems to lie in the possible packing of the SERT helices. Since tyrosine and threonine can both participate in hydrogen bonding, an interaction with other helices, through these hydrogen bonds, could alter the conformation of the recognition site for cocaine. This phenomena could be explained because the threonine hydrogen bond could allow tighter intrahelical packing than the tyrosine hydrogen bond, due to decreased bulk. The tighter packing would subsequently disallow increased steric bulk near the bridgehead amine or the adjacent position on the cocaine molecule. This theory is supported by the inactivity of the Y289F mutant. This mutant preserves the aromatic nature of the side-chain, but the replaced phenylalanine cannot participate in hydrogen bonding, as the threonine and tyrosine residues maintain, and an overall disruption of the SERT helical packing motif may be occurring. Also, the possibility exists that an interaction may be occurring between the tyrosine (or threonine) and the protonated amine on the drug molecule, but I recognize that this is in conflict with several lines of evidence implicating TMD I as being part of the permeation pathway, and particularly of Asp98 in TMD I recognizing the amine of substrates. However, the recognition of 5-HT, involving Asp98 and the amine of 5-HT, may be quite different than the way the amine of cocaine interacts with the transporter. A more thorough discussion of Asp98 is discussed in chapter V.

The mutagenesis studies described in this chapter provide some information about two residues that appear to play subtle roles in the recognition of cocaine derivatives. The current published data, outlined in detail in chapter V, has pointed to residues F287 and Y289 as being important for cocaine recognition. In my hands, the shifts in recognition of cocaine derivatives for two mutants, F287K and Y289T, are subtle, yet significant. The recognition of a subset of cocaine derivatives is undoubtedly affected by these mutations; however the exact nature of the recognition that is being disrupted is unclear. The F287K mutant shows some possible promise in the recognition of 4'-phenyl substituents of cocaine derivatives, and additional mutagenesis studies to explore these interactions are warranted.

The data in this chapter provide some clues about cocaine recognition by SERT, but do not reveal the nature of the interactions between the drug molecule and our mutant SERTS. While I have proposed some possible interaction schemes, it is difficult to determine if I have observed changes in direct drug-protein interaction or perhaps changes in the conformation of SERT itself. The promise of these studies is that an overall disruption of SERT is not as likely an explanation, due to the distinct shifts in potency of only a subset of the cocaine derivatives. The disruption of overall SERT intrahelical interactions would, most likely, result in more universal potency shifts for the cocaine derivatives in this study, unless the subtle shifts in conformation affecting only a small region near the binding sites for key functional groups.

CHAPTER V

Proposed Model of SERT Topology and Ligand Recognition

The arrangement of the twelve TMDs in biogenic amine neurotransmitter transporters has been the subject of much research. The majority of this work can be divided into three groups 1) mutagenesis and ligand interaction studies, 2) substituted-cysteine accessibility method studies (SCAM), and 3) zinc-binding studies focused on DAT. While each of these studies has provided a variety of information about this transporter family, detailed structural information about this family of transporters is still lacking. Structural information, in the form of a high-resolution crystal structure has not yet been available, due to a myriad of difficulties ranging from the production of sufficient quantities of stable, non-aggregating transporters, to the inherent problems of crystallizing a membrane-spanning protein. However, some transport proteins have been crystallized, albeit they are members of different protein families (Williams et al., 1999;Williams, 2000;Abramson et al., 2003;Huang et al., 2003).

Escherichia coli Lactose Permease

The crystal structure of the lactose permease from *Escherichia coli* has been recently solved through the pioneering efforts of research groups under the guidance of H. Ronald Kaback and So Iwata (Abramson et al., 2003). This group of researchers recently reported the 3.5 Å resolution structure of lac permease, which had been catalytically "frozen" through the discovery of a point mutation (C154G) that arrested the conformation of lac permease with a bound substrate. Lac permease is a member of the major facilitator superfamily, which transduces the energy stored in a transmembrane proton gradient into a substrate concentration gradient. Whereas the lac permease is a member of a different transporter family than the biogenic amine neurotransmitter transporters, at least one feature is shared by both families. In both the biogenic amine neurotransmitter transporters and the lac permease, twelve TMDs are proposed for the overall structure, however no other comparable features seem to exist. The lac permease structure revealed the presence of two major domains, one linked to the N- and one to the C-terminus, and each having six TMDs (Abramson et al., 2003). The topology of this permease also indicates four short intracellular helices, one at both the N- and C-termini, and two acting as connectors between the two groups of six TMDs. Mechanistically, this transporter appears to follow the alternating-access model presented in Chapter I, with protons and substrate binding the outward facing transporter sequentially, and causing a conformational shift through the modification of specific amino acid residues to an inward facing conformation, where substrate is released (Abramson et al., 2003).

The level of detail of the mechanism published by Kaback's laboratory is impressive. Key residues for the binding of proton and substrate have been delineated, and the intrahelical interactions that are created and disrupted in order to complete the transport cycle have been identified. The mechanistic detail and structural information that has become available has made the lac permease one of the most highly characterized transporters.

Escherichia coli Glycerol-3-Phosphate Transporter

The structure of the *Escherichia coli* Glycerol-3-Phosphate transporter (GlpT) was solved by Huang and coworkers (2003) at a 3.3Å resolution, and shares overall structure similarity with the lactose permease crystallized by Kaback and coworkers (Abramson et al., 2003). The GlpT consists of six-transmembrane helix bundles, each bundle linked to either an N- or C- terminus (Huang et al., 2003). In this structure, four helices form a central pore, supported by the eight remaining scaffolding helices. The mechanism for translocation has been proposed, involving the binding of inorganic phosphate and substrate to the outer face of the transporter, at which time tight helical interactions on the cytoplasmic side of the transporter relax and allow a conformational change to occur that allows substrate to enter the cell (Huang et al., 2003). The proposed mechanism, like that for the lac permease, appears to follow the alternating-access model of transport, with a substrate binding site accessible to a specific side of the membrane depending on the transporter's conformation.

Escherichia coli NhaA Na^+/H^+ Antiporter

The NhaA is an ion-coupled transport protein that uses the energy provided by ionic gradients to facilitate the accumulation of solute and the removal of toxins. Functionally, NhaA uses the proton electrochemical gradient across the inner membrane of *Escherichia coli* to transport Na^+ out of the cytoplasm to adapt to environmental high salinity (Reviewed by Dahl et al., 2004). A three-dimensional electron density map of this transporter was determined by electron cryo-microscopy at a resolution of 7Å (Williams, 2000) and 4Å (Williams et al., 1999). These studies confirmed an overall structure of twelve transmembrane spanning helices and are significant in that the NhaA was the first ion-coupled transporter that was structurally resolved. Briefly, the structure showed 12 tilted, membrane spanning helices, approximately arranged as a dimer of two six-helix bundles, and exhibiting two possible "pores" for the passage of ions (Williams, 2000;Williams et al., 1999). The precise mechanism for ion translocation through this transporter, however, is still under investigation.

Zn^{+2} Inhibition of dopamine transport: a model of three DAT TMDs

An endogenous binding site for the divalent cation Zn^{+2}, was discovered in DAT, as the treatment of DAT-transfected cells with zinc salts shows an inhibition of DA uptake at approximately a 1 micromolar concentration (Norregaard et al., 1998). These studies, coupled with mutagenesis of candidate residues in DAT (H193, H375, and E396), showed that residues at the extracellular faces of TMD VII and TMD VIII, as well

as a residue in extracellular loop II near the extracellular face of TMD III are contributors to a tridentate Zn^{+2} binding site. These features are depicted in Figure 5.1, adapted from data published by Norregaard and others (Norregaard et al., 1998;Loland et al., 1999;Norregaard et al., 2000;Gether et al., 2001), and show a putative binding motif of Zn^{+2} and the key residues in TMDs III, VII, and VIII. The distance requirement for binding Zn^{+2} is quite stringent and limited to approximately 2-2.3 Å (Norregaard et al., 1998;Loland et al., 1999;Norregaard et al., 2000). The ability of zinc to coordinate with these three residues supports the hypothesis that these TMDs must be arranged in close proximity to each other. Also, the ability of zinc to block the inward transport of dopamine supports the hypothesis that interaction of zinc with these three domains, somehow blocks the permeation pathway for DA as a substrate.

Biogenic amine neurotransmitter transporter mutagenesis

Since the cloning of members of the biogenic amine neurotransmitter transporter family, these transporters have been the subject of a significant number of mutagenesis studies. Many residues in the TMDs have been mutated, including TMD I (Barker et al., 1998;Barker et al., 1999;Adkins et al., 2001c;Henry et al., 2003), TMD II (Sato et al., 2004), TMD III (Chen et al., 1997), as well as TMD VII (Penado et al., 1998;Kamdar et al., 2001;Rodriguez, 2004). Key residues have also been found to exist in TMDs V (Lin et al., 2000), XI (Rodriguez, 2004), and XII (Barker and Blakely, 1996;Mitsuhata et al., 1998).

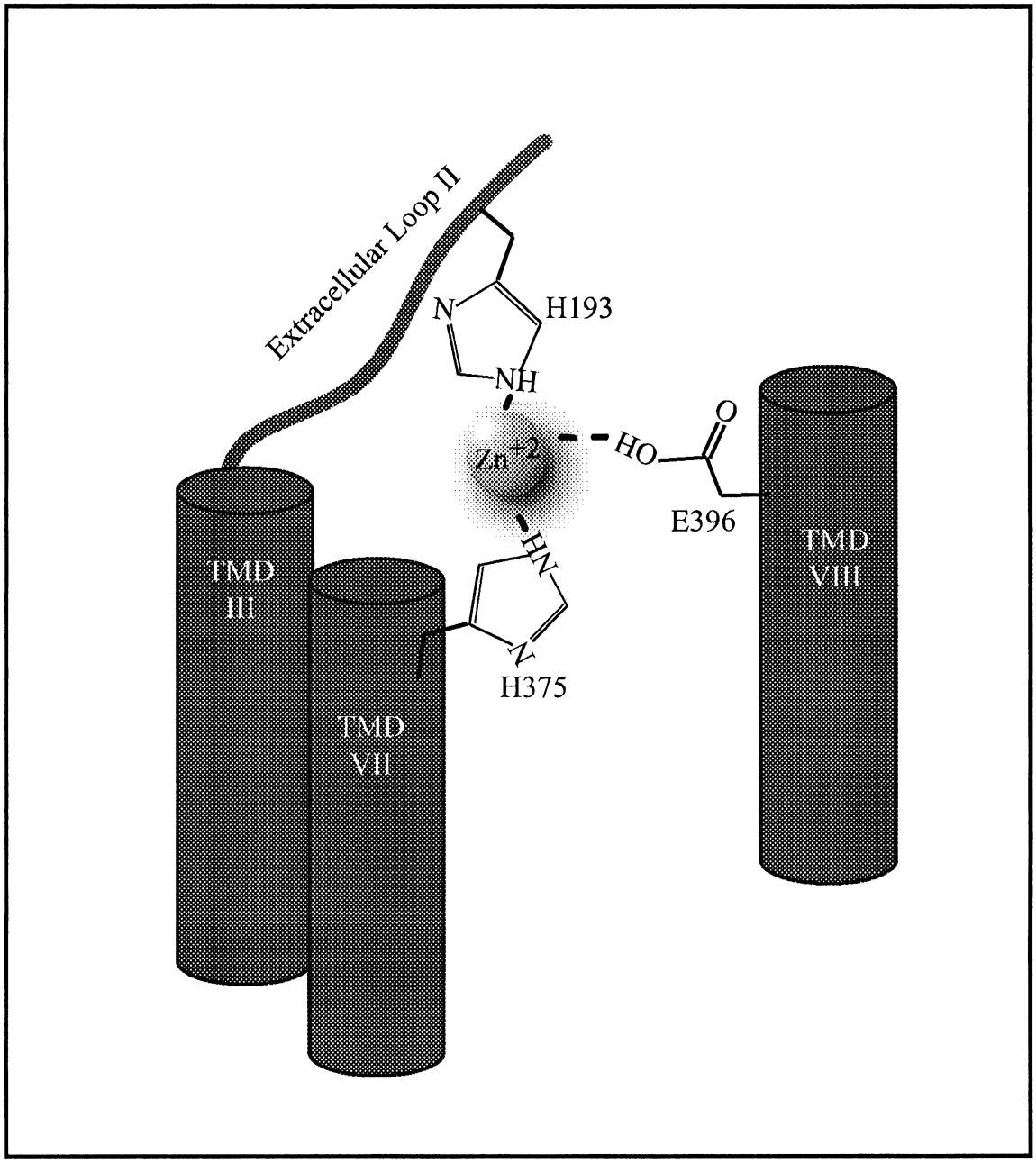

Figure 5.1. An illustration of the endogenous Zn^{+2} binding site on hDAT. Residues H375 (TMD VII), E396 (TMD VIII), and H193 located on extracellular loop II, near the extracellular end of TMD III, coordinate to the divalent cation. The distance constraint for this interaction is 2.0-2.3 Å , which places TMDs III, VII, and VIII within close proximity of one another (Norregaard et al., 1998;Loland et al., 1999).

Mutagenesis studies have provided some fundamental knowledge regarding the role of amino acids in biogenic amine neurotransmitter transporters with regard to antagonist binding, substrate translocation, and structural stability of the protein. Studies by Barker and coworkers identified two residues in TMD I that are critical for the recognition of antagonists and substrates (Barker et al., 1998;1999). Tyr95 (TMD I) in hSERT was found to be critical for the recognition of citalopram and mazindol, and was identified as the primary determinant of hSERT and dSERT species selectivity of those drugs (Barker et al., 1998). Moreover, a recent study that focused on the recognition of tryptamine derivatives, which are SERT substrates, also indicated the role of Tyr95 as a critical determinant of substrate recognition, thus adding another degree of importance to this aromatic residue in TMD I (Adkins et al., 2001c). Furthermore, Barker and coworkers (1999) also showed that Asp98 (TMD I) played a critical role in the recognition of substrates and associated ions. These data are supported by evidence in DAT, that showed the DAT Asp98 equivalent, Asp79, was critical for the recognition of substrate (Kitayama et al., 1993).

An extensive study of TMD I was recently reported by Blakely and coworkers (Henry et al., 2003) that utilized the SCAM method to determine residues of TMD I that were accessible to the aqueous substrate translocation pathway in SERT. This study indicated that SERT mutants D98C, G100C, N101C, W103C, and Y107C were inactivated by MTSET. Moreover, 5-HT provided protection from inactivation at these positions. Interestingly, cocaine also provided protection from MTS inactivation for two of these TMD I mutants, G100C and N101C, indicating a possible role for TMD I in cocaine recognition (Henry et al., 2003).

Mutagenesis and SCAM of TMD II of SERT was also recently reported by Rudnick and coworkers (Sato et al., 2004). In this study, residues in TMD II were mutated to cysteine and reactivity toward membrane-impermeant MTS reagents was determined. Whereas some of the mutants exhibited alterations in cell surface expression levels, no single cysteine mutant was found to have marked reactivity toward the modifying MTS reagents. These data indicate that TMD II, while likely located in close proximity to TMD I due to the short extracellular loop of 7-9 amino acids bridging these domains, does not form a vital face of the membrane-spanning substrate translocation pathway (Sato et al., 2004).

The role of TMD III in cocaine and substrate recognition has also been explored. Two seminal studies, both by Rudnick and coworkers (Chen et al., 1997;Chen and Rudnick, 2000), explored the role of this TMD in SERT function. Briefly, they found that Ile172, when mutated to cysteine, was reactive to MTSET inactivation, indicating that this residue is likely within the substrate permeation pathway (Chen and Rudnick, 2000). Also, the presence of 5-HT prevented this inactivation. Another study revealed that I172C could be protected from inactivation by MTS reagents in the presence of cocaine (Chen et al., 1997). These studies suggest a role for TMD III in ligand recognition, but no clear mechanistic role for residues in TMD III have been determined. Current studies are underway in the Barker lab investigating the role of residues in TMD III for antidepressant and cocaine derivative recognition.

Interestingly, TMD III has provided at least one candidate residue that affects cocaine binding but not substrate recognition. This DAT mutant, F154A, lowers cocaine affinity 10-fold, but does not alter the transport of DA (Lin and Uhl, 2002). These data

could indicate distinct sites of recognition for cocaine and substrate by transporters, although these sites may not be mutually exclusive. The character of this mutant provides evidence that it is possible inhibit these two transporter properties independently. The reported goal of these, and other studies, is to obtain a decrease in cocaine affinity, while leaving substrate transport unaffected. This report provides some hope of the possibility of obtaining a cocaine antagonist for the treatment of addiction. (Lin and Uhl, 2002). Taken together, these studies indicate that TMD III is a likely candidate to form part of the pore-forming region of the transporter as well as a part of the cocaine recognition site.

The role of residues in TMD V has also been investigated with regard to cocaine recognition and conformational stability of the transporter (Kitayama et al., 1996). One residue, Y273 in DAT (equivalent to Y289 in hSERT) was found to affect cocaine binding to DAT, and my data in Chapter IV also show evidence of interaction, but the nature of this interaction is not clear. This particular TMD has not been implicated as part of the permeation pathway, so cocaine interaction may bind to an allosteric location on SERT and modify the ability of substrate to translocate.

TMD VII has also been investigated for its role in the recognition of substrates. One study highlights the importance of a "critical stripe" of residues within TMD VII (Kamdar et al., 2001). Whereas these studies could not detect a difference in MTS reactivity around the putative helix, modification of intrahelical interactions through the addition of cysteine mutations could affect the overall transport mechanism of SERT. Although these studies did not provide evidence that TMD VII has a critical face of the transmembrane-spanning translocation pathway, studies in the Barker lab, as discussed

below, indicate that a face of TMD VII may be accessible to the translocation pore (Rodriguez, 2004).

In contrast to the studies undertaken by Rudnick and coworkers, additional studies utilizing DAT mutants in TMD VII (Kitayama et al., 1992;Kitayama et al., 1993) indicate that residues in TMD VII play a role in substrate translocation in DAT. Also, additional evidence has been reported by Norregaard and coworkers (Norregaard et al., 2003) involving the reactivity of DAT mutant M371C to membrane impermeant MTS reagents, indicating that TMD VII may form part of the pore in DAT. Also, a report by Sur and coworkers (1998) indicates the role of DAT C369 in antidepressant and 5-HT recognition. These studies further implicate a role of TMD VII in the formation of the substrate pore and antagonist binding site(s).

A mutation in TMD XII has demonstrated an importance in the recognition of tricyclic antidepressants (Barker and Blakely, 1996). hSERT F586, located in TMD XII, was mutated to the analogous residue in rSERT, V586. This mutation caused a profound shift in the potency of antidepressants to inhibit 5-HT uptake. Interestingly, the pharmacology of cocaine, *d*-amphetamine, and 5-HT recognition were unaltered by the mutation, indicating a specificity of this aromatic residue for recognizing TCAs (Barker and Blakely, 1996). Another amino acid in TMD XII, S545, was found to affect the interactions of SERT with Na^+ and imipramine (Sur et al., 1997). The interaction of S545 with Na^+ indicates a probable role of TMD XII in the permeation pathway, in addition to its role in the recognition of imipramine. The role of TMD XII in the recognition of cocaine has also been investigated (Mitsuhata et al., 1998). Data from this report indicates a role for DAT Tyr553 in both cocaine recognition and the recognition of

substrate. In consideration with data from the Barker lab (Rodriguez, 2004), the role of TMD XII for forming part of the permeation pore is reasonable, as is the role of TMD XII in the recognition of antagonists.

In another mutagenesis study performed by Norregaard and coworkers (2003), two residues were identified in DAT, M371 in TMD VII and A399 in TMD VIII, that were sensitive to MTSET modification. These residues, equivalent to M386 and A415 in hSERT, showed a unique pattern of protection, whereby M371C modification by MTSET was blocked by DA, but not by cocaine. In contrast, A399C was partially protected from MTS modification by cocaine, but DA had no effect (Norregaard et al., 2003). These data suggest, again, that TMD VII likely bounds the permeation pathway, and perhaps TMD VIII contains part of the cocaine binding site, or perhaps the binding of cocaine produces a conformational change in the transporter that alters the accessibility of A399C to MTSET. Whereas the exact mechanism is unclear, TMD VIII may play a role in cocaine recognition, and due to the proximity restraints explained above, TMD VII may lie very near TMD VIII and contribute to the permeation pathway

Barker lab data involving the putative substrate translocation pathway

Studies in the Barker lab have focused on refining a model of substrate translocation by SERT. In one series of studies by Rodriguez (2004), the role of TMDs VII and XII were explored using the substituted-cysteine accessibility method (SCAM). The results of these studies indicate that two residues in TMD VII, V366 and M370, that were both mutated to cysteine in independent experiments, are both accessible to

modification from the membrane-impermeant methanethiosulfonate reagent, MTSET (Rodriguez, 2004). Additional studies revealed that V366 could be protected from MTS inactivation in the presense of 5-HT and Na^+, indicating that TMD VII likely has a helical face that is exposed to the aqueous pore of the putative translocation pathway. These data are also supported by previous work by Rudnick and coworkers that indicated TMD VII contained a "critical stripe" of residues important for SERT function (Kamdar et al., 2001).

In another series of experiments focused on the role of TMD XI in substrate translocation, a point mutant F556C, located in TMD XI, was reactive to MTSET and 5-HT transport was inhibited. In this scheme, Na^+ and 5-HT were able to partially protect the mutant SERT from MTSET inactivation, indicating that TMD XI is likely to have a helical face exposed to the permeation pathway for 5-HT and associated ions (Rodriguez, 2004).

These studies provide evidence that TMDs VII and XI are likely candidate helices for lining a substrate translocation pathway. A role in cocaine interaction with biogenic amine neurotransmitter transporters in general is also supported, thus any model proposed must take these data into account.

Briefly, my data, as discussed in Chapters III and IV, implicate the region encompassing TMDs V-IX as having critical determinants of psychostimulant recognition. Some of the tested amphetamines, such as DCA and MMAI act as substrates, and determinants for their recognition lies within TMDs V-IX. Also, the recognition of some cocaine derivatives is altered by mutations at positions F287 and Y289, located in

TMD V, indicating a role of these residues as possible cocaine binding contact points, or allosteric regulators of a putative cocaine binding site.

Modeling of biogenic amine neurotransmitter transporters

Recently, researchers have focused on producing putative three-dimensional models of several neurotransmitter transporters. These studies, largely based on available mutagenesis data and the structure of NhaA, provide some insight into the possible arrangement of the twelve TMD structure shared by SERT, DAT and NET.

The first of these recent studies focused on a putative arrangement of hSERT transmembrane helices (Ravna and Edvardsen, 2001). This study focused on ligand interactions with the transporter, as well as data obtained from the Williams projection structure of NhaA (Williams et al., 1999;Williams, 2000). Several key residues in SERT and DAT, established in previous studies were used to model possible interactions with the cocaine molecule, antidepressants, and another substrate, MPP^+. The TMDs containing these residues, TMDs I, III, IV, V, and XI, were arranged as rigid helices, with intermolecular surface contacts with cocaine maintained (Ravna and Edvardsen, 2001).

Briefly, as depicted in Figure 5.2, binding regions were proposed (A), and a putative arrangement of the helices modeled (B). What is distinct about this proposed model are heterogeneous binding sites for cocaine and imipramine, in effect depicting two distinct pores for substrate or ion translocation, with each being occluded by distinct antagonists. Whereas this model fits the "dual pore" model proposed for NhaA (Williams, 2000), data for evidence of more than one pore are lacking for the monoamine

transporters. Also, the role of Asp98 in TMD I as being important for ionic and substrate interactions would not fit with this model containing a more distal, and non-contiguous, imipramine binding site. The proposal of SERT TMD arrangement is a daunting task, as no real structural information is available, and this proposed model fits *some* of the available data in an acceptable manner, but two major problems exist. The first problem is data indicating that the positively charged bridgehead amine on the tropane ring of cocaine is not necessary for binding to biogenic amine neurotransmitter transporters, as discussed in Chapter II (Goulet et al., 2001). If TMD I , namely Asp98 provided a critical contact with the cocaine molecule, the removal of the nitrogen and replacement with an oxygen or carbon, as in the study by Goulet and coworkers (2001) should show loss of potency, and this is not the case. The importance of Asp98 in SERT function has been demonstrated (Barker et al., 1999), and evidence strongly suggests that Asp98 is in the permeation pathway for 5-HT and its cotransported ions, but a direct ionic interaction between this residue and the amine of cocaine has not been firmly established experimentally. The second problem with this model is far more troubling, and is rooted in the arrangement of some of the helices. As previously discussed, zinc binding data indicate

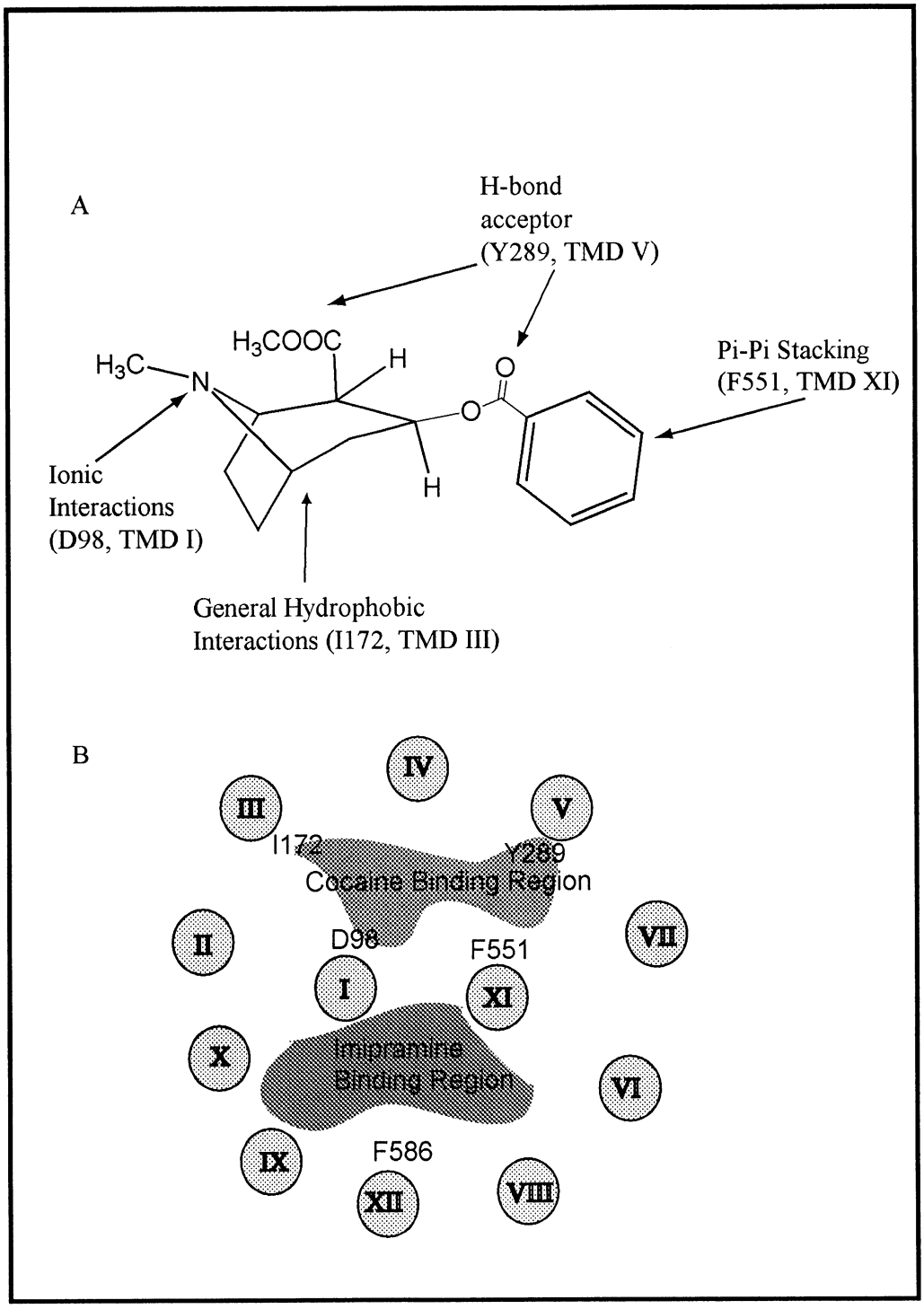

Figure 5.2. (A) Indicates proposed amino acid interactions of SERT with cocaine. (B) Depicts proposed helix packing of SERT, showing two binding regions. Adapted from Ravna and Edvardsen, 2001.

that TMDs III, VII, and VIII are within close proximity to each other. As depicted in Figure 5.2, the model proposed by Ravna and Edvarsen (2001) places TMD VI between TMDs VII and VIII, which violates the proposed distance constraint indicated by zinc binding. Moreover, TMD III is placed on the opposite side of the putative translocation pathway with regard to the placement of TMDs VII and VIII. The arrangement of these helices, in light of current data, does not seem reasonable.

A model for DAT has also been proposed by Ravna and coworkers (Ravna et al., 2003a). This model is similar to the model proposed for SERT, except that the DAT model includes a single translocation pore, which seems more reasonable in light of current data. The DAT model is based on a transport mechanism involving TMDs I, III, IV, V, VII and XI, and key cocaine binding residues Asp79 (hSERT Asp98), Tyr252 (hSERT Tyr267), and Tyr274 (hSERT Tyr289) in hDAT. The proposed model is consistent with the findings of my work (Chapter IV) and others (Kitayama et al., 1996) in that Y289 plays at least a minor role in cocaine recognition. Figure 5.3 is an adaptation of the helix packing and putative binding site for cocaine in this hDAT model. Interestingly, this model lacks the bilateral symmetry common to the solved structures of transporters discussed previously. Also, TMDs VIII, IX, and X seem to be placed in the periphery, having few intrahelical contact points. Moreover, the arrangement of TMDs II, VII, and VIII are still not compatible with the zinc binding data discussed previously. The arrangement of helices I, III, V, VII, XI, and XII seem to be in agreement with current mutagenesis data as discussed previously.

In another report, Ravna and coworkers (2003b) propose possible mechanisms for cocaine and citalopram interactions with monoamine transporters. In this report, the

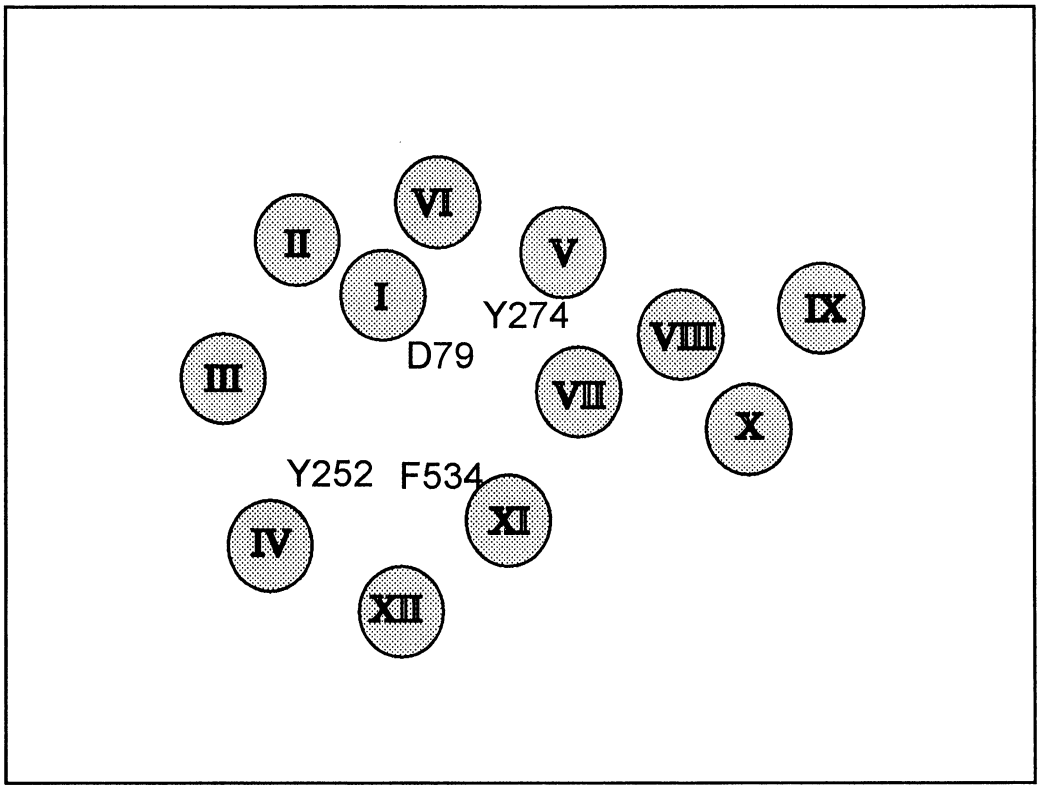

Figure 5.3. Helical packing adapted from the proposed model of hDAT, indicating key amino acids for substrate and cocaine recognition (Ravna et al, 2003).

helical packing model for DAT (as in Figure 5.3) is utilized, and the cocaine binding area includes residues (given according to hSERT positions): Tyr95 (TMD I), Asp98 (TMD I), Ile172 (TMD III), Tyr176 (TMD III), Tyr267 (TMD IV), Tyr289 (TMD V), and Phe551 (TMD II). According to this model, the benzoate of cocaine is proposed to interact and form a hydrogen bond with the hydroxyl group of a tyrosine residue, either Y289 or Y267. Furthermore, the positively charged amine of cocaine is proposed to form a salt bridge with D98. Also, a putative hydrophobic interaction is proposed between Y95 and the tropane ring of cocaine (Ravna et al., 2003b). These proposed interactions are depicted in Figure 5.4.

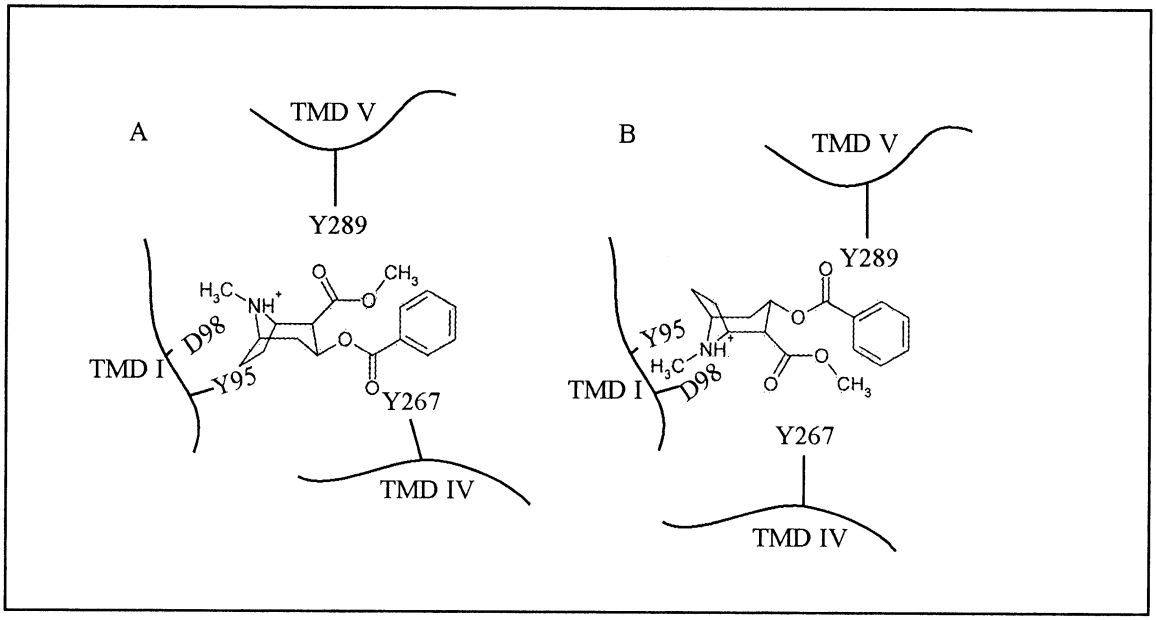

Figure 5.4. Proposed interactions of SERT with cocaine, involving TMDs I, V, and IV, derived from Ravna et al 2003b.

Proposed models considering current data

The models proposed and discussed above each have merit, and are based on information that is currently available about monoamine transporters. However, in light of my data indicating TMDs V-IX contain the major determinants of psychostimulant recognition, the proposal of a new model based on this and previously discussed data is warranted.

The arrangement of the helices in a SERT model must take into account what is known about the transporter, and care must be taken to avoid violating any of the most firmly supported lines of evidence. Primarily, a new model of SERT helix packing should place TMDs III, VII, and VIII within close proximity to each other. The zinc interactions with DAT are well supported, indicating these helices are in very close proximity. Furthermore, in support of the crystal structure data available for other members of the major facilitator superfamily, a model should incorporate an element of bilateral symmetry. Another physical aspect of a model of transporter helix arrangement that must be considered is the length of the intracellular and extracellular loops between the helices. In SERT, these loops range in length from seven to approximately seventy-five amino acids, and the ability of one of these loops to span a reasonable distance, considering its length, must also be considered. Table 5.1 summarizes the putative lengths of the intracellular and extracellular loops.

As reviewed earlier, several TMDs have been shown to be candidates for lining the pore, or translocation pathways for 5-HT and cotransported ions. These helices, in summary, consist of TMDs I, III, V, VII, and XI. Also, when considering the size of

Table 5.1. Putative lengths of intracellular and extracellular loops in SERT.

Loop	Connecting Helices	Approximate Length
EC I	I-II	7 AA
IC I	II-III	19 AA
EC II	III-IV	75 AA
IC II	IV-V	5 AA
EC III	V-VI	25 AA
IC III	VI-VII	11 AA
EC IV	VII-VIII	29 AA
IC IV	VIII-IX	28 AA
EC V	IX-X	12 AA
IC V	X-XI	17 AA
EC VI	XI-XII	14 AA

the cocaine molecule, points of molecular contact with SERT should be within reasonable distance to produce a pocket with the exhibited high-affinity binding. Figure 5.5 depicts an arrangement I propose based on the available data, including data obtained through my own studies and others in the Barker lab. Notably, some features include TMDs I, III, V, VII, XI, and XII providing the major faces of the permeation pathway. Also, TMD IV has a narrow face accessible to the pore. TMDs II, VI, IX, and X, which have not been implicated as being a part of the permeation pathway, are arranged as peripheral helices. The data that support the arrangement of TMDs II, IV, and VI on the peripheral boundaries of SERT come from evidence supporting the formation of SERT oligomers. TMD II has a region of residues identified as a putative leucine-zipper motif that has been suggested as a site of contact for SERT-SERT oligomeric structure formation (Norgaard-Nielsen et al., 2002;Torres et al., 2003a). Furthermore, TMDs IV and VI have also been identified as putative sites for interactions forming DAT dimers, and the positioning of these helices at the outer face of the SERT helix bundle would allow for interactions between transporters to form multimeric units (Hastrup et al., 2001). Finally, my model also incorporates an element of symmetry, as this is a common motif in each of the transporters with solved crystal structures.

The model I propose for the overall structure of SERT is based on the available data. The arrangement of the helices I have presented allows for the established residues to access the permeation pathway. Also, the outer helices arrangement could allow for the formation of SERT higher-ordered structures, such as dimers or multimers. The length of the loops, again, has also been considered.

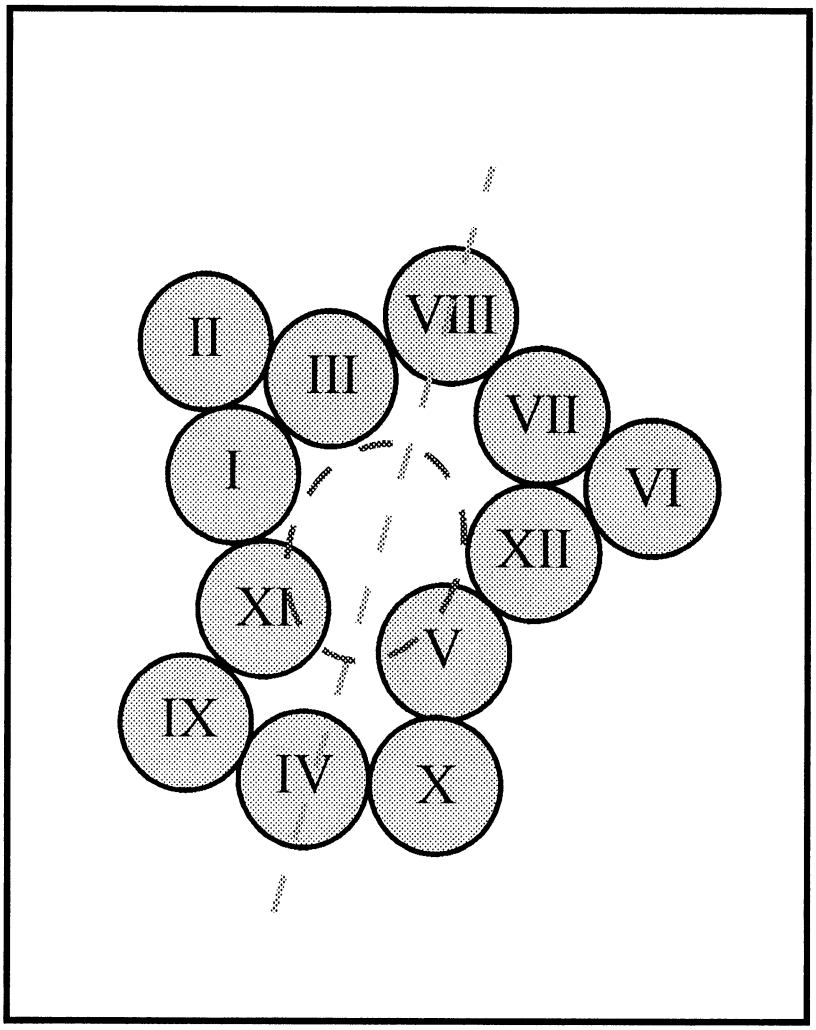

Figure 5.5. Proposed model of helix packing for SERT. The model was constructed utilizing the available data, as discussed, and relative lengths of connecting intrahelical loops. A proposed substrate translocation pathway is outlined in red, and a plane of approximate symmetry is indicated by the broken gray line.

While my proposed model is simply an exploration into a hypothetical structure of SERT helix assembly, I have taken care to not violate any of the established monoamine transporter functional and structural data. The paucity of real structural information for this family of transporters allows for the formulation of such models, which may provide a useful tool for future investigations of biogenic amine neurotransmitter transporters.

I would propose another model for cocaine derivative recognition by SERT. Based upon my data, as well as published reports earlier discussed, the likelihood exists that several candidate residues are important for cocaine derivative recognition. This model, proposed as Figure 5.6, takes into account my data involving the chimeric studies as discussed in chapter III as well as some of the mutagenesis information as discussed in chapter IV.

My model of cocaine derivative interaction with SERT is similar to that proposed by Ravna and coworkers (2003b), with a few key differences. First, I removed the interaction of Asp98 with the protonated amine of the cocaine molecule, or in the case of my model, RTI-55. The importance of Asp98 has been established, and I do not doubt its importance involving substrate recognition. However, the reports by Madras and coworkers (Milius et al., 1991;Goulet et al., 2001) demonstrating that replacement of the amine nitrogen does not affect potency, are convincing evidence that Asp98 is playing another role with the recognition of cocaine as compared to recognition of substrate and other antagonists. Therefore, my model does not include the Asp98-amine site of contact.

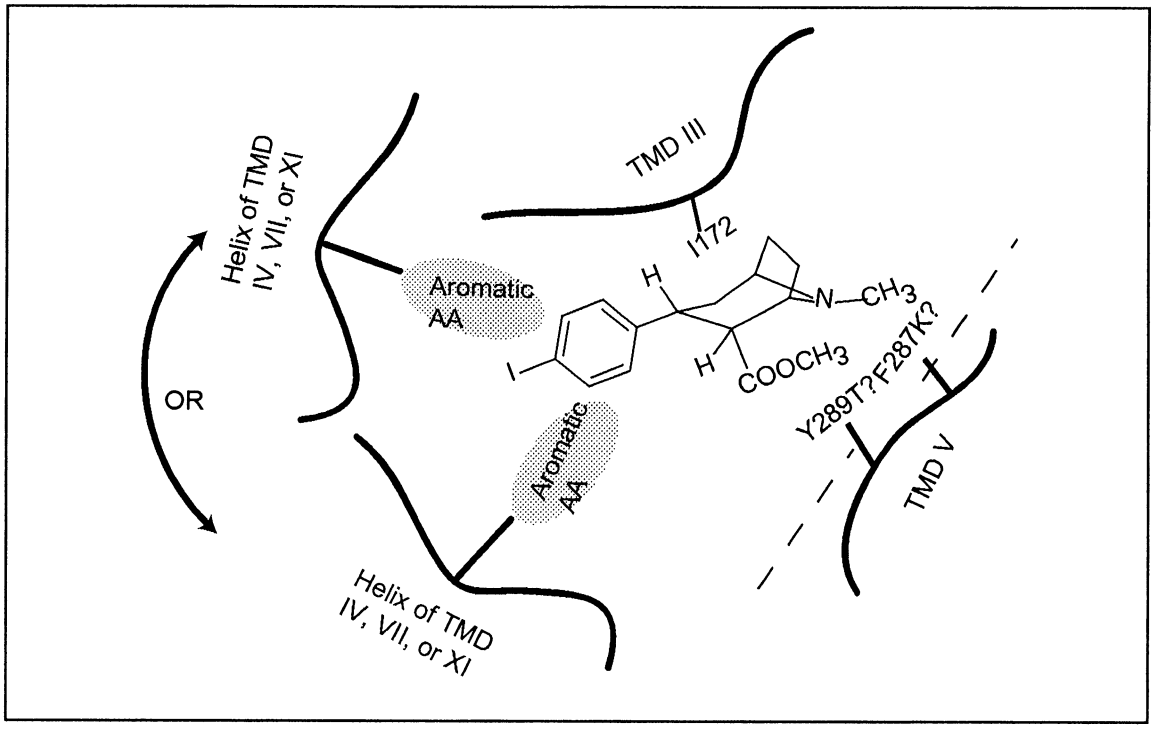

Figure 5.6. Proposed model of cocaine derivative interaction with domains and residues in SERT. RTI-55 is depicted with putative interacting residues within TMDs III, IV, V, XI, or XII.

Second, the interactions with the benzoyl carbonyl oxygen and putative residues Y289 and Y267, which Ravna and coworkers had identified as possibly forming hydrogen bonds is questionable. The presence of these interactions is debatable, as every cocaine derivative tested in my studies, except for CPT-D-tartrate, lacks this functional group and exhibits much higher potency as compared to cocaine. However, this interaction remains in my model, due to consideration of the CPT-D-tartrate data. CPT-D-tartrate is identical to cocaine, with the exception of the benzoyl carbonyl oxygen functional group. The potency of CPT-D-tartrate is markedly lower than cocaine at all transporters discussed in this work, however substitutions on CPT-D-tartrate yield drugs with remarkably higher potency than cocaine. Thus, my model takes into account that these residues, Y289 and/or Y287 may be interacting with this functional group in cocaine, but in substituted derivatives of CPT-D-tartrate, such as RTI-55, alternate stronger interactions are occurring that are not present for either cocaine or CPT-D-tartrate. Possibly, different amino acid interactions are playing a role in the recognition of cocaine and CPT-D-tartrate as compared to the remaining derivatives used in these studies.

A third determinant notable in my model is the presence of an aromatic amino acid at a location within SERT where pi-pi stacking interactions could occur with the aromatic ring on cocaine derivatives. Each of the CoMFA maps generated in chapters III and IV, with regard to cocaine derivatives, has shown a large contribution of positive interacting energy from the aromatic ring. Moreover, Carroll and coworkers (Blough et al., 2002) have demonstrated the presence of a "distal aromatic interaction," in their

models of cocaine interaction with DAT. Whereas this residue has not been identified, I propose this residue exists within TMDs I-IV or IX-XII, as the chimera CoMFA described in chapter III shares this field of positive interaction.

A final interaction, of Ile172 and the tropane ring of the cocaine derivatives is also depicted. Data from the Barker lab (Walline, C.C. and Barker, E.L., unpublished observation) indicates that mutation of this isoleucine, a hydrophobic residue, to methionine, a less bulky and slightly less hydrophobic residue, disrupts the recognition of all cocaine derivatives tested to date. Therefore, an interaction between I172, located in TMD III, and the tropane ring may provide positive binding energy and enhances the recognition of cocaine derivatives by SERT.

Future Studies

The exact mechanism of cocaine interaction with SERT has not yet been established. However, the data presented here and in other studies discussed in this work provide some clues for future experiments that could be performed to more clearly delineate the role of SERT amino acids in the recognition of cocaine derivatives. The investigation of Ile172 is critical in determining the possible role of this residue in the recognition of the tropane ring of cocaine. Studies with this goal could provide information about global binding properties of cocaine to SERT and other monoamine transporters. Further characterization of positions F287 and Y289 are also warranted. Whereas the limited number of mutants described in this study provide some evidence

that these residues may directly interact with cocaine derivatives, additional mutagenesis studies are necessary to more clearly define their possible roles.

A final aspect of investigation is still a relative mystery. The aromatic residues in SERT, and apparently common in DAT and other monoamine transporters, that interact with the phenyl ring of cocaine derivatives have not been identified. Changing the electronic nature of the phenyl ring system, through ring substitution, has been shown to produce profound effects in terms of drug potency. The identification and characterization of these residues is critical to our understanding of cocaine interactions with transporters.

The overall goal of this work has been to determine important features on SERT that play a role in dictating ligand recognition. A more meaningful understanding of how antidepressants, substrates, and cocaine derivatives interact could provide the basis for designing better, more potent, and selective pharmacotherapies for a variety of conditions, from substance abuse to depression and other affective disorders.

As I have described, site-directed mutagenesis, compound library screening, and CoMFA analysis are but a few tools available to investigators seeking to explore molecular recognition of different classes of drugs by biogenic amine transporters.

LIST OF REFERENCES

LIST OF REFERENCES

Mental Disorders in America. http://www.nimh.nih.gov/publicat/numbers.cfm . 1-1-2001.
Internet Reference

Abramson J, Smirnova I, Kasho V, Verner G, Kaback HR, and Iwata S (2003) Structure and Mechanism of the Lactose Permease of Escherichia coli. *Science* **301**:610-615.

Adams SV and DeFelice LJ (2002) Flux coupling in the human serotonin transporter. *Biophys.J.* **83**:3268-3282.

Adams SV and DeFelice LJ (2003) Ionic Currents in the Human Serotonin Transporter Reveal Inconsistencies in the Alternating Access Hypothesis. *Biophys.J.* **85**:1548.

Adkins EM, Barker EL, and Blakely RD (2001a) Interactions of tryptamine derivatives with serotonin transporter species variants implicate transmembrane domain I in substrate recognition. *Mol.Pharmacol.* **59**:514-523.

Adkins EM, Barker EL, and Blakely RD (2001b) Interactions of tryptamine derivatives with serotonin transporter species variants implicate transmembrane domain I in substrate recognition. *Mol.Pharmacol.* **59**:514-523.

Adkins EM, Barker EL, and Blakely RD (2001c) Interactions of Tryptamine Derivatives with Serotonin Transporter Species Variants Implicate Transmembrane Domain I in Substrate Recognition. *Mol.Pharmacol.* **59**:514.

Amara SG and Kuhar MJ (1993) Neurotransmitter transporters: recent progress. *Annu.Rev.Neurosci.* **16**:73-93.

Augustine GJ (2001) How does calcium trigger neurotransmitter release? *Curr Opin Neurobiol* **11**:320-326.

Barker EL and Blakely RD (1995) Norepinephrine and Serotonin Transporters, in *Psychopharmacology: The Fourth Generation of Progress* (Floyd E.Bloom and David J.Kupfer eds) pp 321-333, Raven Press, Ltd., New York.

Barker EL and Blakely RD (1996) Identification of a single amino acid, phenylalanine 586, that is responsible for high affinity interactions of tricyclic antidepressants with the human serotonin transporter. *Mol.Pharmacol.* **50**:957-965.

Barker EL, Kimmel HL, and Blakely RD (1994) Chimeric human and rat serotonin transporters reveal domains involved in recognition of transporter ligands. *Mol.Pharmacol.* **46**:799-807.

Barker EL, Moore KR, Rakhshan F, and Blakely RD (1999) Transmembrane domain I contributes to the permeation pathway for serotonin and ions in the serotonin transporter. *J.Neurosci.* **19**:4705-4717.

Barker EL, Perlman MA, Adkins EM, Houlihan WJ, Pristupa ZB, Niznik HB, and Blakely RD (1998) High affinity recognition of serotonin transporter antagonists defined by species-scanning mutagenesis. An aromatic residue in transmembrane domain I dictates species-selective recognition of citalopram and mazindol. *J.Biol.Chem.* **273**:19459-19468.

Berg JM, Tymoczko JL, and Stryer L (2002) *Biochemistry*. W.H. Freeman and Co., New York.

Berger UV, Gu XF, and Azmitia EC (1992) The substituted amphetamines 3,4-methylenedioxymethamphetamine, methamphetamine, p-chloroamphetamine and fenfluramine induce 5-hydroxytryptamine release via a common mechanism blocked by fluoxetine and cocaine. *Eur J Pharmacol* **215**:153-160.

Blakely RD, Berson HE, Fremeau RT, Jr., Caron MG, Peek MM, Prince HK, and Bradley CC (1991a) Cloning and expression of a functional serotonin transporter from rat brain. *Nature* **354**:66-70.

Blakely RD, Clark J, Rudnick G, and Amara SG (1991b) Vaccinia-T7 RNA polymerase expression system: evaluation for the expression cloning of plasma membrane transporters. *Anal.Biochem.* **194**:302-308.

Blakely RD, De Felice LJ, and Hartzell HC (1994) Molecular physiology of norepinephrine and serotonin transporters. *J.Exp.Biol.* **196**:263-281.

Blakely RD, Ramamoorthy S, Qian Y, Schroeter S, and Bradley CC (1996) Regulation of Antidepressant-Sensitive Serotonin Transporters, in *Neurotransmitter Transporters: Structure, Function and Regulation* (M.E.A.Reith ed) pp 29-72, Humana Press, Inc., Totowa, N.J.

Blough BE, Abraham P, Lewin AH, Kuhar MJ, Boja JW, and Carroll FI (1996) Synthesis and transporter binding properties of 3 beta-(4'-alkyl-, 4'-alkenyl-, and 4'-alkynylphenyl)nortropane-2 beta-carboxylic acid methyl esters: serotonin transporter selective analogs. *J.Med.Chem.* **39**:4027-4035.

Blough BE, Keverline KI, Nie Z, Navarro H, Kuhar MJ, and Carroll FI (2002) Synthesis and transporter binding properties of 3beta-[4'-(phenylalkyl, -phenylalkenyl, and -phenylalkynyl)phenyl]tropane-2beta-carboxylic acid methyl esters: evidence of a remote phenyl binding domain on the dopamine transporter. *J.Med.Chem.* **45**:4029-4037.

Bradford MM (1976) A rapid and sensitive method for the quantitation of microgram quantities of protein utilizing the principle of protein-dye binding. *Anal.Biochem.* **72**:248-254.

Buck KJ and Amara SG (1995) Structural domains of catecholamine transporter chimeras involved in selective inhibition by antidepressants and psychomotor stimulants. *Mol.Pharmacol.* **48**:1030-1037.

Cao Y, Li M, Mager S, and Lester HA (1998) Amino acid residues that control pH modulation of transport-associated current in mammalian serotonin transporters. *J.Neurosci.* **18**:7739-7749.

Carroll FI, Gao YG, Rahman MA, Abraham P, Parham K, Lewin AH, Boja JW, and Kuhar MJ (1991) Synthesis, ligand binding, QSAR, and CoMFA study of 3 beta-(p-substituted phenyl)tropane-2 beta-carboxylic acid methyl esters. *J.Med.Chem.* **34**:2719-2725.

Carroll FI, Mascarella SW, Kuzemko MA, Gao Y, Abraham P, Lewin AH, Boja JW, and Kuhar MJ (1994) Synthesis, ligand binding, and QSAR (CoMFA and classical) study of 3 beta-(3'-substituted phenyl)-, 3 beta-(4'-substituted phenyl)-, and 3 beta-(3',4'-disubstituted phenyl)tropane-2 beta-carboxylic acid methyl esters. *J.Med.Chem.* **37**:2865-2873.

Cavalli A, Poluzzi E, De Ponti F, and Recanatini M (2002) Toward a pharmacophore for drugs inducing the long QT syndrome: insights from a CoMFA study of HERG K(+) channel blockers. *J Med Chem* **45**:3844-3853.

Chapman ER (2002) Synaptotagmin: a Ca(2+) sensor that triggers exocytosis? *Nat Rev Mol Cell Biol* **3**:498-508.

Chen JG, Liu-Chen S, and Rudnick G (1998) Determination of external loop topology in the serotonin transporter by site-directed chemical labeling. *J.Biol.Chem.* **273**:12675-12681.

Chen JG and Rudnick G (2000) Permeation and gating residues in serotonin transporter. *Proc.Natl.Acad.Sci.U.S.A.2000.Feb.1.;97.(3.):1044.-9.* **97**:1044-1049.

Chen JG, Sachpatzidis A, and Rudnick G (1997) The third transmembrane domain of the serotonin transporter contains residues associated with substrate and cocaine binding. *J.Biol.Chem.* **272**:28321-28327.

Chen YA, Scales SJ, Duvvuri V, Murthy M, Patel SM, Schulman H, and Scheller RH (2001) Calcium Regulation of Exocytosis in PC12 Cells. *J.Biol.Chem.* **276**:26680-26687.

Cheng Y and Prusoff WH (1973) Relationship between the inhibition constant (K1) and the concentration of inhibitor which causes 50 per cent inhibition (I50) of an enzymatic reaction. *Biochem.Pharmacol.* **22**:3099-3108.

Corey JL, Quick MW, Davidson N, Lester HA, and Guastella J (1994) A cocaine-sensitive Drosophila serotonin transporter: cloning, expression, and electrophysiological characterization. *Proc.Natl.Acad.Sci.U.S.A* **91**:1188-1192.

Dahl SG, Ravna AW, and Sylte I (2004) Structures and models of transporter proteins. *J Pharmacol Exp.Ther.*

Danek Burgess KS and Justice JB, Jr. (1999) Effects of serine mutations in transmembrane domain 7 of the human norepinephrine transporter on substrate binding and transport. *J.Neurochem.* **73**:656-664.

DeFelice LJ and Galli A (1998) Fluctuation analysis of norepinephrine and serotonin transporter currents. *Methods Enzymol.* **296**:578-593.

Demchyshyn LL, Pristupa ZB, Sugamori KS, Barker EL, Blakely RD, Wolfgang WJ, Forte MA, and Niznik HB (1994) Cloning, expression, and localization of a chloride-facilitated, cocaine-sensitive serotonin transporter from Drosophila melanogaster. *Proc.Natl.Acad.Sci.U.S.A.* **91**:5158-5162.

Dulubova I, Sugita S, Hill S, Hosaka M, Fernandez I, Sudhof TC, and Rizo J (1999) A conformational switch in syntaxin during exocytosis: role of munc18. *EMBO J* **18**:4372-4382.

Duman JG and Forte JG (2003) What is the role of SNARE proteins in membrane fusion? *Am J Physiol Cell Physiol* **285**:C237-C249.

Duman RS (1998) Novel therapeutic approaches beyond the serotonin receptor. *Biological Psychiatry* **44**:324-335.

Eiden LE (2000) The vesicular neurotransmitter transporters: current perspectives and future prospects. *FASEB J* **14**:2396-2400.

Erickson JD and Varoqui H (2000) Molecular analysis of vesicular amine transporter function and targeting to secretory organelles. *FASEB J* **14**:2450-2458.

Fang H, Yanhong L, Jian F, Lihe G, and Schwartz W (1998) Identification of Ser354 and Ser357 involved in the function of norepinephrine transporter. *Chinese Science Bulletin* **43**:1541-1544.

Fon EA and Edwards RH (2001) Molecular mechanisms of neurotransmitter release. *Muscle Nerve* **24**:581-601.

Fuerst TR, Niles EG, Studier FW, and Moss B (1986) Eukaryotic transient-expression system based on recombinant vaccinia virus that synthesizes bacteriophage T7 RNA polymerase. *Proc.Natl.Acad.Sci.U.S.A* **83**:8122-8126.

Gainetdinov RR, Mohn AR, Bohn LM, and Caron MG (2001) Glutamatergic modulation of hyperactivity in mice lacking the dopamine transporter. *Proc.Natl.Acad.Sci.U.S.A* **98**:11047-11054.

Gainetdinov RR, Sotnikova TD, and Caron MG (2002) Monoamine transporter pharmacology and mutant mice. *Trends Pharmacol Sci* **23**:367-373.

Galli A, Blakely RD, and DeFelice LJ (1996) Norepinephrine transporters have channel modes of conduction. *Proc.Natl.Acad.Sci U.S.A* **93**:8671-8676.

Galli A, Petersen CI, deBlaquiere M, Blakely RD, and DeFelice LJ (1997) Drosophila serotonin transporters have voltage-dependent uptake coupled to a serotonin-gated ion channel. *J Neurosci* **17**:3401-3411.

Ganong WF (1995) *Review of Medical Physiology*. Appleton and Lange, Norwalk, Connecticut.

Geppert M, Goda Y, Hammer RE, Li C, Rosahl TW, Stevens CF, and Sudhof TC (1994) Synaptotagmin I: a major Ca2+ sensor for transmitter release at a central synapse. *Cell* **79**:717-727.

Gether U, Norregaard L, and Loland CJ (2001) Delineating structure-function relationships in the dopamine transporter from natural and engineered Zn2+ binding sites. *Life Sci* **68**:2187-2198.

Giros B, Wang YM, Suter S, McLeskey SB, Pifl C, and Caron MG (1994) Delineation of discrete domains for substrate, cocaine, and tricyclic antidepressant interactions using chimeric dopamine-norepinephrine transporters. *J.Biol.Chem.* **269**:15985-15988.

Goulet M, Miller GM, Bendor J, Liu S, Meltzer PC, and Madras BK (2001) Non-amines, drugs without an amine nitrogen, potently block serotonin transport: novel antidepressant candidates? *Synapse* **42**:129-140.

Green AR, Mechan AO, Elliott JM, O'Shea E, and Colado MI (2003) The Pharmacology and Clinical Pharmacology of 3,4-Methylenedioxymethamphetamine (MDMA, "Ecstasy"). *Pharmacol.Rev.* **55**:463-508.

Hastrup H, Karlin A, and Javitch JA (2001) Symmetrical dimer of the human dopamine transporter revealed by cross-linking Cys-306 at the extracellular end of the sixth transmembrane segment. *Proc.Natl.Acad.Sci.U.S.A* **98**:10055-10060.

Henry LK, Adkins EM, Han Q, and Blakely RD (2003) Serotonin and Cocaine-sensitive Inactivation of Human Serotonin Transporters by Methanethiosulfonates Targeted to Transmembrane Domain I. *J.Biol.Chem.* **278**:37052-37063.

Hille B (2001) *Ion Channels of Excitable Membranes*. Sinauer Associates, Inc..

Hoffman BJ, Mezey E, and Brownstein MJ (1991) Cloning of a serotonin transporter affected by antidepressants. *Science* **254**:579-580.

Holmquist CR, Keverline-Frantz KI, Abraham P, Boja JW, Kuhar MJ, and Carroll FI (1996) 3 alpha-(4'-substituted phenyl)tropane-2 beta-carboxylic acid methyl esters: novel ligands with high affinity and selectivity at the dopamine transporter. *J.Med.Chem.* **39**:4139-4141.

Horn AS (1973) Structure activity relations for the inhibition of 5-HT uptake into rat hypothalamic homogenates by serotonin and tryptamine analogues. *J.Neurochem.* **21**:883-888.

Horn AS, Baumgarten HG, and Schlosserberger HG (1973) Inhibition of the uptake of 5-hydroxytryptamine, noradrenaline and dopamine into rat brain homogenates by various hydroxylated tryptamines. *J.Neurochem.* **21**:233-236.

Horn AS and Trace RC (1974) Structure-activity relations for the inhibition of 5-hydroxytryptamine uptake by tricyclic antidepressants into synaptosomes from serotoninergic neurones in rat brain homogenates. *Br.J.Pharmacol.* **51**:399-403.

Hotchkiss AJ and Gibb JW (1980) Long-term effects of multiple doses of methamphetamine on tryptophan hydroxylase and tyrosine hydroxylase activity in rat brain. *J Pharmacol Exp.Ther* **214**:257-262.

Howell LL and Wilcox KM (2001) The Dopamine Transporter and Cocaine Medication Development: Drug Self-Administration in Nonhuman Primates. *J.Pharmacol.Exp.Ther.* **298**:1-6.

Huang X, Marona-Lewicka D, and Nichols DE (1992) p-methylthioamphetamine is a potent new non-neurotoxic serotonin-releasing agent. *Eur J Pharmacol* **229**:31-38.

Huang Y, Lemieux MJ, Song J, Auer M, and Wang DN (2003) Structure and Mechanism of the Glycerol-3-Phosphate Transporter from Escherichia coli. *Science* **301**:616-620.

Humphreys CJ, Wall SC, and Rudnick G (1994) Ligand binding to the serotonin transporter: equilibria, kinetics, and ion dependence. *Biochemistry* **33**:9118-9125.

Jones SR, Joseph JD, Barak LS, Caron MG, and Wightman RM (1999) Dopamine neuronal transport kinetics and effects of amphetamine. *J.Neurochem.* **73**:2406-2414.

Jones SR, Gainetdinov RR, Wightman RM, and Caron MG (1998) Mechanisms of Amphetamine Action Revealed in Mice Lacking the Dopamine Transporter. *J.Neurosci.* **18**:1979-1986.

Kahlig KM, Javitch JA, and Galli A (2003) Amphetamine regulation of dopamine transport: Combined measurements of transporter currents and transporter imaging support the endocytosis of an active carrier. *J Biol Chem*.

Kamdar G, Penado KM, Rudnick G, and Stephan MM (2000) Functional role of critical stripe residues in transmembrane span 7 of the serotonin transporter: effects of Na{super+}, Li{super+} and methanethiosulfonate reagents. *J.Biol.Chem.* **75**.

Kamdar G, Penado KM, Rudnick G, and Stephan MM (2001) Functional role of critical stripe residues in transmembrane span 7 of the serotonin transporter: effects of Na{super+}, Li{super+} and methanethiosulfonate reagents. *J.Biol.Chem.* **276**:4038-4045.

Kasai H (1993) Cytosolic Ca2+ gradients, Ca2+ binding proteins and synaptic plasticity. *Neurosci Res* **16**:1-7.

Keyes SR and Rudnick G (1982) Coupling of transmembrane proton gradients to platelet serotonin transport. *J Biol Chem* **257**:1172-1176.

Kitayama S, Morita K, Dohi T, Wang JB, Davis SC, and Uhl GR (1996) Dissection of dopamine and cocaine binding sites on the rat dopamine transporter expressed in COS cells. *Ann.N.Y.Acad.Sci.* **801**:388-393.

Kitayama S, Shimada S, Xu H, Markham L, Donovan DM, and Uhl GR (1992) Dopamine Transporter site-directed mutations differentially alter substrate transport and cocaine binding. *Proc.Natl.Acad.Sci U.S.A* **89**:7782-7785.

Kitayama S, Wang JB, and Uhl GR (1993) Dopamine transporter mutants selectively enhance MPP transport. *Synapse* **15**:58-62.

Kogan FJ, Nichols WK, and Gibb JW (1976) Influence of methamphetamine on nigral and striatal tyrosine hydroxylase activity and on striatal dopamine levels. *Eur J Pharmacol* **36**:363-371.

Kuczenski R and Segal DS (1994) Neurochemistry of Amphetamine, in *Amphetamine And Its Analogs* (Cho AK and Segal DS eds) pp 81-113, Academic Press, Inc., San Diego.

Kuo CL, Assefa H, Kamath S, Brzozowski Z, Slawinski J, Saczewski F, Buolamwini JK, and Neamati N (2004) Application of CoMFA and CoMSIA 3D-QSAR and docking studies in optimization of mercaptobenzenesulfonamides as HIV-1 integrase inhibitors. *J Med Chem* **47**:385-399.

Li AH, Moro S, Forsyth N, Melman N, Ji XD, and Jacobson KA (1999) Synthesis, CoMFA analysis, and receptor docking of 3,5-diacyl-2, 4-dialkylpyridine derivatives as selective A3 adenosine receptor antagonists. *J.Med.Chem.* **42**:706-721.

Lin RC and Scheller RH (2000) Mechanisms of synaptic vesicle exocytosis. *Annu.Rev Cell Dev.Biol* **16**:19-49.

Lin Z and Uhl GR (2002) Dopamine transporter mutants with cocaine resistance and normal dopamine uptake provide targets for cocaine antagonism. *Mol.Pharmacol.* **61**:885-891.

Lin Z, Wang W, and Uhl GR (2000) Dopamine Transporter Tryptophan Mutants Highlight Candidate Dopamine- and Cocaine-Selective Domains. *Mol.Pharmacol.* **58**:1581.

Loder MK and Melikian HE (2003) The Dopamine Transporter Constitutively Internalizes and Recycles in a Protein Kinase C-regulated Manner in Stably Transfected PC12 Cell Lines. *J.Biol.Chem.* **278**:22168-22174.

Loland CJ, Norregaard L, and Gether U (1999) Defining proximity relationships in the tertiary structure of the dopamine transporter. Identification of a conserved glutamic acid as a third coordinate in the endogenous Zn(2+)-binding site. *J.Biol.Chem.* **274**:36928-36934.

Lonart G and Sudhof TC (2000) Assembly of SNARE core complexes prior to neurotransmitter release sets the readily releasable pool of synaptic vesicles. *J Biol Chem* **275**:27703-27707.

Mager S, Cao Y, and Lester HA (1998) Measurement of transient currents from neurotransmitter transporters expressed in Xenopus oocytes. *Methods Enzymol.* **296**:551-566.

Martelli AM, Baldini G, Tabellini G, Koticha D, Bareggi R, and Baldini G (2000) Rab3A and Rab3D control the total granule number and the fraction of granules docked at the plasma membrane in PC12 cells. *Traffic.* **1**:976-986.

Milius RA, Saha JK, Madras BK, and Neumeyer JL (1991) Synthesis and receptor binding of N-substituted tropane derivatives. High-affinity ligands for the cocaine receptor. *J.Med.Chem.* **34**:1728-1731.

Mitsuhata C, Kitayama S, Morita K, Vandenbergh D, Uhl GR, and Dohi T (1998) Tyrosine-533 of rat dopamine transporter: involvement in interactions with 1-methyl-4-phenylpyridinium and cocaine. *Brain Res Mol Brain Res* **56**:84-88.

Moriyama Y and Futai M (1990a) H(+)-ATPase, a primary pump for accumulation of neurotransmitters, is a major constituent of brain synaptic vesicles. *Biochem Biophys Res Commun* **173**:443-448.

Moriyama Y and Futai M (1990b) Presence of 5-hydroxytryptamine (serotonin) transport coupled with vacuolar-type H(+)-ATPase in neurosecretory granules from bovine posterior pituitary. *J Biol Chem* **265**:9165-9169.

Nelson PJ and Rudnick G (1979) Coupling between platelet 5-hydroxytryptamine and potassium transport. *J Biol Chem* **254**:10084-10089.

Neumeyer JL, Tamagnan G, Wang S, Gao Y, Milius RA, Kula NS, and Baldessarini RJ (1996) N-substituted analogs of 2 beta-carbomethoxy-3 beta- (4'-iodophenyl)tropane

Neumeyer JL, Tamagnan G, Wang S, Gao Y, Milius RA, Kula NS, and Baldessarini RJ (1996) N-substituted analogs of 2 beta-carbomethoxy-3 beta- (4'-iodophenyl)tropane (beta-CIT) with selective affinity to dopamine or serotonin transporters in rat forebrain. *J.Med.Chem.* **39**:543-548.

Neumeyer JL, Wang S, Gao Y, Milius RA, Kula NS, Campbell A, Baldessarini RJ, Zea-Ponce Y, Baldwin RM, and Innis RB (1994) N-omega-fluoroalkyl analogs of (1R)-2 beta-carbomethoxy-3 beta-(4-iodophenyl)-tropane (beta-CIT): radiotracers for positron emission tomography and single photon emission computed tomography imaging of dopamine transporters. *J.Med.Chem.* **37**:1558-1561.

Newman AH, Izenwasser S, Robarge MJ, and Kline RH (1999) CoMFA study of novel phenyl ring-substituted 3alpha-(diphenylmethoxy)tropane analogues at the dopamine transporter. *J.Med.Chem.* **42**:3502-3509.

Nichols DE (1986) Differences between the mechanism of action of MDMA, MBDB, and the classic hallucinogens. Identification of a new therapeutic class: entactogens. *J Psychoactive Drugs* **18**:305-313.

Nichols DE (1994) Medicinal Chemistry and Structure-Activity Relationships, in *Amphetamine and Its Analogs* (Cho AK and Segal D.S. eds) pp 3-41, Academic Press, San Diego.

Nichols DE, Brewster WK, Johnson MP, Oberlender R, and Riggs RM (1990) Nonneurotoxic tetralin and indan analogues of 3,4-(methylenedioxy)amphetamine (MDA). *J Med Chem* **33**:703-710.

Norgaard-Nielsen K, Norregaard L, Hastrup H, Javitch JA, and Gether U (2002) Zn2+ site engineering at the oligomeric interface of the dopamine transporter. *FEBS Letters* **524**:87-91.

Norregaard L, Frederiksen D, Nielsen EO, and Gether U (1998) Delineation of an endogenous zinc-binding site in the human dopamine transporter. *EMBO J.* **17**:4266-4273.

Norregaard L, Visiers I, Loland CJ, Ballesteros J, Weinstein H, and Gether U (2000) Structural probing of a microdomain in the dopamine transporter by engineering of artificial Zn2+ binding sites. *Biochemistry* **39**:15836-15846.

Norregaard L, Loland CJ, and Gether U (2003) Evidence for Distinct Sodium-, Dopamine-, and Cocaine-dependent Conformational Changes in Transmembrane Segments 7 and 8 of the Dopamine Transporter. *J.Biol.Chem.* **278**:30587-30596.

Owens MJ, Morgan WN, Plott SJ, and Nemeroff CB (1997) Neurotransmitter receptor and transporter binding profile of antidepressants and their metabolites. *J.Pharmacol.Exp.Ther.* **283**:1305-1322.

Paczkowski FA and Bryan-Lluka LJ (2001) Tyrosine residue 271 of the norepinephrine transporter is an important determinant of its pharmacology. *Brain Res.Mol.Brain Res.* **97**:32-42.

Paczkowski FA and Bryan-Lluka LJ (2002) Amino acids involved in differences in the pharmacological profiles of the rat and human noradrenaline transporters. *Naunyn Schmiedebergs Arch.Pharmacol.* **365**:312-317.

Padbury JF, Tseng YT, McGonnigal B, Penado K, Stephan M, and Rudnick G (1997) Placental biogenic amine transporters: cloning and expression. *Brain Res.Mol.Brain Res.* **45**:163-168.

Parsons SM (2000) Transport mechanisms in acetylcholine and monoamine storage. *FASEB J* **14**:2423-2434.

Penado KM, Rudnick G, and Stephan MM (1998) Critical amino acid residues in transmembrane span 7 of the serotonin transporter identified by random mutagenesis. *J.Biol.Chem.* **273**:28098-28106.

Peter D, Finn III JP, Merickel A, Liu Y, and Edwards RH (1997) Molecular Analysis of Serotonin Packaging into Secretory Vesicles, in *Serotonergic Neurons and 5-HT Receptors in the CNS* (Baumgarten HG and Gothert M eds) pp 131-148, Springer-Verlag, Berlin.

Petersen CI and DeFelice LJ (1999) Ionic interactions in the Drosophila serotonin transporter identify it as a serotonin channel. *Nat.Neurosci.* **2**:605-610.

Ramamoorthy S, Bauman AL, Moore KR, Han H, Yang-Feng T, Chang AS, Ganapathy V, and Blakely RD (1993) Antidepressant- and cocaine-sensitive human serotonin transporter: molecular cloning, expression, and chromosomal localization. *Proc.Natl.Acad.Sci.U.S.A* **90**:2542-2546.

Ravna AW and Edvardsen O (2001) A putative three-dimensional arrangement of the human serotonin transporter transmembrane helices: a tool to aid experimental studies. *J.Mol.Graph.Model.* **20**:133-144.

Ravna AW, Sylte I, and Dahl SG (2003a) Molecular model of the neural dopamine transporter. *J Comput Aided Mol Des* **17**:367-382.

Ravna AW, Sylte I, and Dahl SG (2003b) Molecular Mechanism of Citalopram and Cocaine Interactions with Neurotransmitter Transporters. *J.Pharmacol.Exp.Ther.* **307**:34-41.

Ricaurte GA, Seiden LS, and Schuster CR (1984) Further evidence that amphetamines produce long-lasting dopamine neurochemical deficits by destroying dopamine nerve fibers. *Brain Res* **303**:359-364.

Ritz MC, Lamb RJ, Goldberg SR, and Kuhar MJ (1987) Cocaine receptors on dopamine transporters are related to the self-administration of cocaine. *Science* **237**:1219-1223.

Robertson DW, Jones ND, Swartzendruber JK, Yang KS, and Wong DT (1988) Molecular structure of fluoxetine hydrochloride, a highly selective serotonin-uptake inhibitor. *J.Med.Chem.* **31**:185-189.

Rocha BA, Fumagalli F, Gainetdinov RR, Jones SR, Ator R, Giros B, Miller GW, and Caron MG (1998a) Cocaine self-administration in dopamine-transporter knockout mice. *Nat.Neurosci.* **1**:132-137.

Rocha BA, Fumagalli F, Gainetdinov RR, Jones SR, Ator R, Giros B, Miller GW, and Caron MG (1998b) Cocaine self-administration in dopamine-transporter knockout mice [see comments] [published erratum appears in Nat Neurosci 1998 Aug;1(4):330]. *Nat.Neurosci.* **1**:132-137.

Rodriguez, G. J. Molecular Insights Into the Translocation Mechanism for Substrates by the Serotonin Transporter. 2004. Purdue University.
Ref Type: Thesis/Dissertation

Rodriguez GJ, Roman DL, White KJ, Nichols DE, and Barker EL (2003) Distinct Recognition of Substrates by the Human and Drosophila Serotonin Transporters. *J.Pharmacol.Exp.Ther.* **306**:338-346.

Roman DL, Saldana SN, Nichols DE, Carroll FI, and Barker EL (2004) Distinct molecular recognition of psychostimulants by human and Drosophila serotonin transporters. *J Pharmacol Exp.Ther* **308**:679-687.

Roubert C, Cox PJ, Bruss M, Hamon M, Bonisch H, and Giros B (2001) Determination of residues in the norepinephrine transporter that are critical for tricyclic antidepressant affinity. *J.Biol.Chem.* **276**:8254-8260.

Rudnick G (1977) Active transport of 5-hydroxytryptamine by plasma membrane vesicles isolated from human blood platelets. *J Biol Chem* **252**:2170-2174.

Rudnick G (1998) Bioenergetics of neurotransmitter transport. *J Bioenerg Biomembr* **30**:173-185.

Rudnick G and Clark J (1993) From synapse to vesicle: the reuptake and storage of biogenic amine neurotransmitters. *Biochim.Biophys.Acta* **1144**:249-263.

Rudnick G and Wall SC (1992) The molecular mechanism of "ecstasy" [3,4-methylenedioxy-methamphetamine (MDMA)]: serotonin transporters are targets for MDMA-induced serotonin release. *Proc.Natl.Acad.Sci U.S.A* **89**:1817-1821.

Sandhu SK, Ross LS, and Gill SS (2002) A cocaine insensitive chimeric insect serotonin transporter reveals domains critical for cocaine interaction. *Eur.J.Biochem.* **269**:3934-3944.

Sato Y, Zhang YW, Androutsellis-Theotokis A, and Rudnick G (2004) Analysis of transmembrane domain 2 of rat serotonin transporter by cysteine scanning mutagenesis. *J.Biol.Chem.*M312194200.

Scheffel U, Lever JR, Abraham P, Parham KR, Mathews WB, Kopajtic T, Carroll FI, and Kuhar MJ (1997) N-substituted phenyltropanes as in vivo binding ligands for rapid imaging studies of the dopamine transporter. *Synapse* **25**:345-349.

Schneggenburger R and Neher E (2000) Intracellular calcium dependence of transmitter release rates at a fast central synapse. *Nature* **406**:889-893.

Seiden LS, Fischman MW, and Schuster CR (1976) Long-term methamphetamine induced changes in brain catecholamines in tolerant rhesus monkeys. *Drug Alcohol Depend.* **1**:215-219.

Shafqat S, Velaz-Faircloth M, Guadano-Ferraz A, and Fremeau RT, Jr. (1993) Molecular characterization of neurotransmitter transporters. *Mol.Endocrinol.* **7**:1517.

Sora I, Hall FS, Andrews AM, Itokawa M, Li XF, Wei HB, Wichems C, Lesch KP, Murphy DL, and Uhl GR (2001) Molecular mechanisms of cocaine reward: combined dopamine and serotonin transporter knockouts eliminate cocaine place preference. *Proc.Natl.Acad.Sci.U.S.A* **98**:5300-5305.

Spafford JD and Zamponi GW (2003) Functional interactions between presynaptic calcium channels and the neurotransmitter release machinery. *Curr Opin Neurobiol* **13**:308-314.

Sprague JE, Everman SL, and Nichols DE (1998) An integrated hypothesis for the serotonergic axonal loss induced by 3,4-methylenedioxymethamphetamine. *Neurotoxicology* **19**:427-441.

Stokes PE and Holtz A (1997) Fluoxetine tenth anniversary update: the progress continues. *Clinical Therapeutics* **19**:1135-1250.

Sur C, Betz H, and Schloss P (1998) Distinct effects of imipramine on 5-hydroxytryptamine uptake mediated by the recombinant rat serotonin transporter SERT1. *J.Neurochem.* **70**:2545-2553.

Sur C, Betz H, and Scholss P (1997) A single serine residue controls the cation dependence of substrate transport by rat serotonin transporter. *Proc.Natl.Acad.Sci U.S.A* **94**:7639-7644.

Takahashi T and Momiyama A (1993) Different types of calcium channels mediate central synaptic transmission. *Nature* **366**:156-158.

Torres GE, Carneiro A, Seamans K, Fiorentini C, Sweeney A, Yao WD, and Caron MG (2003a) Oligomerization and trafficking of the human dopamine transporter. Mutational analysis identifies critical domains important for the functional expression of the transporter. *J.Biol.Chem.* **278**:2731-2739.

Torres GE, Gainetdinov RR, and Caron MG (2003b) Plasma membrane monoamine transporters: structure, regulation and function. *Nat.Rev.Neurosci.* **4**:13-25.

Tucker WC and Chapman ER (2002) Role of synaptotagmin in Ca2+-triggered exocytosis. *Biochem J* **366**:1-13.

Uhl GR, Nobu T, Kaor I, Zhic L, Masa H, and Ichi S (2000) The VMAT2 gene in mice and humans: amphetamine responses, locomotion, cardiac arrhythmias, aging, and vulnerability to dopaminergic toxins. *FASEB J.* **14**:2459-2465.

Usdin TB, Mezey E, Chen C, Brownstein MJ, and Hoffman BJ (1991) Cloning of the cocaine-sensitive bovine dopamine transporter. *Proc.Natl.Acad.Sci.U.S.A* **88**:11168-11171.

Wagner GC, Preston K, Ricaurte GA, Schuster CR, and Seiden LS (1982) Neurochemical similarities between d,l-cathinone and d-amphetamine. *Drug Alcohol Depend.* **9**:279-284.

Wang YM, Xu F, Gainetdinov RR, and Caron MG (1999) Genetic approaches to studying norepinephrine function: knockout of the mouse norepinephrine transporter gene. *Biol.Psychiatry* **46**:1124-1130.

Weihe E and Eiden LE (2000) Chemical neuroanatomy of the vesicular amine transporters. *FASEB J* **14**:2435-2449.

Wellsow J, Machulla H.J., and Kovar K-A (2002) 3D QSAR of Serotonin Transporter Ligands: CoMFA and CoMSIA Studies. *Quantitative Structure-Activity Relationships* **21**:577-589.

Wilcox RE, Tseng T, Brusniak MY, Ginsburg B, Pearlman RS, Teeter M, DuRand C, Starr S, and Neve KA (1998) CoMFA-based prediction of agonist affinities at recombinant D1 vs D2 dopamine receptors. *J.Med.Chem.* **41**:4385-4399.

Williams KA (2000) Three-dimensional structure of the ion-coupled transport protein NhaA. *Nature* **403**:112-115.

Williams KA, Geldmacher-Kaufer U, Padan E, Schuldiner S, and Kuhlbrandt W (1999) Projection structure of NhaA, a secondary transporter from Escherichia coli, at 4.0 A resolution. *EMBO J.* **18**:3558-3563.

Wong DT, Bymaster FP, Horng JS, and Molloy BB (1975) A new selective inhibitor for uptake of serotonin into synaptosomes of rat brain: 3-(p-trifluoromethylphenoxy). N-methyl-3-phenylpropylamine. *J.Pharmacol.Exp.Ther.* **193**:804-811.

Wong DT, Horng JS, Bymaster FP, Hauser KL, and Molloy BB (1974) A selective inhibitor of serotonin uptake: Lilly 110140, 3-(p-trifluoromethylphenoxy)-N-methyl-3-phenylpropylamine. *Life Sci.* **15**:471-479.

Zahniser NR and Doolen S (2001) Chronic and acute regulation of Na+/Cl- -dependent neurotransmitter transporters: drugs, substrates, presynaptic receptors, and signaling systems. *Pharmacol.Ther.* **92**:21-55.

VITA

VITA

David Lance Roman was born in Evergreen Park, Illinois on October 26th, 1976. He was greeted into this world by his parents, David Benedict and Marie Elizabeth, and his elder sister, Elizabeth Marie.

David attended St. Rene de Goupil elementary school in Chicago, Illinois and then progressed to St. Laurence High School in Burbank, Illinois, where he graduated in 1994. David's scholarly career began in 1994 with his decision to attend Quincy University in Quincy, Illinois in pursuit of an undergraduate degree in Biology with an intention of attending medical school. However, he became somewhat bored with biology courses and keenly interested in the chemistry behind those biological processes. At the behest of his General Chemistry professor, Dr. Scott T. Luaders, David declared himself a dual-degree candidate in Biological Sciences and Chemistry. Four years later, in May 1998, David graduated Magna Cum Laude with a Bachelor of Science in Biological Sciences and a Bachelor of Science in Chemistry. His goal of attaining both degrees within four years was aided by taking a short summer semester set of courses in Italy, including time spent in La Verna, Greccio, Rome, Assisi, Gubbio, the Reti Valley, and San Damiano.

Following graduation from Quincy University, David began his Doctoral studies in Purdue University's Department of Medicinal Chemistry and Molecular Pharmacology under the guidance of Dr. Eric L. Barker. His research has focused on the recognition of

distinct drug classes (such as psychostimulants and antidepressants) by the serotonin transporter (SERT). During his tenure at Purdue, he was awarded an ASPET Graduate Student Travel Award, and also spearheaded efforts to obtain department-wide training with molecular modeling software through Tripos, Inc., a technique used extensively throughout his graduate career.

One highlight of David's time at Purdue was the selection of a set of figures depicting cocaine analog interactions with the serotonin transporter for the cover of the Journal of Pharmacology and Experimental Therapeutics, February 2004 issue.

Upon completion of his studies at Purdue, David accepted a position as a Postdoctoral fellow in the Department of Pharmacology at the University of Michigan Medical Center (Ann Arbor), under the guidance of Dr. Richard R. Neubig. At Michigan, David plans to study the role of RGS (regulators of G-protein signaling) proteins in relation to the kinetics, assembly, and signaling pathways of G-protein coupled receptors, as well as undertaking studies to determine the possible role of RGS proteins as therapeutic targets.